Studies on
Preparation of Carbonaceous Thin Films and Their Electrochemical Properties

Tomokazu FUKUTSUKA

2004

Studies on
Preparation of Carbonaceous Thin Films and Their Electrochemical Properties

Tomokazu FUKUTSUKA

Department of Materials Science and Chemistry
Graduate School of Engineering
University of Hyogo
Hyogo, Japan

2004

Preface

The present thesis is a result of the research work for the preparation of carbonaceous thin films by plasma-assisted chemical vapor deposition (plasma CVD) and their electrochemical properties for lithium-ion batteries.

This work has been carried out under the supervision of *Professor Zempachi Ogumi* at Department of Energy and Hydrocarbon Chemistry, Graduate School of Engineering, Kyoto University and *Professor Yosohiro Sugie* at Department of Materials Science and Chemistry, Graduate School of Engineering, University of Hyogo. The author would like to express their sincere gratitude for their valuable advice and instruction throughout the course of this work.

The author is also grateful to *Professors Yasuhiro Awakura* and *Takashi Kakiuchi*, Graduate School of Engineering, Kyoto University, for their useful comments and discussion.

The author is also grateful to *Professors Akimasa Tasaka* (Doshisha University), *Minoru Inaba* (Doshisha University), *Yoshiaki Matsuo* (University of Hyogo), *Takeshi Abe* (Kyoto University), *Drs. Atsushi Mineshige* (University of Hyogo), and *Yasutoshi Iriyama* (Kyoto University) for many fruitful discussions.

The author greatly appreciates all the members of *Professor* Ogumi's laboratory and *Professor* Sugie's laboratory for their devoted contributions to this work. In particular, the author would like to appreciate *Messrs. Takayuki Doi* (Kyoto University), *Shigeki Yamate* (Kyoto University), and *Kazuhisa Takeda* (Kyoto University) and *Misses. Kaori Gonda* (Doshisha University) and *Naoko Tsuji* (Doshisha University).

Finally, the author wishes to thank his parents for their continuous encouragement.

Tomokazu Fukutsuka

Contents

Chapter 4

Synthesis of highly graphitized carbonaceous thin films by plasma-assisted chemical vapor deposition and their electrochemical properties in propylene carbonate solution

Part 2.

Surface plasma modification of carbonaceous thin film electrodes and their electrochemical properties

Chapter 5

Surface modification of carbonaceous thin films by NF_3 plasma and their effects on electrochemical properties

Chapter 6

Surface modification of carbonaceous thin-film electrodes by using oxygen plasma

Part 3.

Lithium-ion transfer at interface between carbonaceous thin-film electrode and electrolyte

General Introduction

Background of the work

1. *Lithium-ion batteries (LIBs)*

Ever since lithium-ion batteries (LIBs) were commercialized in 1991 [1], many researchers in Japan and elsewhere have aggressively studied [2, 3] their characteristics for the development of portable electronics, such as cellular telephones, camcorders, notebook computers, and so on. Furthermore, LIBs are being considered as power sources for electric vehicles (EVs) and hybrid electric vehicles (HEVs) because of their high energy density.

The main components of LIBs are positive electrodes, negative electrodes, and electrolytes. Lithium transition metal oxides, such as $LiCoO_2$, $LiMn_2O_4$, and $LiNiO_2$, and carbonaceous materials, such as graphitic carbons, hard carbons, and soft carbons, are used as positive and negative electrode materials, respectively, since the insertion/extraction of lithium ion into/from these materials can occur reversibly. The electrolytes consist of non-aqueous organic solvents containing a lithium salt, such as $LiPF_6$, $LiClO_4$, $LiBF_4$, or $LiCF_3SO_3$. The non-aqueous organic solvents consist of a mixed system of two or more kinds of solvents, and include those with a high dielectric constant, such as ethylene carbonate (EC) and propylene carbonate (PC), and those with low viscosity, such as dimethyl carbonate (DMC), diethyl carbonate (DEC), and ethyl methyl carbonate (EMC).

The electrode reactions of LIBs can be described as (negative electrode; carbon and positive electrode; $LiMeO_2$):

<Negative electrode> $x\mathrm{Li}^+ + x\mathrm{e}^- + \mathrm{C} \rightleftarrows \mathrm{Li}_x\mathrm{C}$

<Positive electrode> $\mathrm{LiMeO_2} \rightleftarrows \mathrm{Li}_{1-x}\mathrm{MeO_2} + x\mathrm{Li}^+ + x\mathrm{e}^-$

<Overall reaction> $\mathrm{LiMeO_2} + \mathrm{C} \rightleftarrows \mathrm{Li}_{1-x}\mathrm{MeO_2} + \mathrm{Li}_x\mathrm{C}$

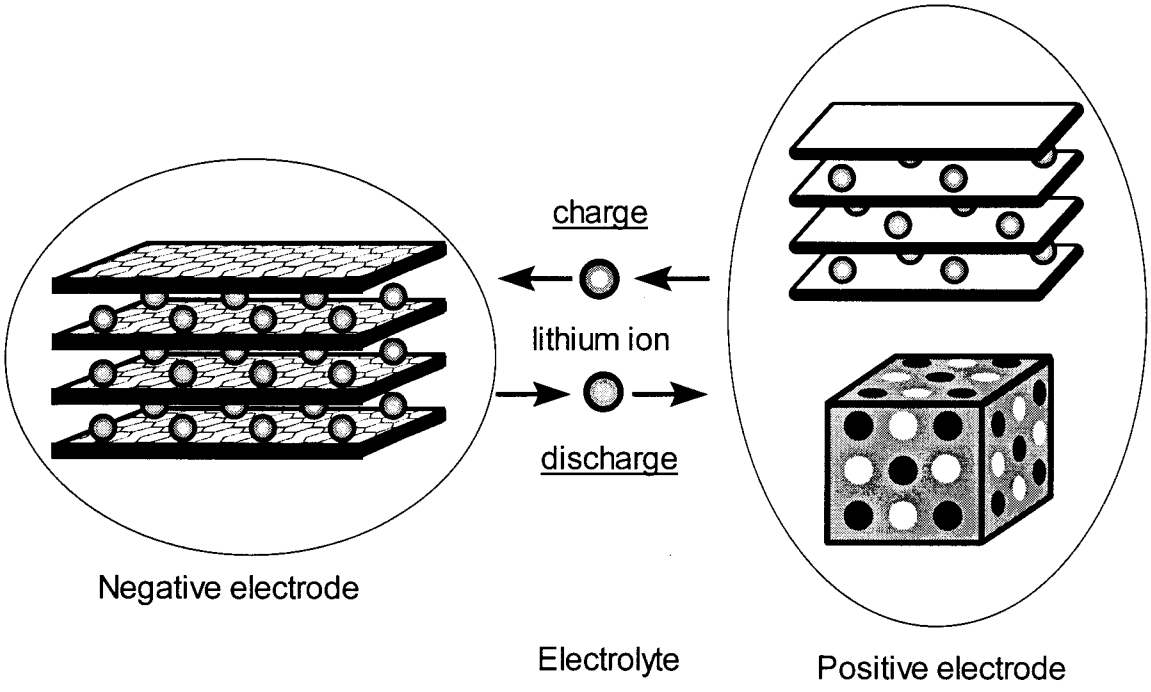

Fig. 1. Principle of battery reaction for lithium-ion batteries.

The principle of LIBs is shown in Fig. 1. The reaction proceeds by the transfer of lithium ion between the positive and negative electrodes through the electrolyte (back and forth rocking movement of lithium ion), and metallic lithium does not exist in the battery system. This is why commercial rechargeable lithium batteries are called "lithium-ion batteries" or "rocking chair batteries"[4].

2. *Carbonaceous material as a negative electrode for LIBs*

Early attempts at the electrochemical insertion of lithium ion into graphite in a PC solution, which was used as a solvent in primary lithium batteries, did not succeed [5], since PC is decomposed by electrochemical reduction at a potential higher than that at which lithium ion is inserted into graphite and graphite undergoes exfoliation due to the co-intercalation of solvated (PC) lithium ion [6]. The electrochemical intercalation of lithium ion into graphite in an electrolyte solution (EC+PC) was first reported in 1990 [7]. The surface of graphite is covered with a passivating film (Fig.2), which is conductive for lithium ion but electronically insulating, and is formed via the reductive decomposition of EC. This surface film, which is called the solid electrolyte interface (SEI) [8], suppresses further solvent decomposition and leads to a coulombic efficiency of almost 100 %. The problem in SEI formation is that the charge consumed for decomposition of EC cannot be used as capacity, and this accounts for most of the irreversible capacity. However, this process is essential for the reaction of LIBs. Although the problem of irreversible capacity remains unsolved, the investigation of various carbonaceous materials suitable for use as the negative electrodes of LIBs has been extended following the discovery of SEI formation by the reduction of EC.

Carbonaceous materials for negative electrodes of LIBs can be divided into four types [9]: (1) graphitic carbons, (2) soft carbons heat-treated at relatively high temperature (1000 – 2400 °C), (3) soft carbons heat-treated at low temperature (< 1000 °C), and (4) hard carbons heat-treated at low temperature (< 1000 °C).

2.1. Graphitic carbons

It is well-known that the intercalation of lithium ion into graphite leads to the formation of lithium-graphite intercalation compounds (Li-GICs) [10, 11]. Electrochemical

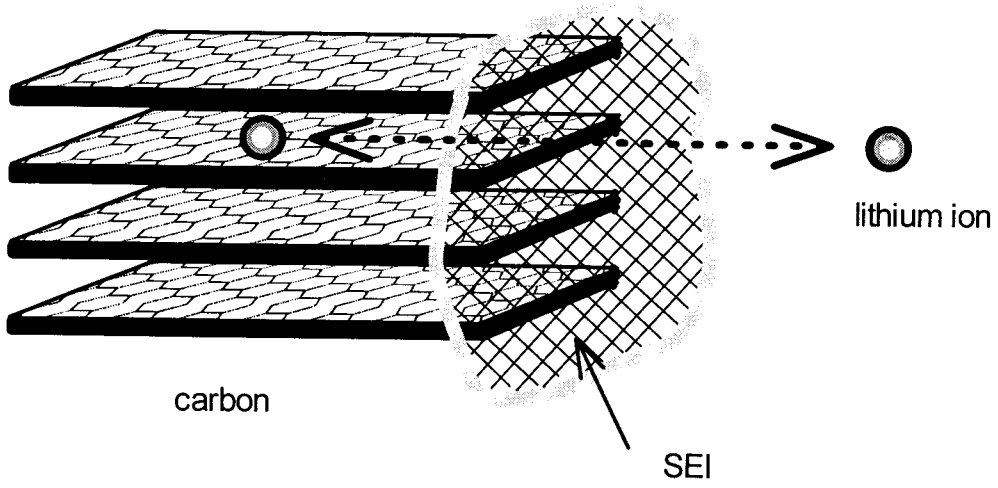

Fig. 2. Schematic image of solid electrolyte interface (SEI) formed on carbon negative electrode.

intercalation of lithium ion occurs below 0.25 V vs. Li/Li^+ with a two-phase reaction and the maximum composition of Li-GICs is restricted to LiC_6 which corresponds to a stage 1 structure. In GICs, the stage number (n) is defined as the number of graphene layers between two intercalate layers. The structures of GICs are shown in Fig. 3. Figure 4 shows charge-discharge curves for graphite at the 1st cycle. Graphitic carbon as a negative electrode shows a flat low potential for charge-discharge curves and a maximum capacity of 372 $mAhg^{-1}$ (theoretical capacity calculated from LiC_6). Moreover, the use of graphitic carbon as a negative electrode gives good cycle performance. Due to these characteristics, graphitic carbon is widely used as a negative electrode for commercial LIBs.

2.2. Soft carbons heat-treated at relatively high temperature

A soft carbon is a carbon that can be graphitized by heat-treatment at high-temperature. For soft carbons, the reversible capacity decreases and a low and long potential plateau is not observed with decreasing HTT (heat-treatment-temperature) (Fig. 5) [3]. Dahn [9] and Tatsumi [12] reported that the degree of graphitization is related to the reversible capacity. For these carbons, lithium-ion insertion and extraction occurs at an interlayer of the graphitized part. Therefore, the reversible capacities of these carbons are lower than those of graphitic carbons, since there is a smaller proportion of graphitic part than with graphitic carbons. The mechanism of lithium-ion insertion/extraction into/from carbonaceous materials with a graphitic structure is very interesting. However, while these carbons have been the subject of considerable study, they have not been commercialized because of their low reversible capacity.

2.3. Soft carbons heat-treated at low temperature

These carbons are also called disordered carbons. For these soft carbons, it is thought that lithium-ion insertion and extraction occur not only at interlayers but also at other parts. Charge-discharge curves for these carbons are shown in Fig. 6 [13]. The reversible capacities of these carbons are greater than the theoretical capacity of graphite (about 500 - 1000 $mAhg^{-1}$) and their irreversible capacities are very large. Moreover, the charge-discharge curves show large hysteresis; i.e., lithium-ion insertion occurs at 0 V and extraction occurs at about 1 V. To explain these unique characteristics, various mechanisms of lithium-ion

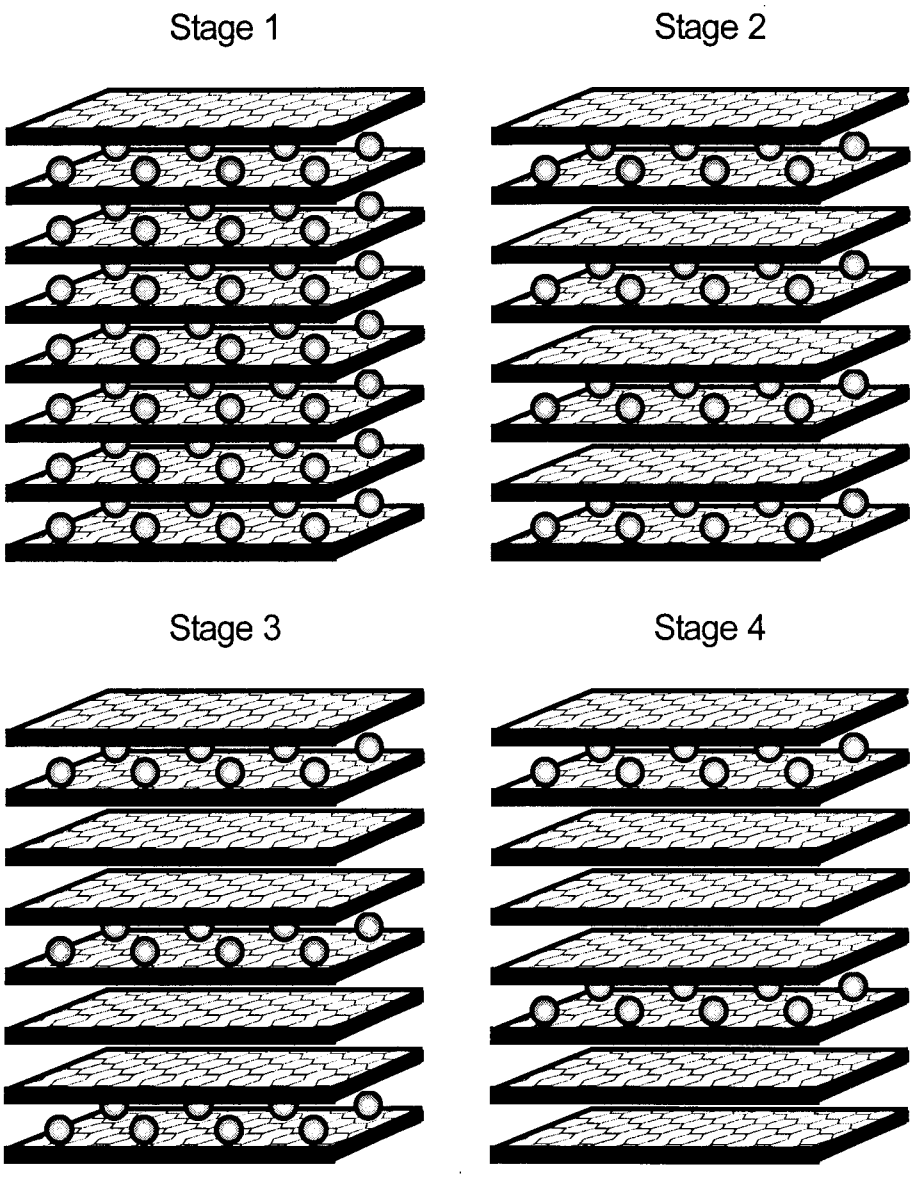

Fig. 3. Schematic images of graphite-intercalation compounds (GICs) for various stage structures.

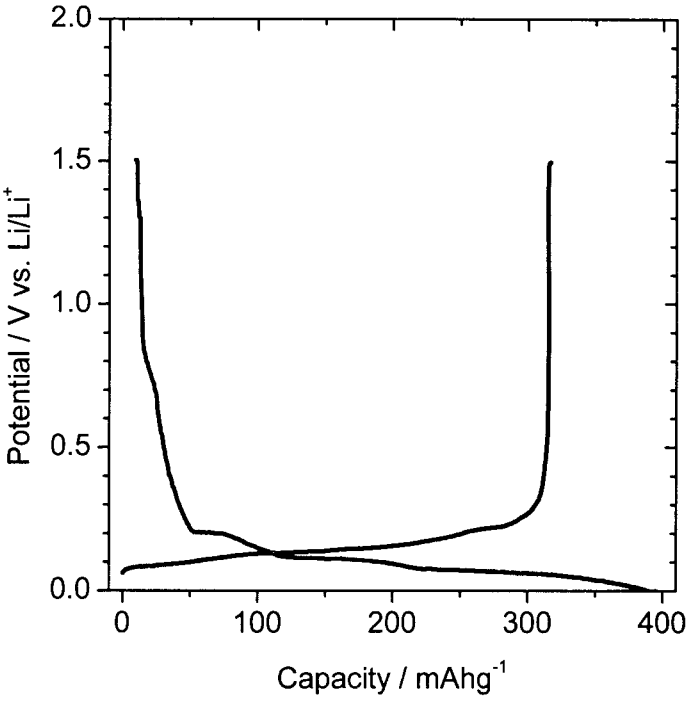

Fig. 4. Schematic illustration of typical charge and discharge curves for graphite electrode.

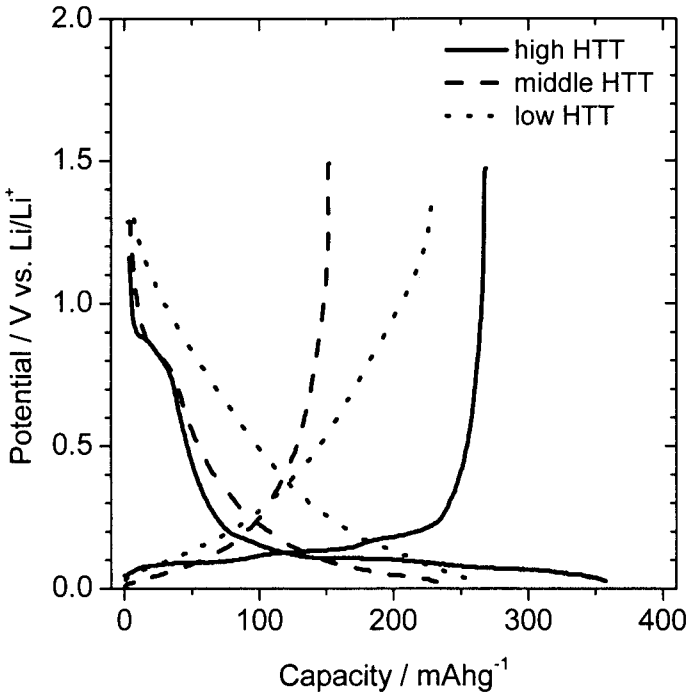

Fig. 5. Schematic illustration of charge and discharge curves for soft carbons heat-treated at various temperatures.

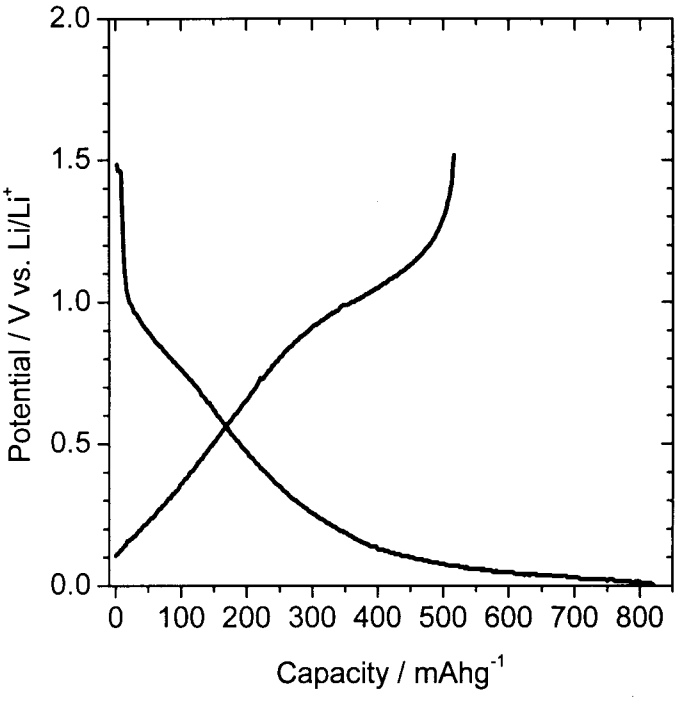

Fig. 6. Schematic illustration of typical charge and discharge curves for soft carbons heat-treated at low temperature.

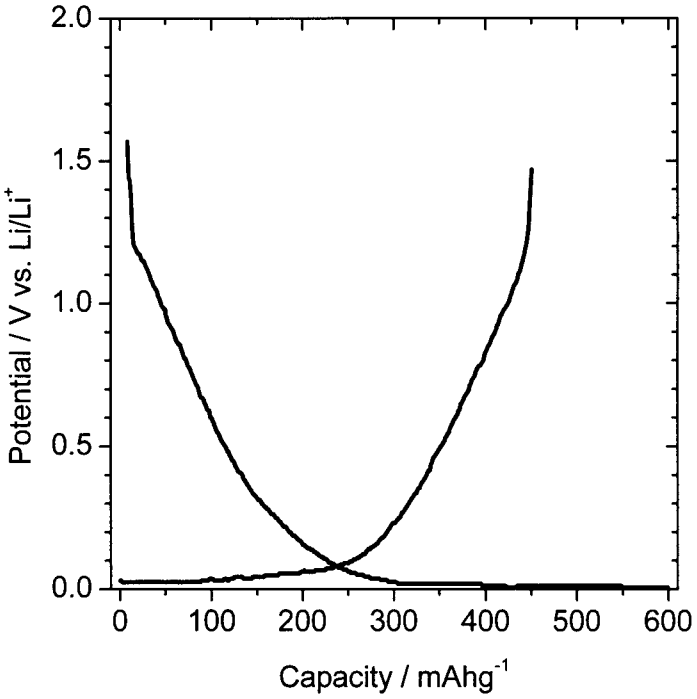

Fig. 7. Schematic illustration of typical charge and discharge curves for hard carbons heat-treated at low temperature.

insertion/extraction have been proposed; e.g., LiC_2 formation at the interlayer [14], formation of an ionic complex [15], storage in nano-cavities [16], and exchange of hydrogen atoms at a hydrogen-terminated edge for lithium [17]. However, these models cannot completely explain the above characteristics. Although these soft carbons may be difficult to commercialize, their large reversible capacities are very attractive for practical applications.

2.4. Hard carbons heat-treated at low temperature

Hard carbons show (1) high reversible capacities and (2) lithium-ion insertion/extraction below 0.1 V (Fig. 7) [3]. Various mechanism of lithium-ion insertion/extraction below 0.1 V have been proposed: formation of a lithium cluster in micropores [18], and adsorption at the surface of a single graphene layer (house-of-cards model) [19]. These properties could be very useful for applications in EVs or HEVs. However, there is a difficulty in the practical use of hard carbons; i.e., the deposition of dendritic lithium can occur during lithium-ion insertion at about 0 V, which leads to a problem regarding the safety of LIBs. This type of carbon is a very promising candidate as a negative electrode in high-capacity LIBs and has been commercialized in some LIBs.

3. *Binder-free electrodes for kinetic analysis*

The negative/positive electrodes for practical use are composite electrodes. For the positive electrode, the composite electrode is a mixture of lithium transition metal oxide (active material), polytetrafluoroethylene; PTFE (binder), and carbon black or acetylene black (conductive additive). For the negative electrode, the composite electrode is a mixture of carbonaceous materials (active material) and poly(vinylidene fluoride) (PVdF; binder). Figure 8 shows a schematic illustration of a composite electrode (positive electrode). The composite electrodes have a porous structure. Since composite electrodes do not provide an exact reaction area and show a non-uniform potential or current distribution, the detailed analysis of the kinetics of lithium-ion insertion/extraction for the active material itself is not easy. To overcome these difficulties, the fabrication of binder-free electrodes has been widely studied [20-53]. Moreover, the use of thin-film electrodes offers some advantages: (1) it is possible to determine the reaction area because of the flat surface and (2) there is a short diffusion path because the material is so thin.

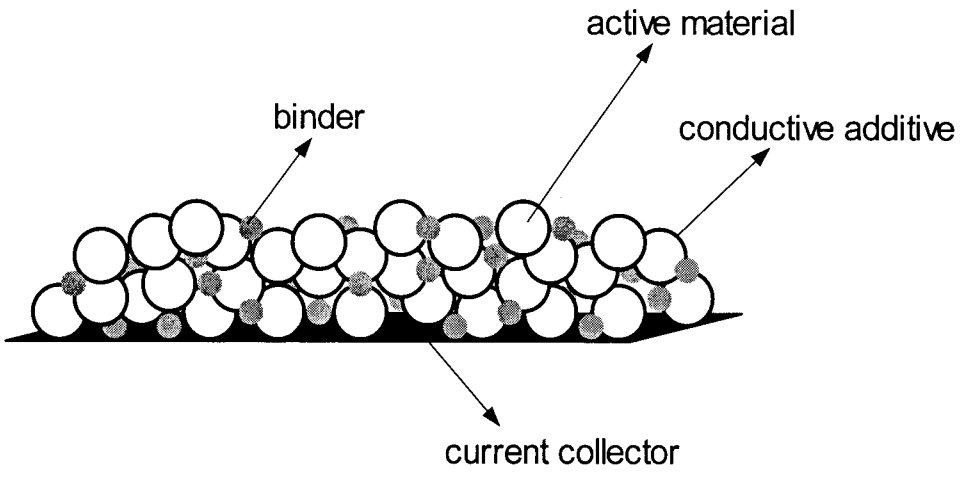

Fig. 8. Schematic illustration of composite positive electrode.

3.1. Classification of binder-free electrodes

Binder-free electrodes can be divided into two types: those in which the electrode only contains active material, such as single-particle, single-crystal and block materials (e.g., high oriented pyrolytic graphite; HOPG), and thin-film electrodes. The former is attractive for determining the nature of electrode materials. However, measurements with single-particle and single-crystal electrodes require complex equipment [54-58], and single-crystal and block materials are quite expensive. Therefore, these may not be suitable for practical use. In contrast, thin-film electrodes are widely used as positive electrodes, since positive electrodes are composed of lithium transition metal oxides (i.e., ceramics) and are easily prepared by physical vapor deposition (PVD), such as by sputtering [35, 39-41, 44] and pulsed laser deposition (PLD) [27, 32, 36, 37, 42, 46, 48, 52], and other processes such as solution methods [21, 23, 26, 38, 43, 49-51] and electrospray deposition (ESD) [25, 30, 31, 33, 45, 47].

3.2. Carbonaceous thin-film electrodes as binder-free electrodes

For reasons mentioned later, few studies have been conducted using carbonaceous thin-film electrodes. Unfortunately, it is difficult to prepare sp^2-type carbonaceous thin films with a flat surface, since PVD methods give mainly sp^3-type carbonaceous thin films (diamond or diamond-like carbon (DLC)) [59-70] and CVD methods give particle-like sp^2-type films due to vapor growth of carbon [71-76]. Despite these difficulties, some carbonaceous thin-film electrodes have been reported for kinetic analysis using CVD (chemical vapor deposition) carbon [20], ESD carbon [24, 29], sputtering carbon [22, 28], and so on [34, 53]. However, these materials are not necessarily suitable for kinetic analysis because of their surface roughness, low crystallinity, relatively large thickness, etc. Therefore, sp^2-type carbonaceous thin-film electrodes that are flat and show high crystallinity must be prepared by other method.

4. Use of plasma to prepare thin films

Plasma-assisted chemical vapor deposition (plasma CVD) and plasma polymerization have been widely used to prepare thin films with the properties described

above. For example, thin films of amorphous silicon (a-Si) for solar cells [77, 78], diamond or DLC thin films [59-70], and lithium-ion conductive polymer for solid-state lithium batteries [79-83], have all been prepared by using plasma.

4.1. Characteristics of plasma

Plasma is a partially ionized gas that consists of equal numbers of positive and negative charges and several non-ionized neutral atoms. When an electric field acts on a gas molecule, some of the free electrons in the gas are accelerated and obtain kinetic energy. If the electric field is extraordinary strong or the gas pressure is quite low (which means that the mean free path is very long), electrons are sufficiently accelerated. Molecules that are impacted by electrons dissociate and a discharge phenomenon is observed. This discharge phenomenon is called plasma. Examples of plasma in an extraordinary strong electron field include thunder, arc plasma, etc. In such plasma, T_e (electron temperature) equals T_g (gas temperature) which is over several thousands K, and therefore such plasma is called thermal plasma. Due to this high T_g, thermal plasma is used as a heat source in thermal spraying, melting furnaces, etc. For plasma obtained at low pressure, $T_e > T_g$, and T_g is below 1000 K. This plasma is called non-equilibrium plasma or cold plasma. Non-equilibrium plasma used for chemical applications is mainly dc (direct current) plasma, rf (radio frequency) plasma, microwave plasma, etc. In particular, rf plasma has been widely used, because stable rf discharge can be easily generated over a large area. Many rf discharge processes operate at 13.56 MHz, since this frequency was allotted by international communications authorities at which a certain amount of energy can be radiated without interfering with communications. A pair of electrodes is necessary to obtain rf discharge: an rf electrode and a ground electrode. The rf discharge is generated between these electrodes, and this is where chemically reactive species are formed.

4.2. Preparation of thin films by plasma CVD

Thin films prepared by plasma CVD have a smooth, dense, pin-hole-free surface. In plasma, active species etch the deposition products, and hence the surface of the thin film is etched and becomes smooth [84]. Sufficient reactive species are available for the substrate and these species fill empty space, and hence the thin film is dense and pin-hole-free.

Moreover, the large number of active species and the high T_e enable the low-temperature synthesis of thin films and high crystallinity if the reaction temperature is equal to that of thermal CVD. The parameters in plasma CVD are the applied rf power, gas pressure, kinds of dilute gas, etc. These parameters affect the properties of the thin films. The applied rf power is in proportion to the current in the reaction chamber. A high rf power gives a large number of active species with high energy according to the Boltzmann distribution, and thus, thin films are obtained with considerable energy and their crystallinity is increased. Gas pressures affect the mean free path in the plasma. The mean free path is the distance that active species in plasma can move before colliding with other active and neutral species. If the mean free path increases, the distance that active species can move increase, and therefore active species can obtain more energy from the electric field. For carbonaceous thin films, dilute gas is a very important parameter. If a carbon source gas and hydrogen gas are used for the plasma source, DLC or diamond thin films are deposited preferentially. Since active species of hydrogen can etch sp^2 carbons preferentially, sp^3 carbons remain and DLC or diamond thin films are deposited [85]. In contrast, there is no deposition of DLC or diamond thin films without hydrogen. Thus, the applied rf power and gas pressure affects the crystallinity of thin films and dilute gas affects the components of thin films. The optimization of these parameters is a key point in the preparation of thin films.

Outline of the work

As mentioned above, carbonaceous materials are important for the development of LIBs and more information on lithium-ion insertion/extraction of carbonaceous materials is needed. The preparation of carbonaceous thin films suitable for use as binder-free electrodes is needed for this purpose. The present work focuses on the preparation of carbonaceous thin-film electrodes and electrochemical lithium-ion insertion/extraction in the resulting thin-film electrodes. First, carbonaceous thin films were prepared by plasma CVD as binder-free electrodes and their electrochemical properties as the negative electrodes of LIBs were examined. Second, surface modifications of carbonaceous thin-film electrodes by plasma were carried out and their effects on the electrochemical properties were examined. Finally, lithium-ion transfer at the interface between carbonaceous thin-film electrodes and electrolyte were examined.

In part 1, carbonaceous thin-film electrodes were prepared by plasma CVD. The resultant thin films were characterized by Raman spectroscopy, X-ray diffraction measurement (XRD), Auger electron spectroscopy (AES), scanning electron microscopy (SEM), and transmission electron microscopy (TEM). Lithium-ion insertion/extraction properties were examined by cyclic voltammetry (CV) and charge-discharge measurements. Based on the results of these measurements, lithium-ion insertion/extraction properties are discussed.

In chapter 1, carbonaceous thin films were prepared by plasma CVD from acetylene/argon plasma at 873 K. The resultant thin films were characterized by Raman spectroscopy, AES, and TEM. Carbonaceous thin films in this study showed relatively high crystallinity. Based on the results of Raman spectroscopy, the crystallinity of carbonaceous thin films found to be depended on the applied rf power.

In chapter 2, carbonaceous thin-film electrodes prepared by plasma CVD from acetylene/argon were examined by electrochemical methods such as CV and charge-discharge measurements in ethylene carbonate (EC)-based solution. The lithium-ion insertion/extraction mechanism for carbonaceous thin-film electrodes is discussed based on electrochemical measurements.

In chapter 3, the electrochemical properties of carbonaceous thin-film electrodes prepared using NF_3 plasma were examined. Carbonaceous thin-film electrodes were prepared by plasma CVD from ethylene/NF_3/argon plasma at 773 K. The difference between carbonaceous thin-film electrodes with and without NF_3 plasma was investigated.

In chapter 4, carbonaceous thin films were prepared by plasma CVD from acetylene/argon plasma at 1073 K. The resultant thin films were characterized by Raman spectroscopy and XRD measurement. The carbonaceous thin-film electrodes in this study were highly graphitized. The electrochemical properties of the resultant thin-film electrodes were measured in propylene carbonate (PC) solution.

In part 2, the surface of carbonaceous thin-film electrodes was modified by plasma (NF_3 or O_2) and the effects of surface modification on solvent decomposition were investigated. So far, various surface modifications of carbonaceous materials have been studied to improve the performance of LIBs [86-92]. These modifications have brought good performance to LIBs. Therefore, it is valuable to clarify the detail of surface modifications by

using carbonaceous thin-film electrodes with flat surface.

In chapter 5, carbonaceous thin-film electrodes were treated by NF_3 plasma. The surface was characterized by AES and X-ray photoelectron spectroscopy (XPS). NF_3 plasma introduced C-F bonding to the surface of carbonaceous thin-film electrodes. The effects of C-F bonding on the decomposition of electrolyte are discussed.

In chapter 6, carbonaceous thin-film electrodes were treated by O_2 plasma. The surface was characterized by AES and X-ray photoelectron spectroscopy (XPS). O_2 plasma had the same effects on thin-film electrodes as NF_3 plasma. Various electrolyte solutions and additives were used to identify the peak of CV affected by surface treatment.

In part 3, lithium-ion transfer at the interface of carbonaceous thin-film electrodes/electrolyte solutions was elucidated by AC impedance spectroscopy. Fast charge and discharge reactions are required for LIBs used for HEVs, and therefore the kinetics of lithium-ion transfer at electrodes should be clarified [52]. Lithium-ion transfer at the negative electrode in LIBs is mainly as follows: (1) migration in electrolyte, (2) migration in SEI, (3) charge-transfer, and (4) diffusion in carbonaceous materials. These processes are shown in Fig. 9. Fast ion transfer in electrolyte (1) is achieved by using an electrolyte with high ionic conductivity and a thin-electrolyte layer. For fast ion transfer in the SEI (2), electrolytes and additives that form thinner SEI with high ionic conductivities must be selected. The length of the diffusion path affects the diffusion process (4), and hence the use of fine particles of carbonaceous materials can decrease the diffusion path and the diffusion of lithium ion is accelerated. However, lithium-ion transfer at the electrode/electrolyte interface (3) has been ignored because of the difficulty of estimating ion transfer and fabricating structural ordered electrodes. Therefore, it is important to clarify lithium-ion transfer at the interface for fast charge and discharge reactions of LIBs. The carbonaceous thin-film electrodes mentioned above are suitable for the analysis of lithium-ion transfer at the electrode/electrolyte interface. In this part, lithium-ion transfer at the electrode/electrolyte interface is investigated.

In chapter 7, lithium-ion transfer for carbonaceous thin-film electrodes with different crystallinities was investigated by AC impedance spectroscopy. Characterization of Nyquist plots for carbonaceous thin-film electrodes was carried out. The activation energy for lithium-ion transfer at the interface was evaluated from the relation between charge-transfer (lithium-ion transfer) resistance and temperature.

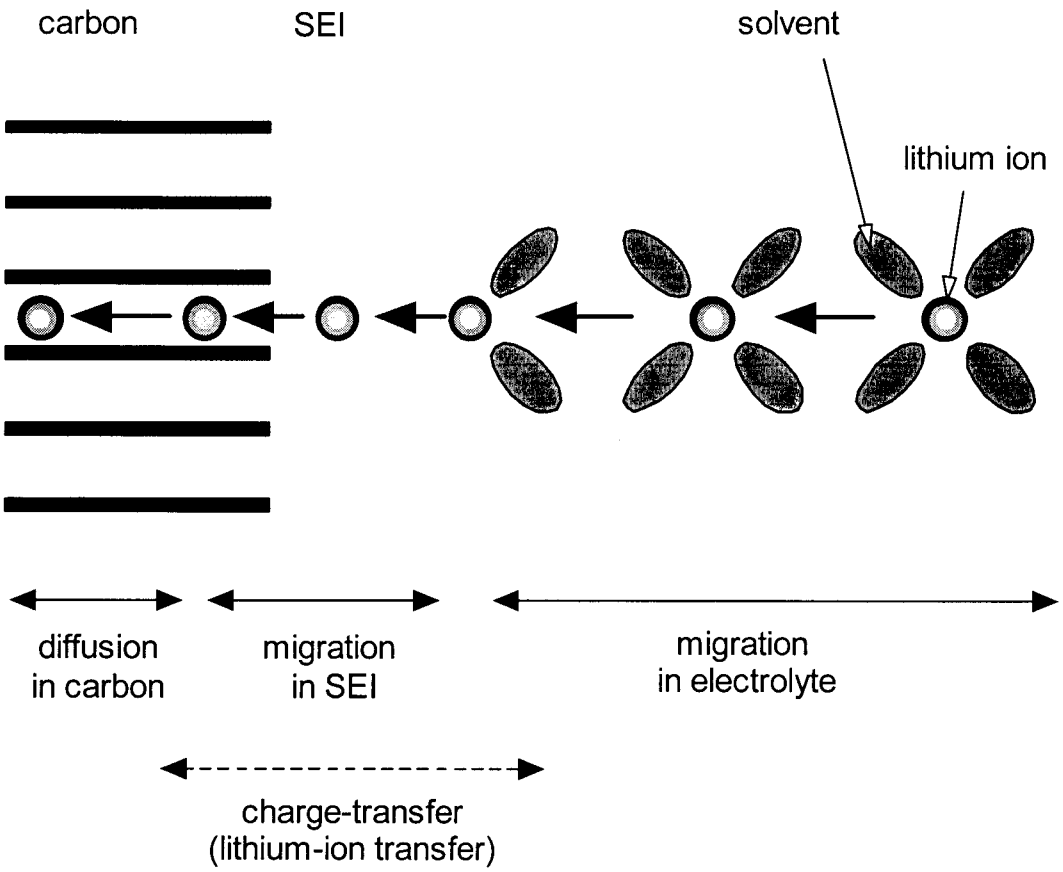

Fig. 9. Schematic image of lithium-ion transfer at carbon negative electrode.

In chapter 8, the effect of the solvent on the activation energy for lithium-ion transfer at the carbonaceous thin-film electrode/electrolyte interface was investigated. The interface was fabricated using two methods to obtain detailed information regarding the activation barrier. Ion-solvent interaction in lithium-ion transfer at the interface is discussed.

In chapter 9, lithium-ion transfer for highly graphitized carbonaceous thin-film electrodes was investigated by AC impedance spectroscopy. Lithium-ion transfer at the interface between a highly graphitized carbonaceous thin-film electrode and electrolyte is discussed.

References

[1] *Advanced in Lithium-Ion Batteries* edited by W. A. van Schalkwijk and B. Scrosati (Kluwer Academic / Plenum Publishers, New York, 2002).

[2] M. Winter, J. O. Besenhard, M. E. Spahr, and P. Novák, *Adv. Mater.*, **10,** 725 (1998).

[3] Z. Ogumi and M. Inaba, *Bull. Chem. Soc. Jpn.*, **71**, 521 (1998).

[4] B. Scrosati, *J. Electrochem. Soc.*, **139**, 2776 (1992).

[5] A. N. Day and B. P. Sullivan, *J. Electrochem. Soc.*, **117**, 222 (1970).

[6] J. O. Besenhard, M. Winter, J. Yang, and W. Biberacher, *J. Power Sources*, **54**, 228 (1995).

[7] R. Fong, U. V. Sacken, and J. R. Dahn, *J. Electrochem. Soc.*, **137**, 2009 (1990).

[8] E. Peled, *J. Electrochem. Soc.*, **126**, 2047 (1979).

[9] J. R. Dahn, T. Zheng, Y. Liu, and J. S. Xue, *Science*, **270**, 590 (1995).

[10] J. R. Dahn, *Phys. Rev.* **B 44**, 9170 (1991).

[11] T. Ohzuku, Y. Iwakoshi, and K. Sawai, *J. Electrochem. Soc.*, **140**, 2490 (1993).

[12] K. Tatsumi, N. Iwashita, H. Sakaebe, H. Shioyama, S. Higuchi, A. Mabuchi, and H. Fujimoto, *J. Electrochem. Soc.*, **142**, 716 (1995).

[13] M. Inaba, H. Yoshida, and Z. Ogumi, *J. Electrochem. Soc.*, **143**, 2572 (1996).

[14] K. Sato, M. Noguchi, A. Demachi, N. Oki, and M. Endo, *Science*, **264**, 556(1994).

[15] S. Yata, H. Kinoshita, M. Komori, N. Ando, T. Kashiwamura, T. Harada, K. Tanaka and T. Yamabe, *Synth. Met.*, **62**,153 (1994).

[16] A. Mabuchi, K. Tokumitsu, H. Fujimoto, and T. Kasuh, *J. Electrochem. Soc.*, **142**, 1041

(1995).

[17] T. Zheng, W. R. McKinnon, and J. R. Dahn, *J. Electrochem. Soc.*, **143**, 2137 (1996).

[18] M. Ishikawa, N. Sonobe, H. Nakamura, and T. Iwasaki, *Extended Abstracts of 35 th Battery Symposium in Japan*, Nagoya, Japan, pp. 49-50, 1994.

[19] T. Zheng, J. S. Xue and J. R. Dahn, *Chem. Mater.*, **8**, 389 (1996).

[20] M. Mohri, N. Yanagisawa, Y. Tajima, T. Tanaka, T. Mitate, S. Nakajima, M. Yoshida, M. Yoshimoto, T. Suzuki, and H. Wada, *J. Power Sources*, **26**, 545 (1989).

[21] I. Uchida and H. Sato, *J. Electrochem. Soc.*, **142**, L139 (1995).

[22] E. Cazzanelli, G. Mariotto, F. Decker, and J. M. Rosolen, *J. Appl. Phys.*, **80**, 2442 (1996).

[23] H. Sato, D. Takahashi, T. Nishina, and I. Uchida, *J. Power Sources*, **68**, 540 (1997).

[24] S.-J. Lee, T. Itoh, M. Nishizawa, K. Yamada, and I. Uchida, *DENKI KAGAKU* (presently *Electrochemistry*), **66**, 1276 (1998).

[25] M. Nishizawa, T. Uchiyama, K. Dokko, K. Yamada, T. Matsue, and I. Uchida, *Bull. Chem. Soc. Jpn.*, **71**, 2011 (1998).

[26] R. Kostecki, F. Kong, Y. Matsuo, and F. McLarnon, *Electrochim. Acta*, **45**, 225 (1999).

[27] M. Inaba, T. Doi, Y. Iriyama, T. Abe, and Z. Ogumi, *J. Power Sources*, **82**, 554 (1999).

[28] S.-I. Pyun and S.-J. Orr, *J. Mater. Sci. Lett.*, **18**, 591 (1999).

[29] S.-J. Lee, M. Nishizawa, and I. Uchida, *Electrochim. Acta*, **44**, 2379 (1999).

[30] M. Nishizawa, T. Uchiyama, T. Itoh, T. Abe, and I. Uchida, *Langmuir*, **15**, 4949 (1999).

[31] T. Uchiyama, M. Nishizawa, T. Itoh, and I. Uchida, *J. Electrochem. Soc.*, **147**, 2057 (2000).

[32] Y. Iriyama, T. Abe, M. Inaba, and Z. Ogumi, *Solid State Ionics*, **135**, 95 (2000).

[33] M. Nishizawa, T. Ise, H. Koshika, and I. Uchida, *Chem. Mater.*, **12**, 1367 (2000).

[34] N. Koura, H. Tsuiki, N. Terakura, Y. Idemoto, K. Ui, K. Yamada, and T. Mitate, *HYOMEN GIJUTSU*, **52**, 143 (2001).

[35] J. C. Dupin, D. Gonbeau, H. B. Moudden, Ph. Vinatier, and A. Levasseur, *Thin Solid Films*, **384**, 23 (2001).

[36] Y. Iriyama, M. Inaba, T. Abe, and Z. Ogumi, *J. Power Sources*, **94**, 175 (2001).

[37] C. Julien, M. A. C. Lopez, L. E. Alarcon, and E. H. Poniatowski, *Mater. Chem. Phys.*, **68**, 210 (2001).

[38] Y. Matsuo, R. Kostecki, and F. McLarnon, *J. Electrochem. Soc.*, **148**, A687 (2001).

[39] J. F. Whitacre, W. C. West, E. Brandon, and B. V. Ratnakumar, *J. Electrochem. Soc.*, **148**, A1078 (2001).

[40] S. H. Lee, H. M. Cheong, C. E. Tracy, A. Mascarenhas, R. Pitts, G. Jorgensen, and S. K. Deb, *Electrochim. Acta*, **46**, 3415 (2001).

[41] Y.-S. Kang, H. Lee, S.-C. Park, P. S. Lee, and J.-Y. Lee, *J. Electrochem. Soc.*, **148**, A1254 (2001).

[42] J. D. Perkins, C. S. Bahn, J. M. McGraw, P. A. Parilla, and D. S. Ginley, *J. Electrochem. Soc.*, **148**, A1302 (2001).

[43] Y. H. Rho, K. Kanamura, and T. Umegaki, *Chem. Lett.*, 1322 (2001).

[44] S.-I. Pyun and H.- C. Shin, *J. Power Sources*, **97-98**, 277 (2001).

[45] M. Mohamedi, D. Takahashi, T. Itoh, M. Umeda, and I. Uchida, *J. Electrochem. Soc.*, **149**, A19 (2002).

[46] K. A. Striebel, E. Sakai, and E. J. Cairns, *J. Electrochem. Soc.*, **149**, A61 (2002).

[47] F. Cao and J. Prakash, *Electrochim. Acta*, **47**, 1607 (2002).

[48] P. J. Bouwman, B. A. Boukamp, H. J. M. Bouwmeester, and P. H. L. Notten, *J. Electrochem. Soc.*, **149**, A699 (2002).

[49] S.-W. Kim and S.-I. Pyun, *J. Electroanal. Chem.*, **528**, 114 (2002).

[50] S.-W. Song, H. Fujita, and M. Yoshimura, *Adv. Mater.*, **14**, 268 (2002).

[51] Y. H. Rho, K. Kanamura, and T. Umegaki, *J. Electrochem. Soc.*, **150**, A107 (2003).

[52] I. Yamada, T. Abe, Y. Iriyama, and Z. Ogumi, *Electrochem. Commun.*, **5**, 502 (2003).

[53] K. Kwon, F. Kong, F. McLarnon, and J. W. Evans, *J. Electrochem. Soc.*, **150**, A229 (2003).

[54] M. Umeda, K. Dokko, Y. Fujita, M. Mohamedi, I. Uchida, and J. R. Selman, *Electrochim. Acta*, **47**, 885 (2002).

[55] K. Dokko, Y. Fujita, M. Mohamedi, M. Umeda, I. Uchida, and J. R. Selman, *Electrochim. Acta*, **47**, 933 (2002).

[56] S. Waki, K. Dokko, Y. Matsue, and I. Uchida, *DENKI KAGAKU* (presently *Electrochemistry*), **65**, 954 (1997).

[57] M. Nishizawa, H. Koshita, and I. Uchida, *J. Phys. Chem. B*, **103**, 192 (1999).

[58] K. Dokko, M. Nishizawa, M. Mohamedi, M. Umeda, I. Uchida, J. Akimoto, Y.

Takahashi, Y. Gotoh, and S. Mizuta, *Electrochem. Solid-State Lett.*, B, A151 (2001).

[59] E. I. Zorin, V. V. Sukhorukov, and D. I. Tetel'baum, *Sov. Phys. Tech. Phys.*, **25**, 103 (1980).

[60] J. C. Angus, J. E. Stultz, P. J. Shiller, J. R. MacDonald, M. J. Mirtich, and S. Domitz, *Thin Solid Films*, **118**, 311 (1984).

[61] S. Matsumoto, *J. Mater. Sci. Lett.*, **4**, 600 (1985).

[62] J. C. Angus and C. C. Hayman, *Science*, **241**, 913 (1988).

[63] T. Fujita and O. Matsumoto, *J. Electrochem. Soc.*, **136**, 2624 (1989).

[64] H. Minagawa, I. Fujita, T. Hino, and T. Yamashita, *Surf. Coat. Technol.*, **43/44**, 813 (1990).

[65] N. Awaya and Y. Arita, *Jpn. J. Appl. Phys.*, **30**, 1813 (1991).

[66] J. Seth and S. V. Babu, *J. Appl. Phys.*, **73**, 2496 (1993).

[67] L. H. Chou and W. T. Hsieh, *J. Appl. Phys.*, **75**, 2257 (1994).

[68] N. Mutsukura and K. Yoshida, *Diamond Relat. Mater.*, **5**, 919 (1996).

[69] J. H. Lee, D. S. Kim, Y. H. Lee, and B. Farouk, *J. Electrochem. Soc.*, **143**, 1451 (1996).

[70] S. Chiu, S. Turgeon, B. Terreaul, and A. Sarkissian, *Thin Solid Films*, **359**, 275 (2000).

[71] B. C. Banerjee, and T. J. Hirt, and P. L. Walker, *Nature*, **192**, 450 (1961).

[72] T. Baird, J. R. Fryer, and B. Grant, *Carbon*, **12**, 591 (1974).

[73] S. Otani, A. Kojima, Y. Kohama, and S. Sakurai, *Nippon Kagaku Kaishi*, **4**, 494 (1979).

[74] T. Baird, *Fuel*, **63**, 1081 (1984).

[75] M. Yudasaka, R. Kikuchi, T. Matsui, Y. Ohki, M. Baxendale, S. Yoshimura, E. Ota, *Thin Solid Films*, **305**, 351 (1997).

[76] H. A. Yu, T. Kaneko, S. Otani, Y. Sasaki, and S. Yoshimura, *Carbon*, **36**, 137 (1998).

[77] R. C. Chittick, J. H. Alexander, and H. F. Sterling, *J. Electrochem. Soc.*, **116**, 77 (1969).

[78] W. E. Spear and P. G. LeComber, *Solid State Communications*, **17**,1193 (1975).

[79] Z. Ogumi, Y. Uchimoto, Z. Takehara, and R. F. Foulkes, *J. Electrochem. Soc.*, **137**, 29 (1990).

[80] Y. Uchimoto, Z. Ogumi, and Z. Takehara, *J. Electrochem. Soc.*, **137**, 35 (1990).

[81] Z. Takehara, Z. Ogumi, Y. Uchimoto, E. Endo, and Y. Kanamori, *J. Electrochem. Soc.*, **138**, 1574 (1991).

[82] Z. Takehara, Z. Ogumi, Y. Uchimoto, K. Yasuda, and H. Yoshida, *J. Power Sources*,

43–44, 377 (1993).

[83] Z. Ogumi, T. Abe, S. Nakamura, and M. Inaba, *Solid State Ionics*, **121**, 289 (1999).

[84] H. Yasuda and T. Hsu, *Surf. Sci.*, **76**, 232 (1978).A.

[85] A. Hiraki and H. Kawarada, *Tanso*, **128**, 41 (1987).

[86] E. Peled, C. Menachem, D. Bar-Tow, and A. Melman, *J. Electrochem. Soc.*, **143**, L4 (1996).

[87] M. Kurihara, S. Maruyama, K. Oh'e, and T. Ishigaki, *Chem. Lett.*, 715 (1998).

[88] T. Nakajima, M. Koh, R. N. Singh, and M. Shimada, *Electrochim. Acta*, **44**, 2879 (1999).

[89] S.-S. Kim, Y. Kadoma, H. Ikuta, Y. Uchimoto, and M. Wakihara, *Electrochem. Solid-State Lett.*, **4**, A109 (2001).

[90] I. R. M. Kottegoda, Y. Kadoma, H. Ikuta, Y. Uchimoto, and M. Wakihara, *Electrochem. Solid-State Lett.*, **5**, A275 (2002).

[91] T. Takamura, *Bull. Chem. Soc. Jpn.*, **75**, 21 (2002).

[92] H. Tanaka, T. Osawa, Y. Moriyoshi, M. Kurihara, S. Maruyama, T. Ishigaki, and H. Kanda, *Thin Solid Films*, **435**, 205 (2003).

Part 1

Preparation and electrochemical properties of carbonaceous thin-film electrode by glow discharge plasma

Chapter 1

Synthesis of sp^2-type carbonaceous thin films by glow discharge plasma

1.1 Introduction

Plasma-assisted chemical vapor deposition (plasma CVD) has been extensively used for the preparation of various kinds of inorganic materials [1-2]. This is because plasma CVD is one of the best methods for preparing dense and pin-hole-free thin films.

The preparation of carbonaceous films by the use of a glow discharge plasma has been carried out by many workers, however, most studies have focused on the preparation of diamond or diamond-like carbon [3-5], and little attention has been paid to the synthesis of sp^2-type carbonaceous thin films. Recently, sp^2-type carbonaceous materials have attracted much attention because of their use in lithium-ion batteries, where they have been used as negative electrodes. For the studies of carbonaceous negative electrodes of lithium-ion batteries, thin films of sp^2-type carbon are very useful because they can be used as a negative electrode without conductor of acetylene black and poly(vinylidene fluoride) binder, which enables one to study the precise electrochemical properties of the carbon.

In this chapter, the preparation of sp^2-type carbonaceous thin films by using glow discharge plasma is reported and in particular the effect of applied rf power on the properties of resultant carbonaceous thin films is investigated.

1.2 Experimental

Figure 1.1 shows a schematic of the plasma CVD apparatus used in this study. The starting materials were acetylene as a carbon source and argon as a plasma assist gas. Carbonaceous thin films were deposited on substrates of nickel sheets and Pyrex® glass plates whose temperature was kept at 873 K. Plasma was generated by an rf power supply at 13.56 MHz, and the applied rf power ranged from 10 to 90 W. The flow rate of argon and acetylene was set at 20 and 10 sccm, respectively, and the total pressure of reaction chamber

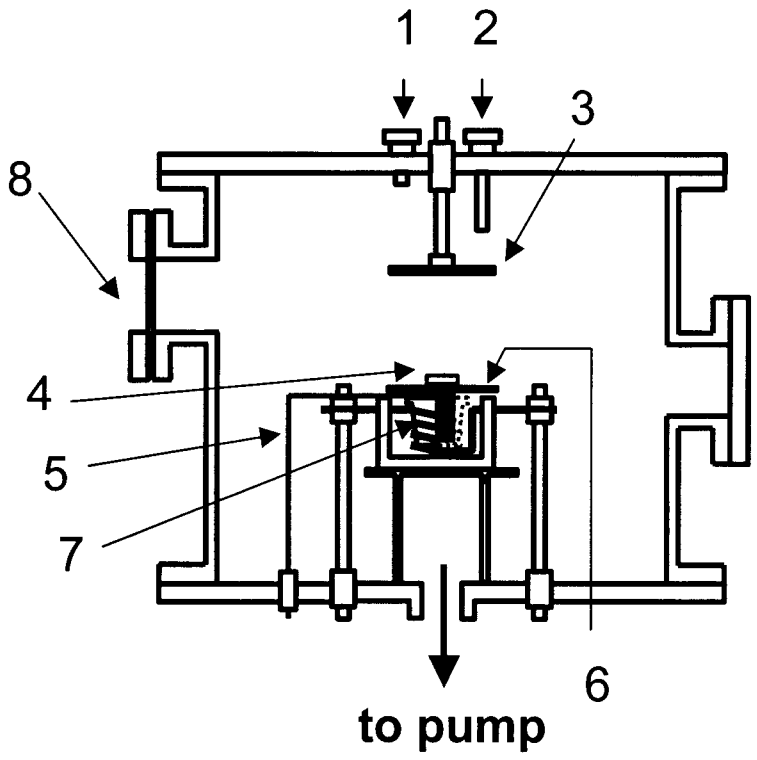

Fig. 1.1. Schematic image of rf reactor for the plasma CVD apparatus. 1; Ar inlet, 2; C_2H_2 inlet, 3; rf electrode, 4; substrate, 5; thermocouple, 6; ground electrode, 7; tungsten heater, 8; view port.

was kept at 133 Pa.

The resultant carbonaceous thin films were mainly characterized by Raman spectroscopy and Auger electron spectroscopy (AES). Transmission electron microscopy (TEM) was also used. The Raman spectra were excited by using a 514.5 nm line (50 mW) of an argon ion laser, and the scattered light was collected in a backscattering geometry. All spectra were recorded using a spectrometer (Jobin-Yvon, T64000) equipped with a multi-channel CCD detector. Each measurement was carried out at room temperature with an integration time of 300 s.

1.3 Results and Discussion

The morphology of the carbonaceous thin films was investigated by scanning electron microscopy (SEM) at first, and very flat and pin-hole-free thin films of less than 1 μm thickness were observed. Figure 1.2 shows Raman spectra of carbonaceous thin films prepared using various rf powers of 10 - 90 W. Mainly two peaks appeared around 1350 and 1600 cm^{-1}, which have been known as Raman active A_{1g} and E_{2g} mode frequencies, respectively [6]. As shown in Fig. 1.2, the peaks around 1600 cm^{-1} become sharper with increasing applied rf power. The full width at half maximum of the peak around 1600 cm^{-1} is correlated with the crystallinity of carbon [7]. In addition, the peak positions shift toward 1580 cm^{-1} by increasing the applied rf power. Hence, these results indicate that the crystallinity of the carbonaceous thin films in this study increased with increasing applied rf power. However, when we focus on the peaks around 1350 cm^{-1}, their intensities are higher than those of the peaks around 1580 cm^{-1}, and these Raman spectra are very similar to that of non-graphitizable carbon [8]. From these results mentioned above, the carbonaceous thin films prepared in this study should contain both graphitizable and non-graphitizable structures.

Figure 1.3 shows the electrical conductivity of the carbonaceous thin films plotted against applied rf power. The conductivity was measured by 2-probe method. As is clear from Fig. 1.3, the conductivity of carbonaceous thin films increases with the rf power. Furthermore, the conductivity changes drastically at an rf power of 30 W. This change suggests that the crystallinity of the carbonaceous thin films should be improved, which is in good agreement with the Raman results. The electrical conductivity of the carbonaceous thin films prepared

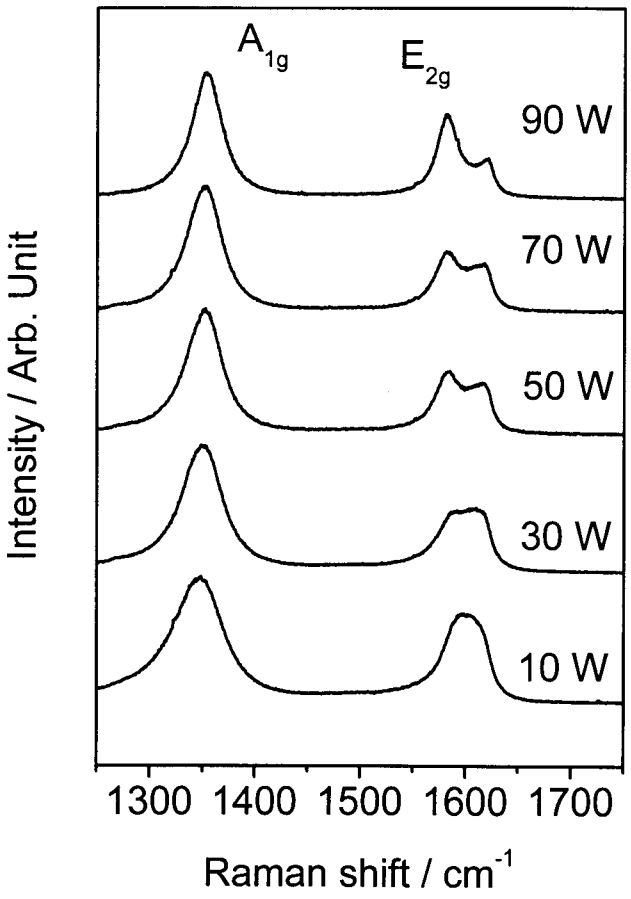

Fig. 1.2. Raman spectra of carbonaceous thin films prepared by plasma CVD. Applied rf powers; 10, 30, 50, 70, 90 W.

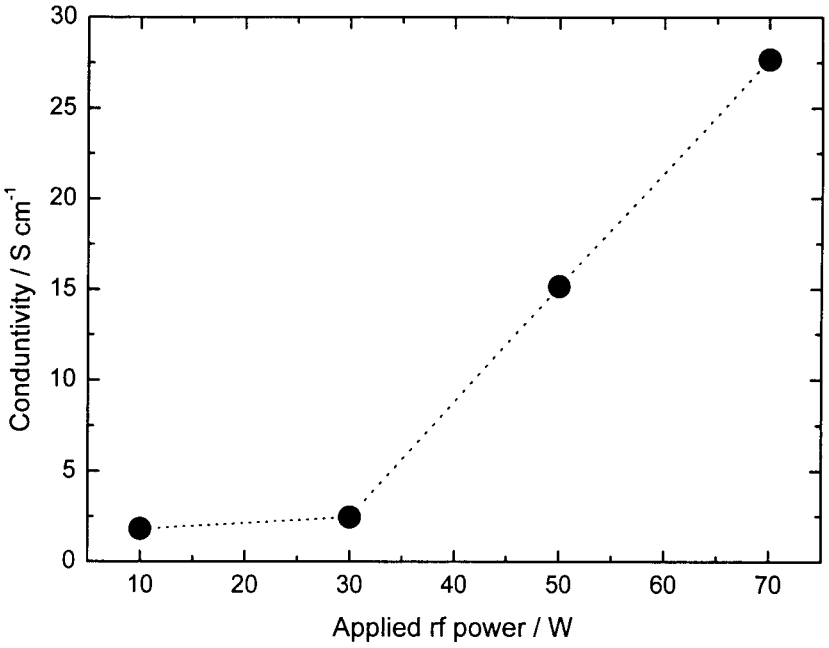

Fig. 1.3. The rf power dependence on conductivity of carbonaceous thin films prepared by plasma CVD.

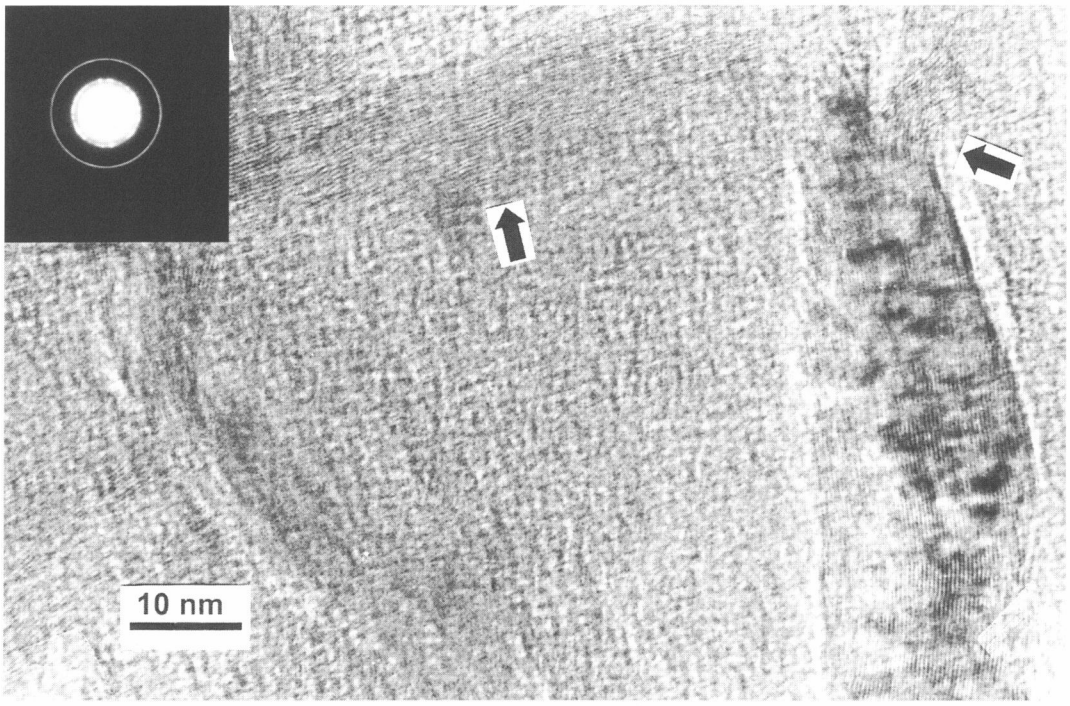

Fig. 1.4. TEM image of carbonaceous thin film prepared by plasma CVD. Applied rf power; 70 W.

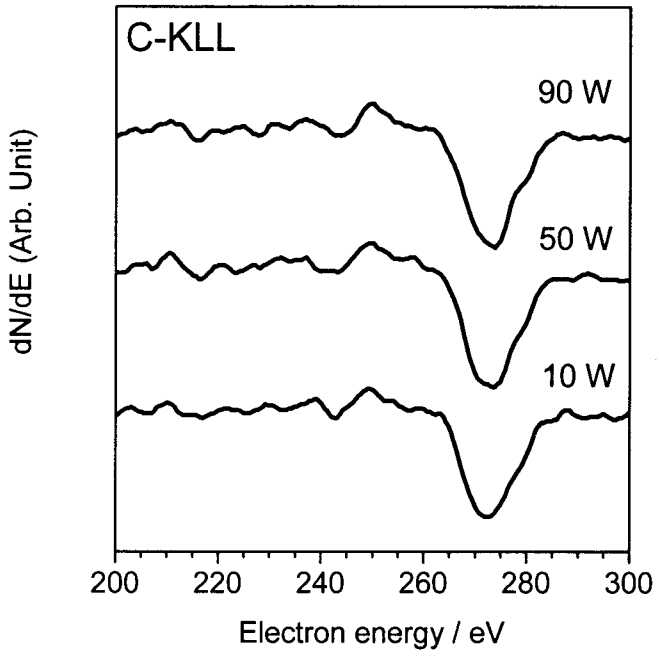

Fig. 1.5. Auger spectra from carbonaceous thin films prepared by plasma CVD. Applied rf powers; 10, 50, and 90 W.

above an rf power of 30 W is in the order of 10^1 S/cm. These values are as high as for carbonaceous films prepared by thermal CVD [9]. From the conductivity, the films prepared in the present work are not diamond-like carbon.

Figure 1.4 shows TEM images and the selected area electron diffraction (SAD) pattern of the carbonaceous thin films prepared using an rf power of 70 W. A graphitizable lamellar structure is observed in the TEM image. In addition, (002) and (10) rings can be observed in the SAD pattern. From this pattern, the value of d_{002} was evaluated to be 0.341 nm, indicating that the carbonaceous thin films were, to some extent, graphitized.

Figure 1.5 shows carbon KLL Auger spectra for the carbonaceous thin films prepared using different levels of applied rf powers. These spectra are very similar to that obtained for graphite [10]. From these spectra, the valence state of carbon atoms in the present samples was found to be sp^2 hybridization.

1.4 Conclusion

The sp^2-type carbonaceous thin films can be synthesized from acetylene and argon gases by using glow discharge plasma at 873 K, and the physical properties of these carbonaceous thin films are strongly dependent on the applied rf power.

References

1. N. Awaya and Y. Arita, *Jpn., J. Appl. Phys.*, **30**, 1813 (1991).
2. E. Kny, L. L. Levenson, W. J. James, and R. A. Auerbach, *Thin Solid Films*, **85**, 23 (1981).
3. J. C. Angus and C. C. Hayman, *Science*, **241**, 913 (1988).
4. J. C. Angus, J. E. Stultz, P. J. Shiller, J. R. MacDonald, M. J. Mirtich, and S. Domitz, *Thin Solid Films*, **118**, 311 (1984).
5. S. Matsumoto, *J. Mater. Sci. Lett.*, **4**, 600 (1985).
6. F. Tuinstra and J. L. Koenig, *J. Chem. Phys.*, **53**, 1126 (1970).
7. G. Katagiri, *Tanso*, **175**, 304 (1996). (in Japanese)
8. D. S. Knight and W. B. White, *J. Mater. Res.*, **4**, 385 (1989).
9. H. A. Yu, T. Kaneko, S. Otani, Y. Sasaki, and S. Yoshimura, *Carbon*, **36**, 137 (1998).

10. P. G. Lurie and J. M. Wilson, *Surface Sci.*, **65**, 476 (1977).

Chapter 2

Electrochemical properties of carbonaceous thin-film electrodes prepared by plasma-assisted chemical vapor deposition

2.1 Introduction

Lithium-ion batteries have been extensively studied because of their high performance and potentialities. Carbonaceous materials with sp^2-type structure have attracted much attention for use as negative electrodes of lithium-ion batteries. Among them, highly crystallized graphite has been employed as negative electrode for lithium-ion batteries in the commercial market. However, various carbonaceous materials have been extensively investigated so far as negative electrode materials to improve the performance of lithium-ion batteries [1-10].

Since carbonaceous materials are generally powders, binders are essential for preparation of electrodes, which makes us difficult to elucidate the precise electrochemical properties of the carbonaceous materials themselves. For the study of carbonaceous negative electrodes, thin films are very useful, because the thin films can be used as electrodes without binders and further it is easy for us to evaluate their surface area of electrodes. However, few studies employing carbonaceous thin films as negative electrodes of lithium-ion batteries have been made [10]. This is because there are some difficulties to prepare thin film electrode of sp^2-type carbonaceous materials due to low adherence on a substrate, etc.

A plasma is an ionized gas containing equal numbers of positive and negative charges, and a number of non-ionized neutral exited species. Glow discharge plasma is unique in that it can generate chemically very reactive species at low temperatures due to the non-equilibrium nature of the plasma state. Plasma assisted chemical vapor deposition (plasma CVD) has been used for the preparation of variety of inorganic materials [11, 12]. The chemical reactions are accelerated in plasma at low temperatures and plasma CVD can easily give dense and pin-hole-free films.

Synthesis of carbonaceous films by use of plasma CVD has been also carried out by many workers. However, most of these studies have been focused on preparation of diamond

films and/or diamond-like carbon films of sp^3-type structure as described in chapter 1 [13, 14], and little attention has been paid to a synthesis of sp^2-type carbonaceous thin films.

In this chapter, electrochemical properties of carbonaceous thin-film electrodes prepared by plasma CVD were studied by cyclic voltammetry (CV), charge-discharge measurements, and linear sweep voltammetry.

2.2 Experimental

Carbonaceous thin films were prepared by plasma CVD as described in chapter 1 [15]. The resultant carbonaceous thin films were characterized by scanning electron microscopy (SEM, Hitachi S-510) and Raman spectroscopy. The Raman spectra were excited by using a 514.5 nm line (50 mW) of an argon ion laser (NEC, GLG3260), and the scattered light was collected in a backscattering geometry. All spectra were recorded using a spectrometer (Jobin-Yvon, T64000) equipped with a multi-channel CCD detector. Each measurement was carried out at room temperature with an integration time of 300 s.

A three-electrode electrochemical cell was used to employee the electrochemical measurements. Lithium metal was used as counter and reference electrodes, and the electrolyte solution was a mixture (1:1 by volume) of ethylene carbonate (EC) and diethyl carbonate (DEC) containing 1 mol dm^{-3} $LiClO_4$ (battery grade by Mitsubishi Petrochemical Company, Limited). The cell was assembled in an argon-filled glove box. Electrochemical properties were examined by cyclic voltammetry and linear sweep voltammetry (RADIOMETER, VoltaLab 32) and charge-discharge measurements using a battery test system (Hokuto Denko, HJ101SM6). Unless otherwise stated, potential was described vs. Li / Li^+.

2.3 Results and Discussion

Figure 2.1 shows a typical SEM image of carbonaceous thin film prepared by plasma CVD at 10 W. From the image, surface of carbonaceous thin film was very flat and free from pin-hole. The film thickness was determined to be less than 1 μm by cross section of SEM image. Carbonaceous thin films prepared using other rf powers also gave the similar surface morphologies to that using an rf power of 10 W.

The Raman spectra of carbonaceous thin films are shown in Fig. 2.2. Mainly three

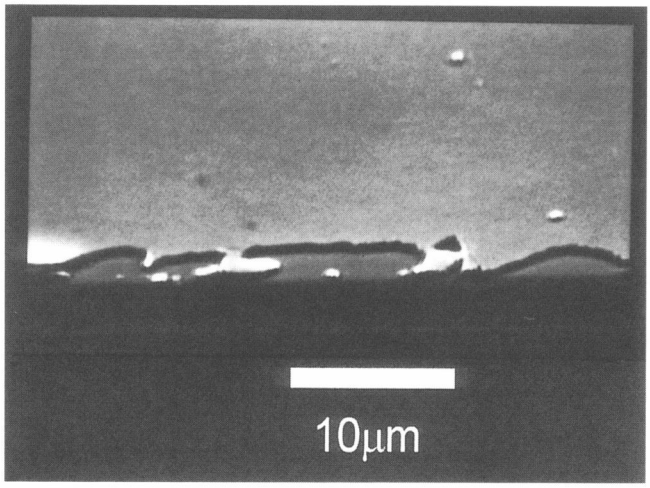

Fig. 2.1. SEM image of carbonaceous thin film prepared by plasma CVD. Reaction time; 6 h, substrate; Pyrex® glass, and applied rf power; 10 W.

peaks around 1360, 1580 and 1620 cm^{-1} were observed. The peak around 1580cm^{-1} is well known to be related with crystallinity of carbonaceous materials, and is assigned to Raman active E_{2g} mode frequency (G band) [16]. The peak around 1360 cm^{-1} is ascribed to Raman inactive A_{1g} mode frequency [16]. Peaks around 1360 and 1620 cm^{-1} appear in the case of finite crystal size and imperfection of carbonaceous materials [17], and the former is called as D band and the latter is as D' band. As is given in Fig. 2.2, the peak around 1580 cm^{-1} of G band became sharper and its position shifted toward 1580 cm^{-1} with increasing the applied rf power. Full width at half maximum (FWHM) of the peak around 1580 cm^{-1} was reported to be correlated with crystallinity of carbonaceous materials [17], and single crystal of graphite gives only one peak around 1580 cm^{-1}. Hence, the result in Fig. 2.2 indicates that crystallinity of the samples increased with increasing the applied rf power, which was also confirmed by the conductivity measurements [15]. The important point of the spectra was that crystallinity of carbonaceous thin film can be easily changed by the applied rf power at fixed temperature as low as 873 K. In other words, high rf power plasma results in the high electron temperature, leading to large energy transfer to carbonaceous thin film at fixed temperature. In Raman spectra, peak intensities around 1360 cm^{-1} are higher than those around 1580 cm^{-1}. This feature indicates that the thin films contained non-graphitized carbon to some extent [18]. From this result, carbonaceous thin films in this study were composed of the graphitized structures with partly non-graphitized structures.

Figure 2.3 shows cyclic voltammograms of carbonaceous thin-film electrode prepared at 90 W. The cyclic voltammogram was measured with a sweep rate of 1 mV/s in the potential range of 0 to 3 V. For the first sweep, large irreversible reduction was observed from the potential around 1.5 to 0.5 V. However, it almost disappeared after the second sweep as is evident from Fig. 2.3. These results indicate that the decomposition of solvent and formation of solid electrolyte interface (SEI) on the surface of carbonaceous thin-film electrodes should occur effectively [19, 20]. For all the carbonaceous thin-film electrodes prepared at any rf powers, large reduction currents at around 1.5 - 0.5 V appeared at the first cycle of cyclic voltammograms.

Figure 2.4 shows cyclic voltammograms at the second sweep for carbonaceous thin-film electrodes prepared by rf powers of 10 W and 90 W. Electrochemical properties were found to be different between carbonaceous thin-film electrodes prepared at 10 W and

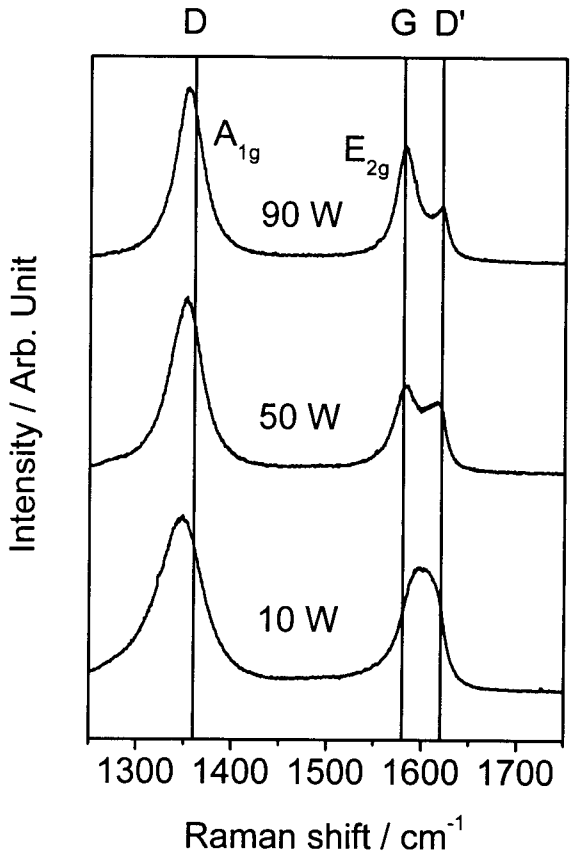

Fig. 2.2. Raman spectra of carbonaceous thin films prepared by plasma CVD. Reaction time; 6 h, substrate; Ni, and applied rf power; 10, 50, and 90 W.

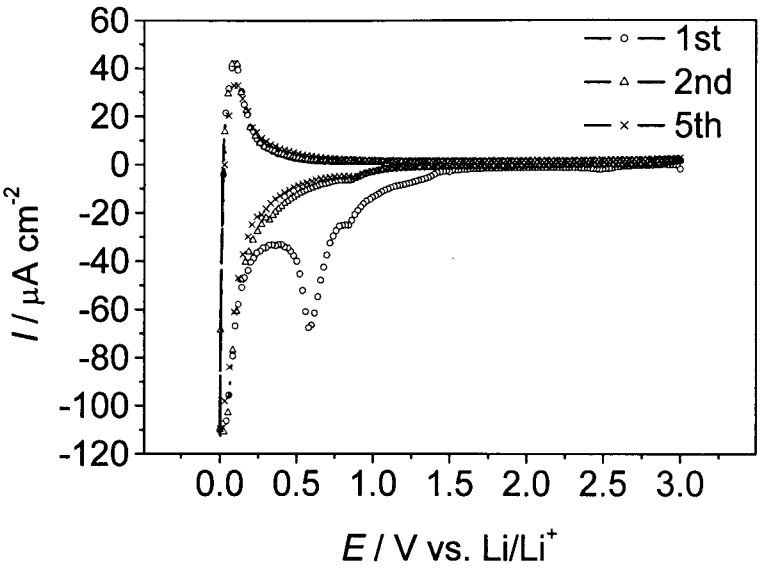

Fig. 2.3. Cyclic voltammograms of carbonaceous thin-film electrode in 1 mol dm^{-3} $LiClO_4$/EC+DEC (1:1). Sweep rate; 1 mV/s. Reaction time; 6 h, substrate; Ni, and applied rf power; 90 W.

90 W as shown in Fig. 2.4. In the oxidation process, the peak of carbonaceous thin-film electrode prepared at 90 W was sharp and had clear shoulder around 0.1 - 0.2 V as shown by an arrow in insertion, while, the peak was broad and did not have such clear shoulder for the film prepared at 10 W. In the reduction process, the peak at 90 W had a clear shoulder around 0.1 V as shown by an arrow in insertion, but the peak near 0 V for the film prepared at 10 W was very smooth. These results were correlated with the formation of stage structures of Li-GICs [21]. The difference of the shape of cyclic voltammograms were also related with Raman spectra shown in Fig. 2.4, that is, crystallinity of the thin film prepared at 90 W was higher than that of the thin film prepared at 10 W. In other words, the degree of crystallinity of the carbonaceous thin films affected the shapes of cyclic voltammograms. From the above results, the intercalation and de-intercalation behavior of carbonaceous thin-film electrodes was found to be dependent on the applied rf powers. In addition, lithium-ion insertion and extraction can occur in propylene carbonate (PC) solution, as well as in the mixed solution of EC and DEC [22].

Figure 2.5(a) shows charge and discharge characteristics of carbonaceous thin-film electrode prepared at 10 W. At the first cycle (inset figure), very large irreversible capacity above 0.5 V appeared. The large irreversible capacity is also reported for other carbonaceous materials [23]. This irreversible capacity decreased dramatically after the second cycle. Insertion curve of sample prepared at 10 W showed about 1100 mAh/g of capacity at the second cycle and extraction curve showed about 600 mAh/g. In the extraction curves, a comparatively large potential plateau appeared at approximately 1 V. These results indicated that the electrochemical properties of carbonaceous thin-film electrode prepared at 10 W was very similar to those for graphitizable carbon heat-treated at lower temperatures [24]. Figure 2.5(b) shows charge and discharge characteristics of carbonaceous thin-film electrode prepared at 90 W. At the first cycle (inset figure), very large irreversible capacity above 0.5 V also appeared as is observed for the film prepared at 10 W. Insertion curve of sample prepared at 90 W showed about 350 mAh/g of capacity at the second cycle and extraction curve showed about 200 mAh/g. On extraction curves, very small potential plateau appeared at approximately 1 V. A small plateau appeared below the potential of 0.25 V. In the case of graphite, lithium-ion de-intercalation from Li-GIC takes place below 0.25 V [24] and therefore this result should be correlated with the formation of stage structures of Li-GIC.

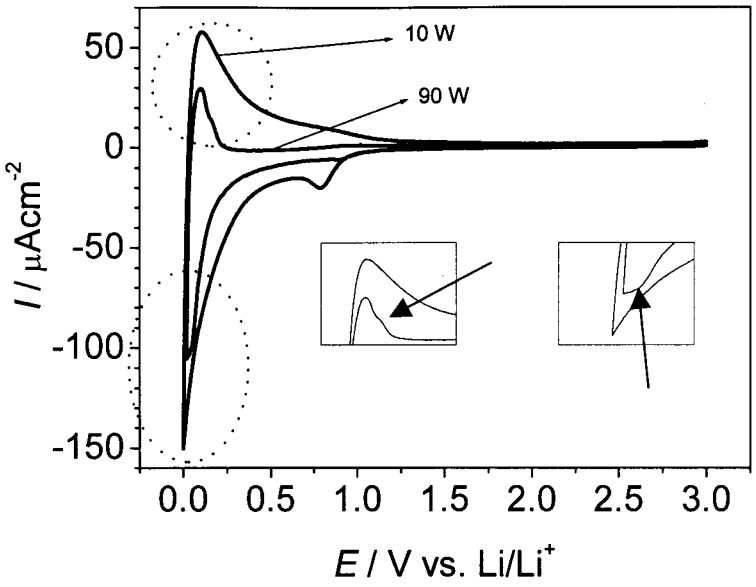

Fig. 2.4. Cyclic voltammograms (2nd cycle) of carbonaceous thin-film electrodes in 1 mol dm^{-3} $LiClO_4$/EC+DEC (1:1). Sweep rate; 1 mV/s. Applied rf power; 10 and 90 W.

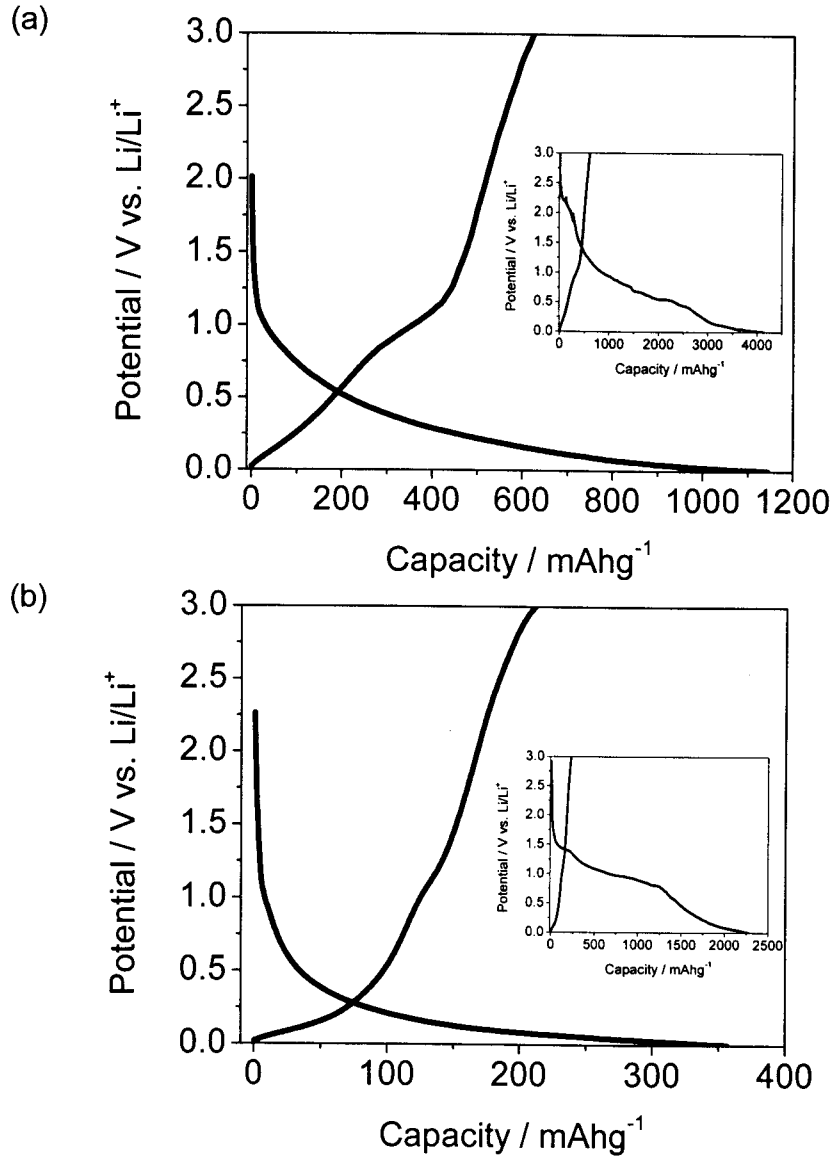

Fig. 2.5. Charge and discharge characteristics (2nd cycle) of carbonaceous thin-film electrodes in 1 mol dm^{-3} $LiClO_4$/EC+DEC (1:1). Applied rf power; (a) 10 W and (b) 90 W. The inset figure is charge and discharge characteristics of 1st cycle.

From these results, charge and discharge characteristics showed similar tendency to the results of cyclic voltammograms for carbonaceous thin-film electrodes in this study. The ratio of capacity in the potential range 0 to 0.25 V to that in the range 0.25 to 3 V was evaluated to be 0.185 for sample at 10 W and 0.498 for sample at 90 W. Tatsumi et al. reported that this ratio of capacity became large with increasing in crystallinity of MCMBs [26]. Hence, the present results of charge-discharge measurements support that the high rf power gave a thin film of high crystallinity.

As is mentioned above, the electrochemical behaviors for lithium-ion insertion and extraction for the present carbonaceous thin-film electrodes are different from those for graphite, but are similar to those for graphitizable carbon heat-treated at lower temperatures [24]. To examine the details of lithium-ion insertion and extraction of the carbonaceous thin-film electrodes, cyclic voltammetry was conducted at various sweep rates. Figures 2.6(a) - 2.6(d) show cyclic voltammograms at the second sweep of sample prepared at 10 W. Sweep rates are (a) 10 mV/s, (b) 1 mV/s, (c) 0.1 mV/s and (d) 0.01 mV/s. As given in Fig. 2.6, change of sweep rate influences not only on values of magnitudes of current but also on shapes of cyclic voltammograms; peak of oxidation current around 0.1 - 0.2 V is relatively large and that around 0.9 - 1.0 V is very small at higher sweep rates, while peak around 0.1 - 0.2 V is small and peak around 0.9 - 1.0 V is large at lower sweep rates. By considering the previous literature [24], oxidation peaks around 0.1 - 0.2 V denoted to A in Fig. 2.6 are due to lithium de-intercalation stored in graphene layers and that peaks around 0.9 - 1.0 V, denoted to B are ascribed to lithium-ion extraction stored in some sites except for graphene layers. In Fig. 2.6, the ratio of peak B to peak A increases with decreasing the sweep rates. Similar tendency was obtained for the sample prepared at 90 W. These results mean that extraction of a potential around 0.9 - 1.0 V is kinetically influenced. This is also obvious by charge-discharge measurements obtained at different current densities as shown in Fig. 2.7. Figure 2.7 shows charge and discharge characteristics at 2nd cycle of carbonaceous thin-film electrodes prepared at 10 W by two current densities (a) 263 mA/g and (b) 26.0 mA/g. In Fig. 2.7, the capacity of (a) is very different from that of (b). This is because the current density for (a) is so large that utilization efficiency of carbonaceous thin-film electrode becomes small, leading to smaller capacity of (a) than that of (b). There is no plateau at around 1 V for extraction curve in Fig. 2.7(a), while a clear plateau can be seen in Fig. 2.7(b), indicating that no

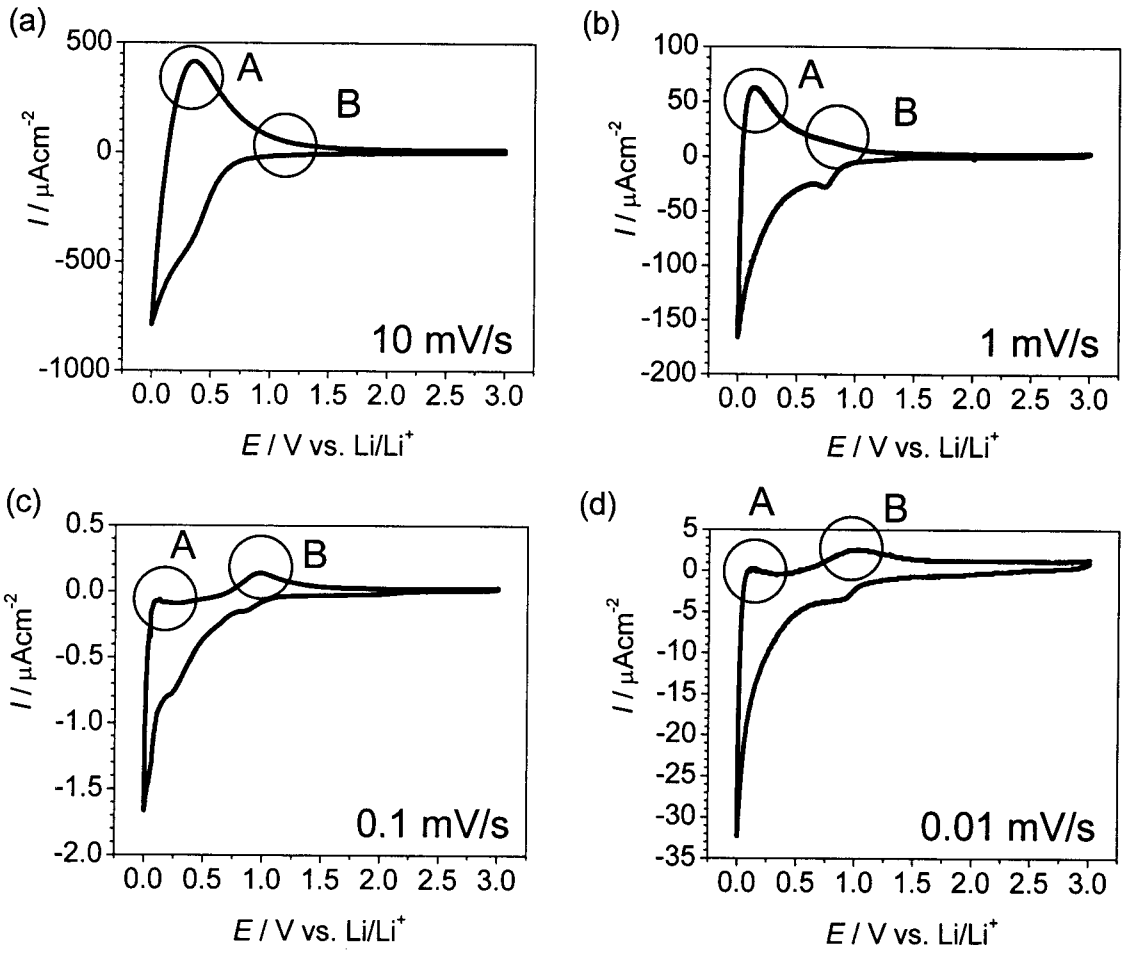

Fig. 2.6. Cyclic voltammograms (2nd cycle) of carbonaceous thin-film electrodes prepared by plasma CVD. Applied rf power; 10 W. Sweep rate; (a) 10 mV/s, (b) 1 mV/s, (c) 0.1 mV/s, and (d) 0.01 mV/s.

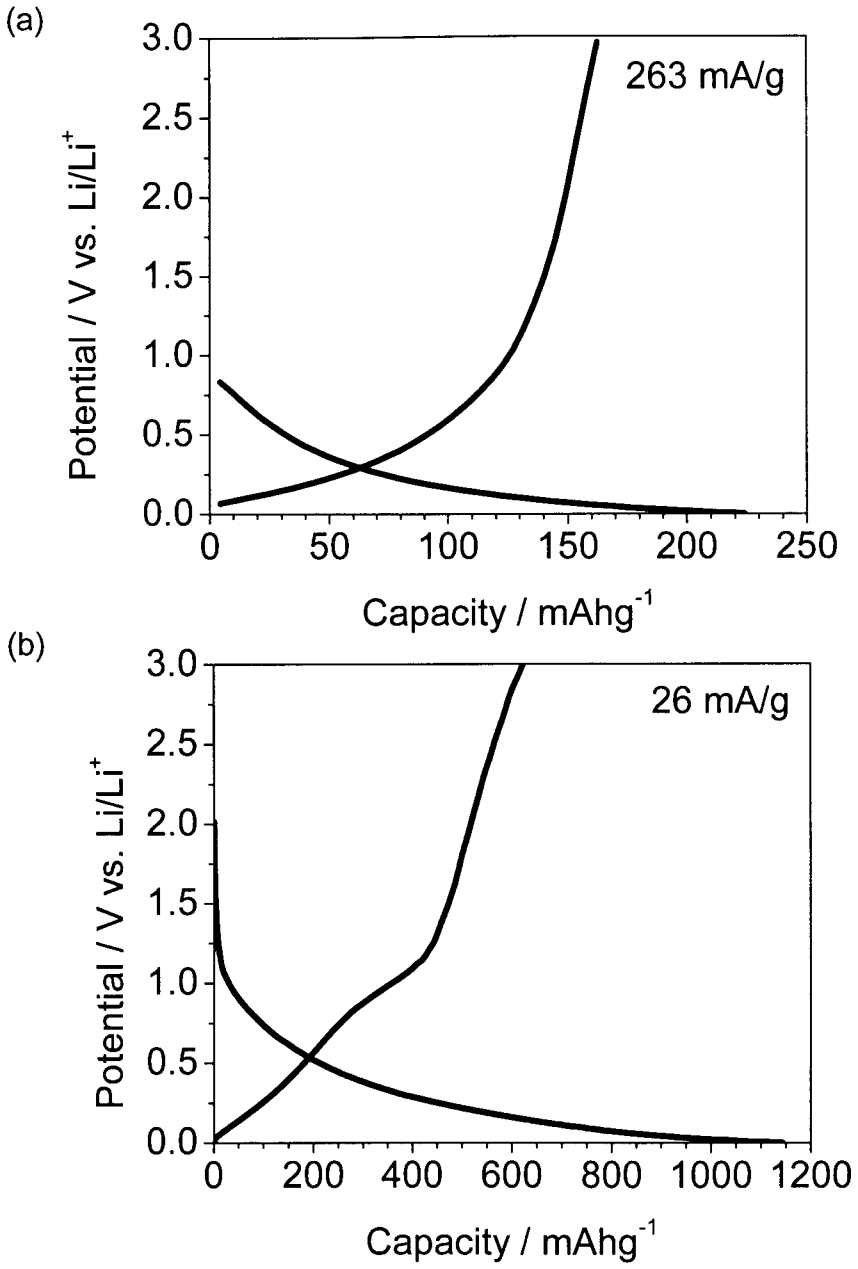

Fig. 2.7. Charge and discharge characteristics of carbonaceous thin-film electrodes at the 2nd charge-discharge cycle in 1 mol dm^{-3} $LiClO_4$/EC+DEC (1:1). Applied rf power; 10 W. Current density; (a) 263 mA/g and (b) 26.0 mA/g.

capacity around 1 V is available for the large current densities, which is in good agreement with results as given in Figs. 2.6(a) – 2.6(d).

Next, the lithium-ion entities, which can be extracted at around 1 V, are focused by linear sweep voltammetry. Lithium-ion was inserted by sweeping the electrode potentials from 3.0 V to 0.3, 0.1 and 0 V, followed by keeping the above potentials for 10 h, and then the potential was reversibly swept linearly to 3.0 V. Figure 2.8 shows positive linear sweep voltammograms of carbonaceous thin-film electrodes prepared at 10 W with a sweep rate of 0.1 mV/s. As shown in Fig. 2.8, the electrodes kept at 0.1 V (dashed line) and 0.3 V (dotted line) did not give any peak at around 1 V, while the electrode kept at 0 V (solid line) exhibited a clear peak around 1 V.

The above results indicated that lithium-ion inserted into the carbonaceous thin-film electrodes at 0 V can be extracted both at about 0 V and 1 V. If the lithium-ion insertion and extraction was a simple redox reaction, the reduction peak at about 1 V should appear even at the higher sweep rate (Fig. 2.6a), but it was not the case. Thus the present lithium-ion insertion and extraction are not a simple reaction, which led us to consider another lithium-ion insertion and extraction mechanism. The above discussion leads to the fact that transfer of lithium ion from A site to B site is necessary for lithium ion to insert into B site. Otherwise lithium ion must directly insert into B site. However, linear sweep voltammetry clear shows that no lithium-ion insertion at around 1 V occurred. Figures 2.6 and 2.7 clearly show that the lithium-ion extraction from B site only occurs at the lower sweep rate and smaller current density, indicating that activation energy should be large for lithium-ion transfer from A site to B site and that the transfer is a slow reaction. In other words, B site occupied by lithium ion is thermodynamically more stable than A site, which is in excellent agreement with the literatures [27, 28].

To further clarify that lithium-ion extraction from B site is a slow process, linear sweep voltammetry with different sweep rates was conducted. Prior to linear sweep voltammetry, the carbonaceous thin-film electrode was scanned from 3 V to 0 V, and held at these potential of 0 V for 10 h. Figure 2.9 shows linear sweep voltammograms of carbonaceous thin-film electrode prepared at 10 W at two sweep rates of 0.1 mV/s (2nd cycle, solid line) and 1 mV/s (3rd cycle, dotted line). Each voltammogram is normalized by maximum peak height. A broad peak appeared near 1 V at the sweep rate of 0.1 mV/s, while

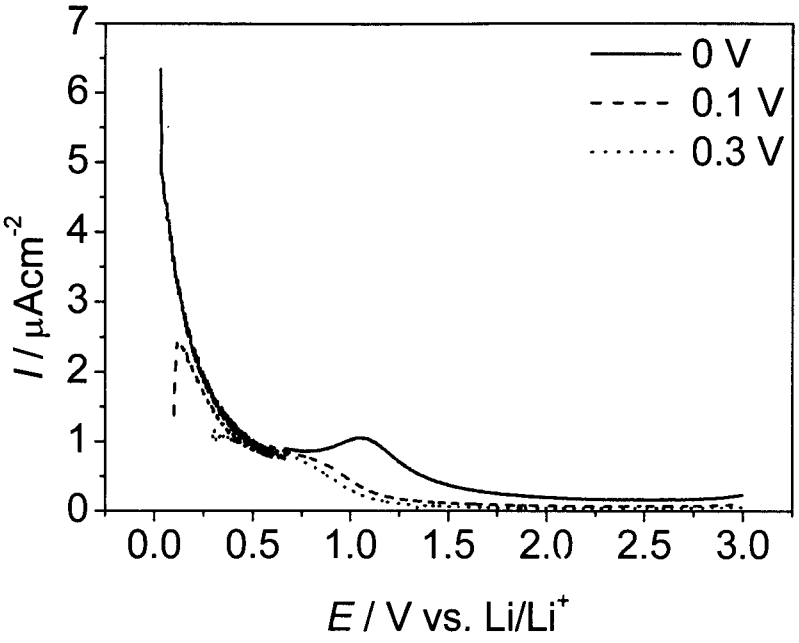

Fig. 2.8. Linear sweep voltammograms (2nd sweep) of carbonaceous thin-film electrodes prepared by plasma CVD in 1 mol dm^{-3} $LiClO_4$/EC+DEC (1:1). Applied rf power; 10 W. Sweep rate; 0.1 mV/s.

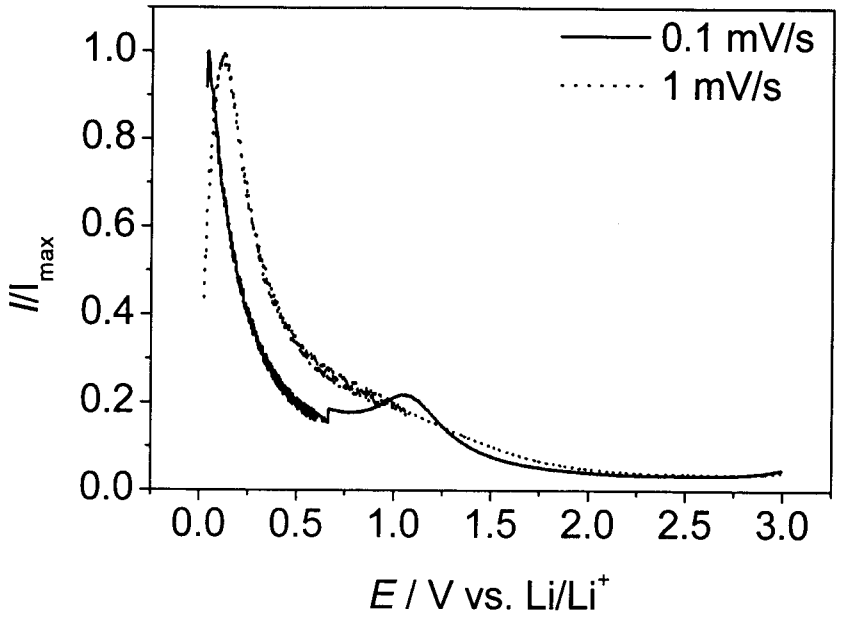

Fig. 2.9. Linear sweep voltammograms of carbonaceous thin-film electrode prepared by plasma CVD in 1 mol dm^{-3} $LiClO_4$/EC+DEC (1:1). Applied rf power; 10 W. Sweep rates are 0.1 mV/s for 2nd cycle and 1 mV/s for 3rd cycle. Each voltammograms is normalized by maximum peak height.

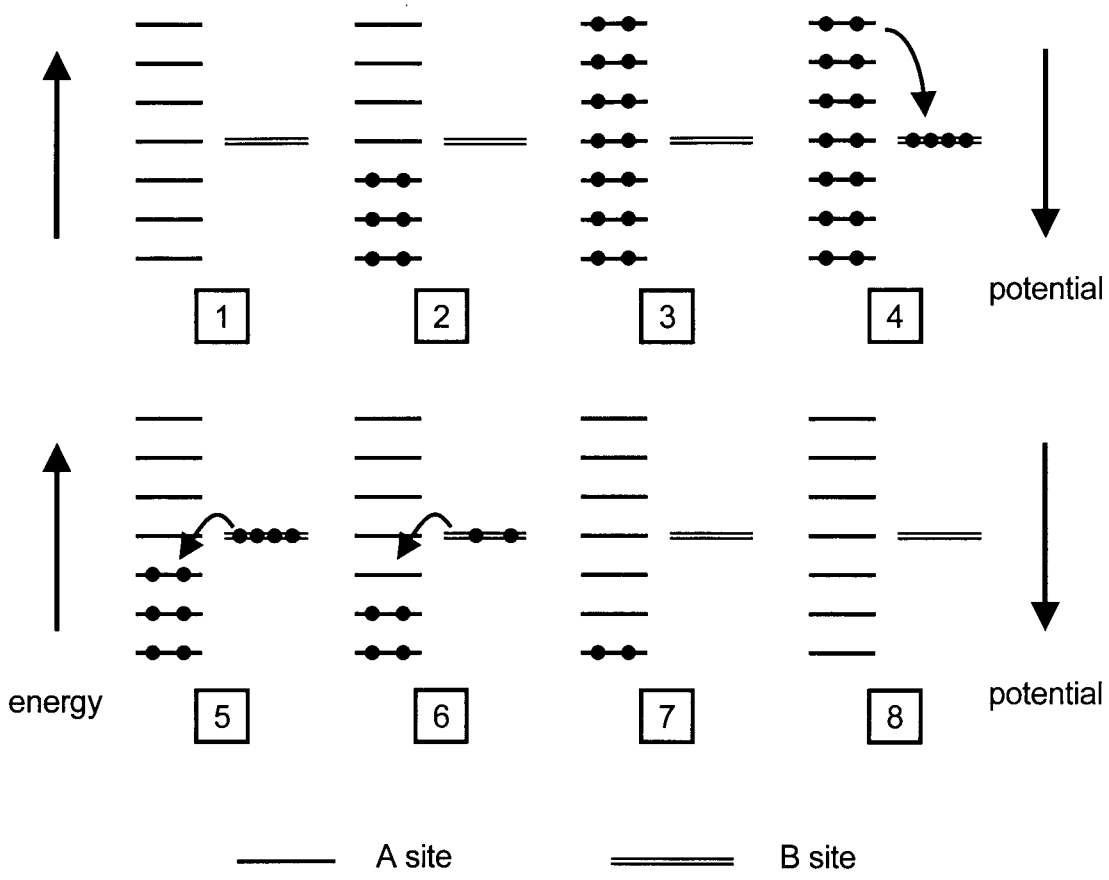

Fig. 2.10. An energy state model to explain lithium-ion insertion and extraction of carbonaceous thin-film electrodes.

no peak appeared at the rate of 1 mV/s. This result indicates that no lithium-ion extraction from B site occurs at high sweep rate, leading to the conclusion again that lithium-ion extraction from B site is a slow process.

The above results suggest that there should be an activation process of lithium-ion transfer from A site to B site. Insertion and extraction mechanism in the present work can be summarized by Fig. 2.10. Here, vertical axis represents the total energy against reaction coordinates. At first, lithium ion inserts into A site as shown by Fig. 2.10(2). After the A site is mostly filled by lithium ion, the electrode potential should reach about 0 V and the transfer of lithium ion from A site to B site occurs, probably accompanying by heat generation due to the energy gap between A site and B site (Fig. 2.10(3), (4)) [28]. During lithium-ion transfer from A site to B site, lithium-ion insertion into A site through electrolyte occurs simultaneously. Finally, A site and B site are filled with lithium ion. As is shown in Fig. 2.10(5), A site filled with lithium ion is thermodynamically more unstable than B site filled with lithium, and hence lithium-ion extraction proceeds from A site. When the lithium-ion extraction from A site occurs, the electrode potential for A site becomes more positive, and then, A site becomes thermodynamically more stable than B site filled with lithium ion. And then lithium ion is extracted from B sites (Fig. 2.10(6)). There are two possible routes for lithium-ion extraction from B site. One route is that lithium ion extract directly from B site with a slow process. Another route is that lithium ion transfers from B site to A site again accompanying by heat generation again and is extracted through A site. Inaba et al. revealed the reasons of hysteresis in the charge-discharge profiles of mesocarbon microbeads heat-treated at lower temperatures by calorimetric study [29]. They observed heat generation during lithium-ion extraction [29]. Hence, the latter route is more probable.

The above mechanism for lithium-ion insertion and extraction is in good agreement with that reported by Zheng et al. [30]. In the case of large current densities, lithium-ion insertion and extraction proceeds by 1→2→3→7→8. For small current densities and keeping 0 V for enough time, the reaction of lithium ion and carbonaceous thin-film electrodes occurs by 1→2→3→4→5→6→7→8.

2.4 Conclusion

Carbonaceous thin films were prepared by C_2H_2 / Ar glow discharge plasma.

Carbonaceous thin films in this study were homogeneous and pin-hole-free. The rf power of plasma was found to influence on the crystallinity of carbonaceous thin films. The lithium-ion storage into different sites for the carbonaceous thin-film electrodes was clarified by using cyclic voltammetry, charge-discharge measurements, and linear sweep voltammetry. Carbonaceous materials give various electrochemical properties for use in lithium-ion batteries, and our present carbonaceous thin-film electrodes can be regarded as a model of carbonaceous materials heat-treated at lower temperatures.

References

1. J. R. Dahn, T. Zheng, Y. Liu, and J. S. Xue, *Science*, **270**, 590 (1995).
2. J. R. Dahn, A. K. Sleigh, H. Shi, J. N. Reimers, Q. Zhong, and B. M. Way, *Electrochim. Acta*, **38**, 1179 (1993).
3. N. Imanishi, H. Kashiwagi, T. Ichikawa, Y. Takeda, O. Yamamoto, and M. Inagaki, *J. Electrochem. Soc.*, **140**, 315 (1993).
4. I. Mochida, C.-H. Ku, S.-H. Yoon, and Y. Korai, *J. Power Sources*, **75**, 214 (1998).
5. T. Zheng, J. S. Xue, and J. R. Dahn, *Chem. Mater.*, **8**, 389 (1996).
6. M. Inaba, Z. Shiroma, A. Funabiki, and Z. Ogumi, *Langmuir*, **12**, 1535 (1996).
7. M. Inaba, H. Yoshida, Z. Ogumi, T. Abe, Y. Mizutani, and M. Asano, *J. Electrochem. Soc.*, **142**, 20 (1995).
8. M. Inaba, H. Yoshida, and Z. Ogumi, *J. Electrochem. Soc.*, **143**, 2572 (1996).
9. Y.-S. Han, J.-S. Yu, G.-S. Park, and J.-Y. Lee, *J. Electrochem. Soc.*, **146**, 3999(1999).
10. M. Mohri, N. Yanagisawa, Y. Tajima, T. Tanaka, T. Mitate, S. Nakajima, M. Yoshida, M. Yoshimoto, T. Suzuki, and H. Wada, *J. Power Sources*, **26**, 545 (1989).
11. N. Awaya and Y. Arita, *Jpn. J. App. Phys.*, **30**, 1813 (1991).
12. E. Kny, L. L. Levenson, W. J. James, and R. A. Auerbach, *Thin Solid Films*, **85**, 23 (1981).
13. S. Matsumoto, *J. Mater. Sci. Lett.*, **4**, 600 (1985).
14. J. C. Angus and C. C. Hayman, *Science*, **241**, 913 (1988).
15. T. Abe, T. Fukutsuka, M. Inaba, and Z. Ogumi, *Carbon*, **37**, 1165 (1999).
16. F. Tuinstra and J. L. Koenig, *J. Chem. Phys.*, **53**, 1126 (1970).

17. G. Katagiri, *Tanso*, **175**, 304 (1996).
18. D. S. Knight and W. B. White, *J. Mater. Res.*, **4**, 385 (1989).
19. E. Peled, *J. Electrochem. Soc.*, **126**, 2047 (1979).
20. J. O. Besenhard, M. Winter, J. Yang, and W. Biberacher, *J. Power Sources*, **51**, 228 (1995).
21. R. Takagi, T. Okubo, K. Sekine, and T. Takamura, *Denki Kagaku* (presently *Electrochemistry*), **65**, 333 (1997).
22. T. Fukutsuka, T. Abe, M. Inaba, Z. Ogumi, Y. Matsuo, and Y. Sugie, *Carbon Science*, **1**, 129 (2001).
23. I. Mochida, C.-H. Ku, M. Egashira, and M. Kimura, *Denki Kagaku* (presently *Electrochemistry*), **66**, 1281 (1998).
24. A. Mabuchi, K. Tokumitsu, H. Fujimoto, and T. Kasuh, *J. Electrochem. Soc.*, **142**, 1041 (1995).
25. T. Ohzuku, Y. Iwakoshi, and K. Sawai, *J. Electrochem. Soc.*, **140**, 2490 (1993).
26. K. Tatsumi, N. Iwashita, H. Sakaebe, H. Shioyama, S. Higuchi, A. Mabuchi, and H. Fujimoto, *J. Electrochem. Soc.*, **142**, 716 (1995).
27. S-J. Lee, T. Itoh, M. Nishizawa, K. Yamada, and I. Uchida, *Denki Kagaku* (presently *Electrochemistry*), **66**, 1276 (1998).
28. S.-J. Lee, M. Nishizawa, and I. Uchida, *Electrochim. Acta*, **44**, 2379 (1999).
29. M. Inaba, M. Fujikawa, T. Abe, and Z. Ogumi, *J. Electrochem. Soc.*, **147**, 4008 (2000).
30. T. Zheng, W. R. McKinnon, and J. R. Dahn, *J. Electrochem. Soc.*, **143**, 2137 (1996).

Chapter 3

Preparation and electrochemical properties of carbonaceous thin films prepared by C_2H_4/NF_3 glow discharge plasma

3.1 Introduction

Plasma-assisted chemical vapor deposition (plasma CVD) has been used for the preparation of inorganic materials [1], mainly because the chemical reactions are accelerated in plasma at low temperature and the resultant films prepared by plasma CVD are dense and pin-hole-free. In previous chapters, carbonaceous thin films were prepared from acetylene (C_2H_2) [2].

For the preparation of carbonaceous thin films by the pyrolysis of hydrocarbon gases, extraction of hydrogen atoms from the hydrocarbon is an essential process. In this sense, the introduction of NF_3 gas may be effective for the extraction of hydrogen atoms, since NF_3 can release fluorine radicals in plasma as is expressed by the following reaction [3, 4];

$$NF_3 \rightarrow NF_2\bullet + F\bullet$$

Fluorine radicals may act as a scavenger of hydrogen atom.

In this chapter, carbonaceous thin films were prepared by C_2H_4 and NF_3 plasma, and the resultant thin films were characterized by scanning electron microscopy (SEM), Raman spectroscopy, and X-ray photoelectron spectroscopy (XPS), and then the electrochemical properties of the carbonaceous thin-film electrodes were investigated.

3.2 Experimental

Figure 3.1 shows a schematic diagram of plasma CVD apparatus used in this chapter. The starting materials were ethylene as a carbon source, argon as a plasma assist gas and NF_3 gas (SHOWA DENKO Co., Ltd.) as a fluorine radical source. The substrates were placed on the ground electrode whose temperature was kept at 773 K. Carbonaceous thin films were deposited on substrates of nickel and Pyrex® glass sheet. Glow discharge plasma was

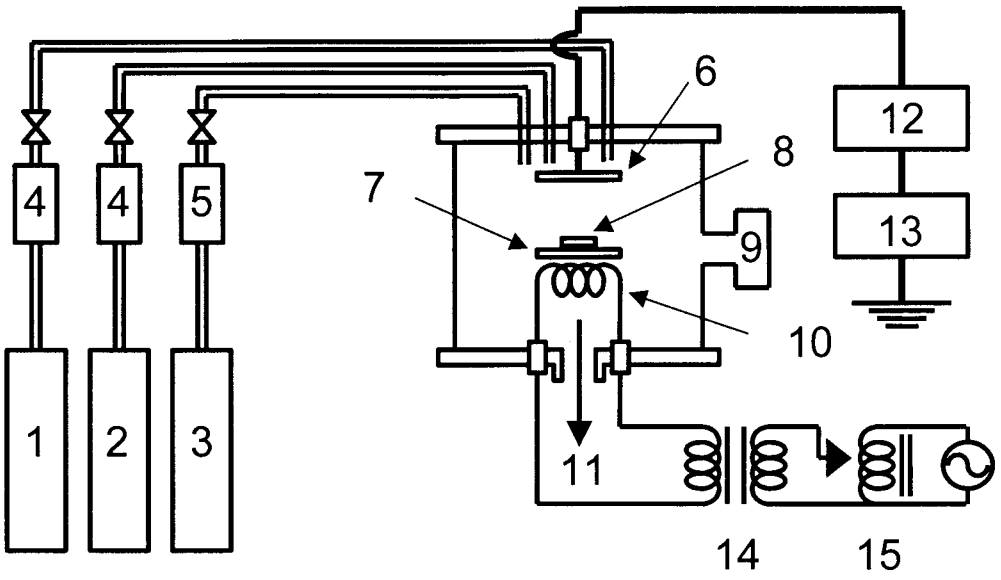

Fig. 3.1. Schematic diagram of carbonaceous thin film deposition apparatus. 1; Ar; 2; C_2H_4, 3; NF_3, 4; flow meter, 5; mass flow meter, 6; rf electrode, 7; ground electrode, 8; substrate, 9; Pirani gauge, 10; tungsten heater, 11; pump unit, 12; impedance matching unit, 13; 13.56 MHz power generator, 14; trans former, 15; slidac®.

generated between rf and ground electrodes by a rf power supply of 13.56 MHz, and the applied rf power was kept at 50 W. The flow rates of argon and ethylene were set at 20 and 10 sccm, respectively, and that of NF_3 was changed from 0 to 20 sccm. The total pressure of reaction chamber was kept at 133 Pa.

The resultant carbonaceous thin films were characterized by Raman spectroscopy and XPS. SEM was used to investigate the surface morphology of carbonaceous thin films. The Raman spectra were excited by using a 514.5 nm line (50 mW) of an argon ion laser, and the scattered light was collected in a backscattering geometry. All spectra were recorded using a spectrometer (Jobin-Yvon, T64000) equipped with a multi-channel CCD detector. Each measurement was carried out at room temperature with an integration time of 300 or 600 s. A Kratos ESCA 1000 electron spectrometer equipped with AlKα X-ray radiation (1400 eV) was used for surface analysis of the carbonaceous thin films. To obtain the depth profile of the film by XPS, the surface was sputtered with an argon ion beam. Experimental conditions were 8 kV and 30 mA (AlKα line).

A three-electrode electrochemical cell was used to employee the electrochemical measurements. Lithium metal was used as counter and reference electrodes, and the electrolyte solution was 1:1 by volume mixture of ethylene carbonate (EC) and diethyl carbonate (DEC) containing 1 mol dm^{-3} $LiClO_4$ (battery grade by Mitsubishi Petrochemical Co, Ltd). The cell was assembled in an argon-filled glove box. Cyclic voltammetry was carried out in the potential range of 0.020 to 3 V vs. Li/Li^+ at a sweep rate of 5 mV/s. Electrochemical lithium insertion (discharge) and extraction (charge) were carried out at a constant current of 26 mA/g in the voltage range of 0 to 3 V.

3.3 Results and Discussion

Figure 3.2 shows a SEM image of carbonaceous thin film prepared by plasma CVD at the flow rate of NF_3 of 15 sccm. From SEM image, surface of carbonaceous thin film was very flat and pin-hole-free as compared with that of carbonaceous thin films without using plasma. The film thickness was less than 1 μm. The surface area of this thin film can be evaluated almost exactly because of this flat morphology.

Since thickness of the resultant thin films were too thin to obtain clear X-ray diffraction patterns, the crystallinity of the thin films was studied by Raman spectroscopy. The

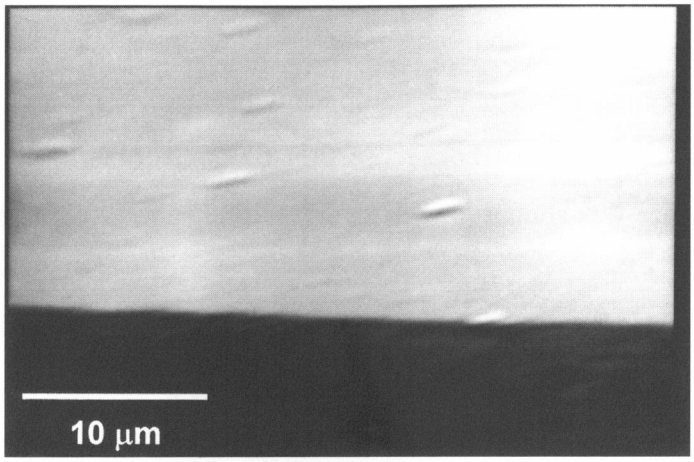

Fig. 3.2. SEM image of carbonaceous thin film prepared by plasma CVD. Flow rate of NF_3; 15 sccm, substrate; Pyrex® glass, and applied rf power; 50 W.

Raman spectra of carbonaceous thin films are shown in Fig. 3.3. Mainly two peaks around 1350 and 1600 cm^{-1} were observed. These peaks have been known as Raman active A_{1g} (due to finite crystal size) and E_{2g} (due to infinite crystal size) mode frequencies, respectively [5]. The peak around 1620 cm^{-1} is also derived from imperfection of graphite crystal [6]. Intense peaks around 1555 cm^{-1} are due to oxygen. As is shown in Fig. 3.3, the shapes of Raman spectra are affected by the flow rates of NF_3. In particular, the spectrum of carbonaceous thin film prepared at NF_3 of 0 sccm is different from that of 15 sccm, in other word, the intensity of the peak around 1360 cm^{-1} (I_{1360}) is higher than that around 1580 cm^{-1} (I_{1580}) of 0 sccm, however, opposite result is observed at the sample prepared by the NF_3 rate of 15 sccm. The former spectrum is similar to that of non-graphitizable carbon [7], and the latter one is similar to that of graphitizable carbon [7]. From the above results, the formation mechanism of carbonaceous thin films may be affected by the flow rate of NF_3.

The spectrum of sample prepared without NF_3 is similar to that prepared by the NF_3 flow rate of 20 sccm. But the ratio of I_{1360}/I_{1580}, which correlates with the degree of crystallinity [8], of sample by the NF_3 flow rate of 0 sccm is very different from that of 20 sccm, indicating the crystallinity of these two samples is not in the same degree.

The S/N ratios of samples prepared by the NF_3 flow rates of 5 and 10 sccm were very small because of the poor growth rate of the films. In contrast, the growth rates of films at the NF_3 flow rate above 15 sccm were fairly large. These results indicated that under the NF_3 flow rate of 10 sccm the role of NF_3 was mainly etching of surface of carbonaceous thin films and that above 15 sccm the role of NF_3 should help the polymerization of ethylene in the gas phase, which enhances the growth rate of the thin films. The noticeable point of this study was that addition of NF_3 enabled us to prepare carbonaceous thin films with different crystallinity.

In Fig. 3.4 is shown the XPS C1s depth profile of the carbonaceous thin film prepared at the NF_3 flow rate of 5 sccm and applied rf power of 50 W. Sputtering time for depth profile measurement was 600 s. The peak shapes and intensities were almost unchanged with increasing sputtering time, indicating that the composition of the carbonaceous thin film was uniform. In Fig. 3.4, a sharp peak at binding energy (E_b) of 284 eV assigned to C-C (graphite) can be seen irrespective of sputtering time. The peaks assigned as -CF- (E_b = 288.5-289.5 eV), $-CF_2-$ (E_b = 291.0-292.0 eV), and CF_3- (E_b = 293.0-294.0 eV) could not be

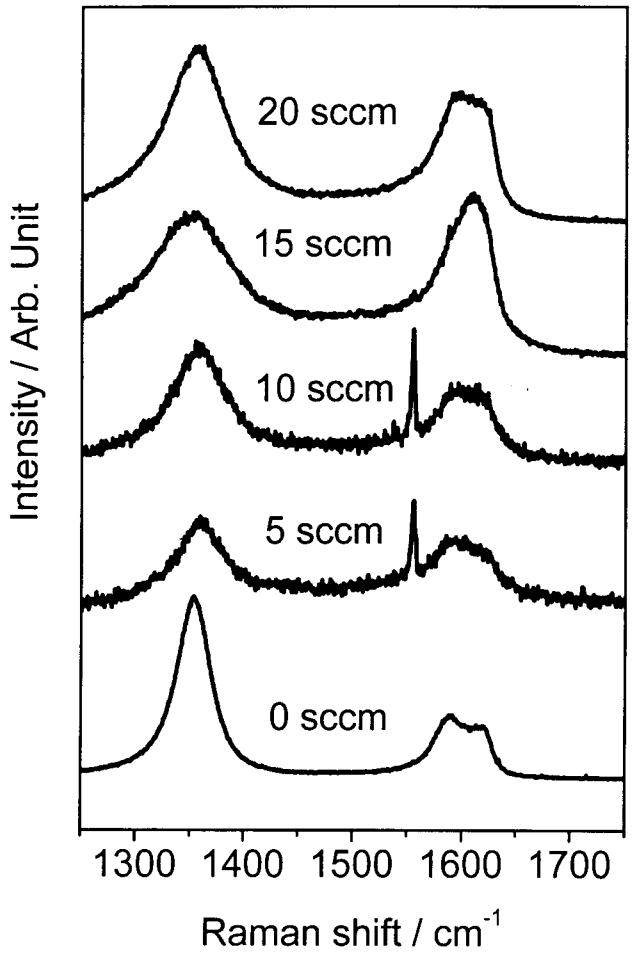

Fig. 3.3. Raman spectra of carbonaceous thin films prepared by plasma CVD at various flow rate of NF_3. Applied rf power; 50 W. Numbers in the figure represent the flow rate of NF_3.

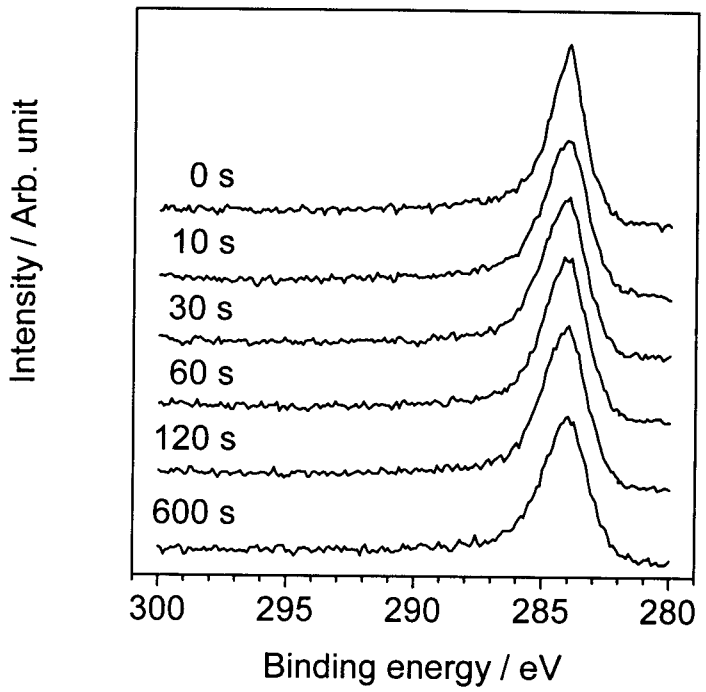

Fig. 3.4. XPS C1s spectra of carbonaceous thin film prepared by plasma CVD exposed with Ar^+ beam for 0 – 600 s. Applied rf power; 50 W.

observed in these XPS C1s spectra. And from XPS F1s spectra and N1s spectra, no clear peaks were observed, which suggest that the thin film contain neither fluorine nor nitrogen atoms.

From the above results, the introduction of NF_3 into plasma does not affect the fluorination of thin film in this study, and hydrogen extraction by fluorine radicals from $-CH_x-$ to form HF may be one of the steps for the preparation of carbonaceous thin films in gas phase [9].

Figure 3.5 shows cyclic voltammograms of carbonaceous thin-film electrodes prepared by the NF_3 flow rate of 20 sccm. Cyclic voltammogram was measured with a sweep rate of 5 mV/s. For the first sweep, mainly two reduction and one oxidation peaks were observed. The reduction peak around 0.6 to 0.5 V vs. Li/Li^+ appeared at the first cycle almost disappeared after second sweep. This result indicates that at the first reduction process the decomposition of solvents and formation of solid electrolyte interface (SEI) occurred on the surface of carbonaceous thin-film electrode [10, 11]. The reduction of the solvents results in the irreversible capacity of carbonaceous electrode for the first cycle. The reduction and oxidation peaks observed at about 0 V vs. Li/Li^+ are due to the lithium-ion intercalation and de-intercalation, but the reduction peak around 0.7 V vs. Li/Li^+ cannot be assigned now. After second sweep the shape of cyclic voltammograms almost unchanged, leading to the conclusion that these carbonaceous thin-film electrodes are suitable for negative electrode of lithium-ion batteries. Fig. 3.6 shows third sweep of cyclic voltammograms for carbonaceous thin-film electrodes prepared at various flow rates of NF_3. The difference of the magnitude of current is due to the difference of thin film thickness. In fact, the deposition rate are determined to be in the order of the NF_3 flow rates as $20 > 15 > 0$ sccm. The shapes of cyclic voltammograms are different between Fig. 3.6(a) and (b). In Fig. 3.6(a) reduction and oxidation peaks are sharper than those in Fig. 3.6(b), and clear shoulder at oxidation peak is shown in Fig. 3.6(a), which may be correlated with the formation of stage structure. The difference of cyclic voltammograms are somehow related with Raman spectra shown in Fig. 3.3, in other word, the degree of crystallinity of the carbonaceous thin-film electrodes affected the shapes of cyclic voltammograms. From the above results, the lithium-ion insertion and extraction behavior of carbonaceous thin-film electrode was quite dependent on the flow rates of NF_3.

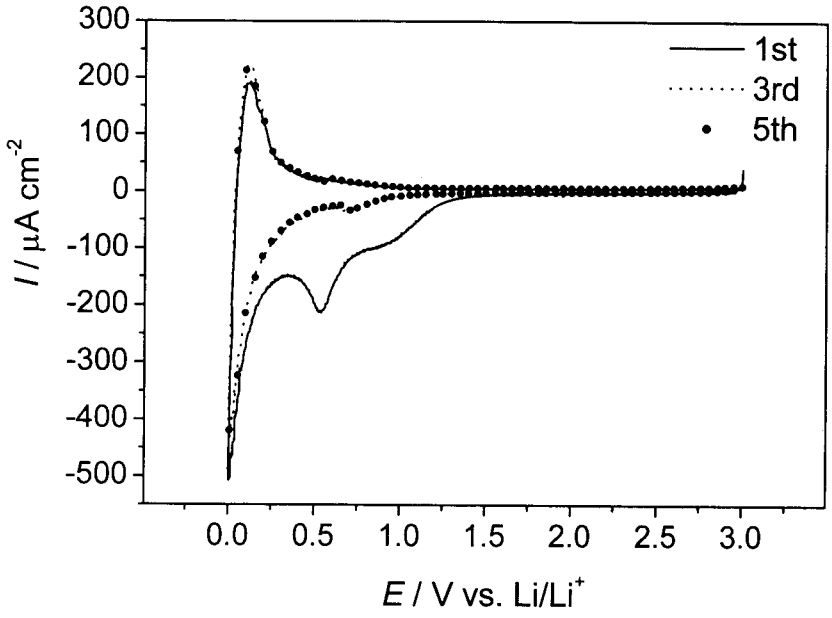

Fig. 3.5. Cyclic voltammograms of carbonaceous thin-film electrodes in 1 mol dm^{-3} $LiClO_4$/EC+DEC (1:1). Sweep rate; 5 mV/s, applied rf power; 50 W, and flow rate of NF_3; 20 sccm.

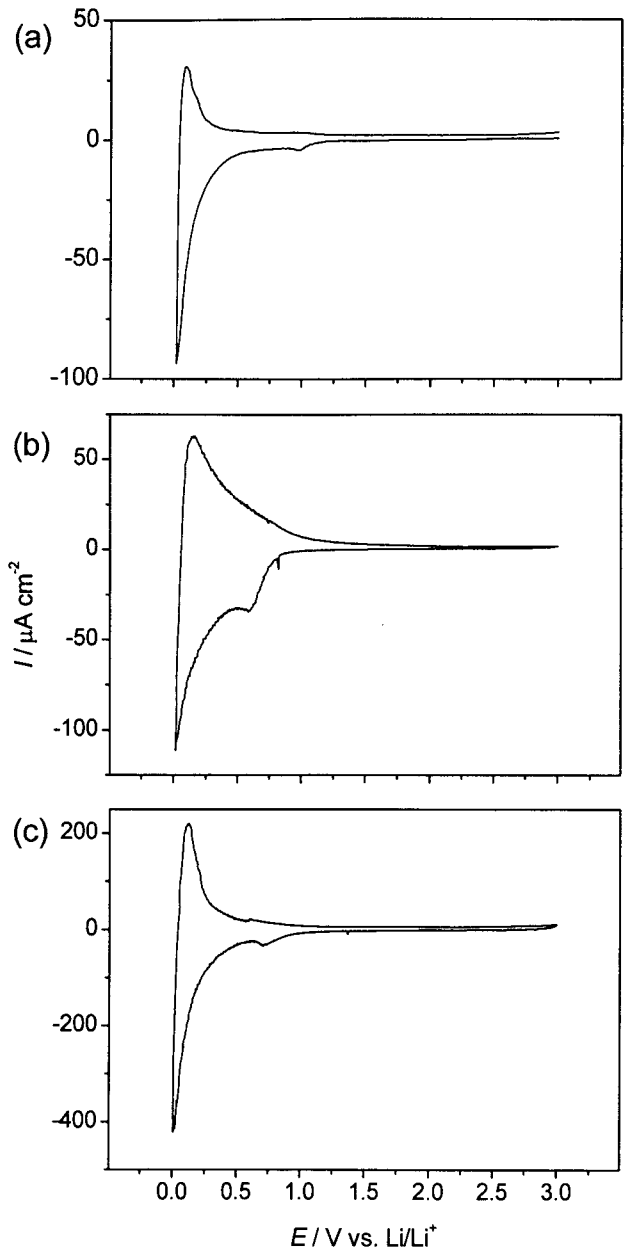

Fig. 3.6. Cyclic voltammograms (3rd cycle) of carbonaceous thin-film electrodes in 1 mol dm^{-3} $LiClO_4$/EC+DEC (1:1). Sweep rate; 5 mV/s. Applied rf power; 50 W. Flow rate of NF_3; (a) 0 sccm, (b) 15 sccm, and (c) 20 sccm.

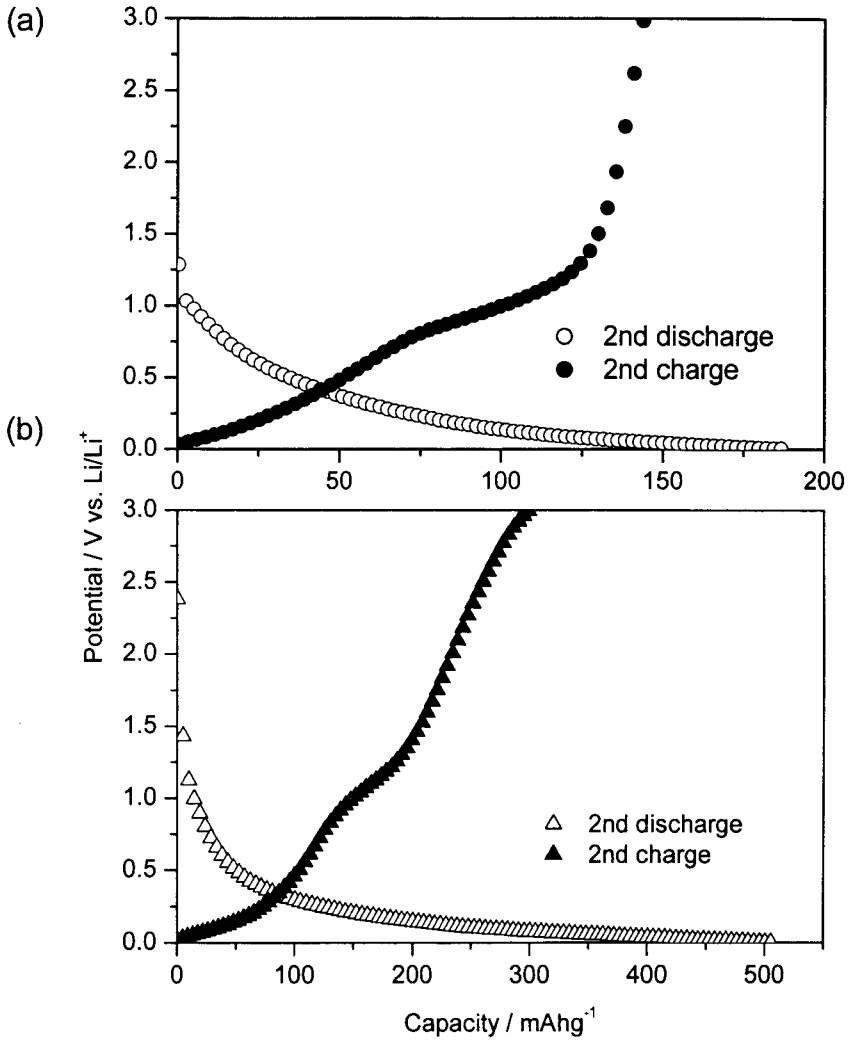

Fig. 3.7. Charge and discharge characteristics of carbonaceous thin-film electrodes prepared at various flow rate of NF_3 of the 2nd charge-discharge cycle in 1 mol dm^{-3} $LiClO_4$/EC+DEC (1:1). Applied rf power; 50 W. Flow rate of NF_3; (a) 15 sccm and (b) 20 sccm.

Figure 3.7 shows charge and discharge characteristics of carbonaceous thin-film electrodes prepared by plasma CVD. These charge and discharge profiles show that a reversible lithium-ion insertion and extraction into carbonaceous thin-film electrodes take place. The feature of these profiles is that in the lithium-ion insertion curves large capacity exist below the potential of 0.25 V vs. Li/Li^+ in which potential range lithium-ion intercalation into graphite occur while in the lithium-ion extraction curves large capacity can not be observed below the potential of 0.25 V. This result suggests that lithium ions should be trapped at some sites among discharge process and these lithium ions are released from the sites followed by extraction from graphite layer [12]. Another experimental approaches will be necessary for the evidence of the trap sites. Figure 3.7(a) shows the result at the NF_3 flow rate of 15 sccm. At the second cycle large irreversible capacity also appeared. Extraction capacity was about 130 $mAhg^{-1}$ and a comparatively large potential plateau appeared at approximately 1 V. These results indicated that the electrochemical properties of carbonaceous thin-film electrodes are similar to those for low graphitized carbon such as low heat-treated mesocarbon microbeads (MCMB) [13]. Figure 3.7(b) shows the result for the NF_3 flow rate of 20 sccm. Extraction capacity was about 290 $mAhg^{-1}$ and similar to the case of the NF_3 flow rate of 15 sccm, and potential plateau appeared at approximately 1 V. The ratio of capacity in the potential range 0 to 0.25 V to that in the range 0.25 to 3 V was evaluated to be 0.262 for 15 sccm and 0.325 for 20 sccm. It has been reported that the de-intercalation capacity in the potential range 0 to 0.25 V becomes large with increasing of crystallinity of MCMB [14]. Hence, the present results of charge-discharge measurements indicate that the crystallinity of carbonaceous thin film at NF_3 of 20 sccm was higher than that of 15 sccm, which is in good agreement with the Raman spectroscopy results.

3.4 Conclusion

Carbonaceous thin films were prepared by C_2H_4 / NF_3 glow discharge plasma. Carbonaceous thin films in this study were flat and pin-hole-free. Addition of NF_3 into plasma was found to affect the growth rates and crystallinity of carbonaceous thin films. Electrochemical properties of the carbonaceous thin-film electrodes were also influenced by the flow rates of NF_3.

References

1. S. Matsumoto, *J. Mater. Sci. Lett.*, **4**, 600 (1985).
2. T. Abe, T. Fukutsuka, M. Inaba, and Z. Ogumi, *Carbon*, **37**, 1165 (1999).
3. G. L. Schott, L. S. Blair, and J. D. Morgan, Jr, *J. Phys. Chem.*, **77**, 2823 (1973).
4. A. Tasaka, A. Komura, Y. Uchimoto, M. Inaba, and Z. Ogumi, *J. Polym. Sci. A*, **34**, 193 (1996).
5. F. Tuinstra and J. L. Koenig, *J. Chem. Phys.*, **53**, 1126 (1970).
6. G. Katagiri, *Tanso*, **175**, 304 (1996). (in Japanese)
7. D. S. Knight and W. B. White, *J. Mater. Res.*, **4**, 385 (1989).
8. G. Katagiri, H. Ishida, and A. Ishitani, *Carbon*, **26**, 565 (1988).
9. T. Abe, A. Funabiki, M. Inaba, Z. Ogumi, K. Gonda, and A. Tasaka, International Symposium on Carbon, Tokyo, 1998.11.8-12, P09-06.
10. E. Peled, *J. Electrochem. Soc.*, **126**, 2047 (1979).
11. J. O. Besenhard, M. Winter, J. Yang, and W. Biberacher, *J. Power Sources*, **51**, 228 (1995).
12. M. Inaba, S. Nohmi, A. Funabiki, T. Abe, and Z. Ogumi, Mat. Res. Soc. Symp. Proc., **496**, 493 (1998).
13. A. Mabuchi, K. Tokumitsu, H. Fujimoto, and T. Kasuh, *J. Electrochem. Soc.*, **142**, 1041 (1995).
14. K. Tatsumi, N. Iwashita, H. Sakaebe, H. Shioyama, S. Higuchi, A. Mabuchi, and H. Fujimoto, *J. Electrochem. Soc.*, **142**, 716 (1995).

Chapter 4

Synthesis of highly graphitized carbonaceous thin films by plasma-assisted chemical vapor deposition and their electrochemical properties in propylene carbonate solution

4.1 Introduction

Natural graphite and highly graphitized carbonaceous materials have been currently used as negative electrode in commercial lithium-ion batteries [1, 2]. Active material of graphite gives advantages as acceptable high capacity, very flat potential as low as lithium metal, etc., while irreversible capacity due to electrolyte decomposition and subsequent formation of solid electrolyte interface (SEI) [3] in the initial stage of charge and discharge cycling should be mentioned as a drawback.

When graphite is employed as a negative electrode in lithium-ion batteries, ethylene carbonate (EC) based electrolytes are essential for practical use. This is because SEI derived from EC based electrolytes on graphite electrode is commonly known to be very available for suppression of further decomposition of solvent, leading to the almost 100 % cycle efficiency of lithium-ion batteries.

Recently, lithium-ion batteries are thought to be one of the candidates of power supply for electric vehicles and hybrid electric vehicles in addition to application areas in the field of portable electronic devices such as cellular phone, notebook computer, and the others. Such expansion of application areas requires lithium-ion batteries to be operated under various severe atmospheres such as low temperatures etc.

Propylene carbonate (PC) possesses as high dielectric constant as EC, and freezing point of PC is much lower than that of EC, indicating that PC should be an ideal choice for an electrolyte of lithium-ion batteries. However, electrochemical lithium-ion intercalation does not take place for graphite electrodes in an electrolyte of PC containing lithium salt [4]. In the PC electrolyte, exfoliation of graphite is explained by the co-intercalation of PC [5, 6]. Much effort has been made for the use of PC solvent as electrolytes in lithium-ion batteries [7-15]. The strategies are mainly addition of additives into a PC electrolyte [7-12] and surface

modification of graphite [13-15]. Among them, carbon coating on graphite may be one of the best approaches for practical use in lithium-ion batteries, because electrochemical properties of graphite will be sustained and SEI on negative active material of carbon can be self-reconstructed.

In this chapter, the preparation of highly graphitized carbonaceous thin film was shown, whose crystallinity differs in surface and bulk, by plasma-assisted chemical vapor deposition (plasma CVD), and its electrochemical properties in electrolyte of PC containing 1 mol dm^{-3} $LiClO_4$ were studied by cyclic voltammetry.

4.2 Experimental

Detailed procedure of plasma CVD is shown in previous chapters [16-18]. Starting materials of acetylene and argon gases were used as a carbon source and plasma assist gas, respectively. Carbonaceous thin films were deposited on substrates of nickel sheets whose temperature was kept at 1023 K. Deposition time was 3 h. Glow discharge plasma was generated between rf and ground electrodes by an rf power supply of 13.56 MHz, and the applied rf power was set at 10 W. The flow rates of argon and acetylene were set at 25 and 10 sccm, respectively. The total pressure of reaction chamber was kept at 133 Pa. The resultant films were characterized by scanning electron microscopy (SEM), X-ray diffraction (XRD), and Raman spectroscopy.

Electrochemical properties were studied by cyclic voltammetry using a three-electrode cell. Carbonaceous thin-film electrode was used as a working electrode. Lithium metal was used as counter and reference electrodes. Cutoff voltage was 0 - 3.0 V vs. Li/Li^+ with a sweep rate of 0.1 mV/s. Electrolyte of PC containing 1 mol dm^{-3} $LiClO_4$ was used. As for comparison, a mixture of EC and diethyl carbonate (DEC) solution containing 1 mol dm^{-3} $LiClO_4$ was also used.

4.3 Results and discussion

Figure 4.1 shows a typical XRD pattern of resultant thin film. Very strong (002) line was observed at 26.6° in 2θ, whose value almost agrees with that of graphite, indicating that obtained thin film is very graphitized. A small broad peak can be observed around 24 - 26° in 2θ and therefore, the thin films possess amorphous region to a certain extent. Raman

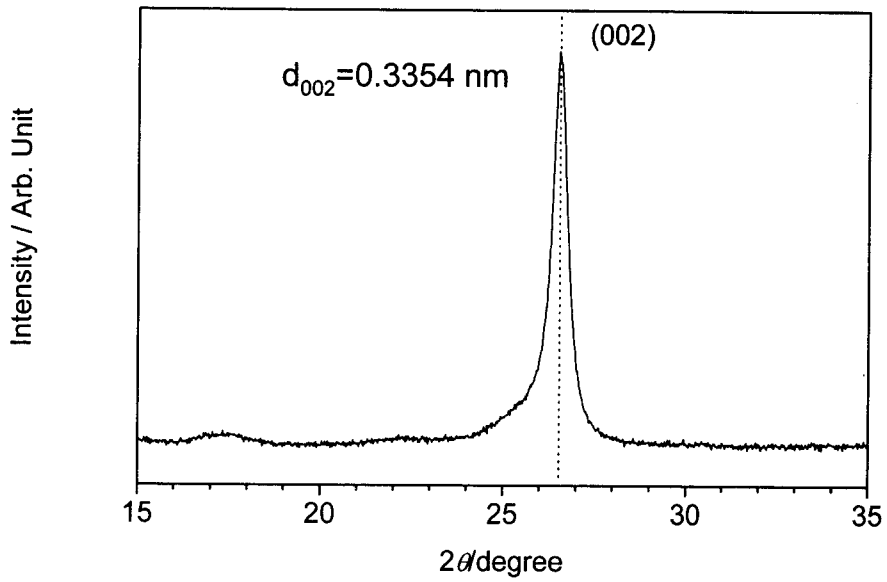

Fig. 4.1. XRD pattern of carbonaceous thin film prepared by plasma CVD. Scan rate; 0.125 °/min. Reaction time; 3h, substrate; Ni, and applied rf power; 10 W. Substrate temperature; 1023 K. Reaction pressure; 133 Pa.

spectroscopy gave different results in crystallinity. In Fig. 4.2 is shown Raman spectrum of carbonaceous thin film. Two peaks around 1350 and 1590 cm^{-1} were observed. Peak around 1590 cm^{-1} is well-known to be related with crystallinity of carbonaceous materials, and is assigned to Raman active E_{2g} mode frequency [19]. Peak around 1350 cm^{-1} is usually inactive and appears in the case of finite crystal size and imperfection of carbonaceous materials [20]. Carbonaceous materials with high degree of graphitization usually give a strong peak at 1580 cm^{-1} with a small peak at around 1360 cm^{-1}. However, the present thin film gives higher intensity of peak at 1360 cm^{-1} than that at 1580 cm^{-1}, indicating that the surface of the thin film is less crystallized. These results reveal that highly graphitized thin films with lower crystallized surface were synthesized.

Figure 4.3 shows the cyclic voltammogram of graphitized carbonaceous thin-film electrode in an electrolyte of PC containing 1 mol dm^{-3} $LiClO_4$. For the first sweep, irreversible reduction current was observed from the potential around 1.5 to 0.5 V vs. Li/Li^+, but it almost disappeared after the second sweep, indicating SEI was formed on carbonaceous thin-film electrode. As is readily apparent, oxidation peak at around 0.1 V were split. The splitting of the peak at around 0 V is observed for graphite negative electrode due to the stage transformation [21-24]. Hence, the electrochemical properties of the carbonaceous thin-film electrodes are very similar to those for graphite negative electrodes [25], which is in good agreement with a structural aspect. As for comparison, cyclic voltammogram of the thin-film electrode in an electrolyte of a mixture of EC and DEC containing 1 mol dm^{-3} $LiClO_4$ is given in Fig. 4.4 over the potential range of 0.3 to 0 V. The cyclic voltammogram given in Fig. 4 is very similar to that observed in Fig. 4.3.

Cyclic voltammograms of graphite negative electrode in PC electrolyte usually give continuous large reduction current around the potential of 1.0 V vs. Li/Li^+, and no electrochemical intercalation of lithium ion into graphite takes place. As mentioned above, this is due to the exfoliation of graphite caused by the co-intercalation of PC. However, the present graphitized film showed quite different cyclic voltammogram as given in Fig. 4.3. This should be explained by the surface crystallinity of this thin film. It is commonly known that lithium ion can intercalate into less crystallized carbonaceous materials with turbostratic structure in PC electrolyte. Although the crystallinity of the present thin film is very high inside its bulk, surface crystallinity is much lower as compared with the inside bulk.

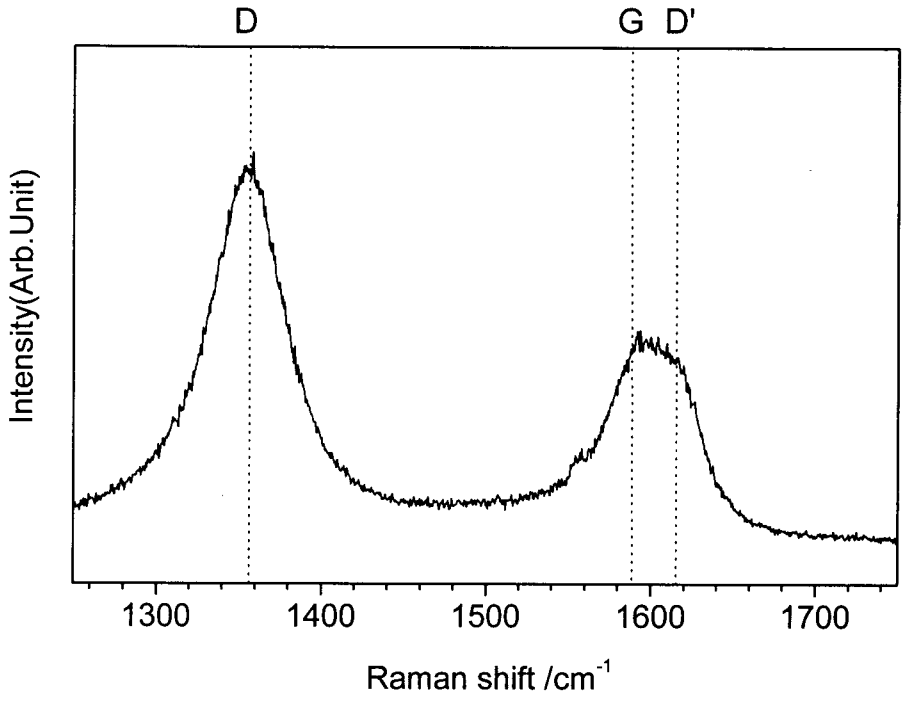

Fig. 4.2. Raman spectrum of carbonaceous thin film prepared by plasma CVD. Reaction time; 3 h, substrate; Ni, and applied rf power; 10 W. Substrate temperature; 1023 K. Reaction pressure; 133 Pa.

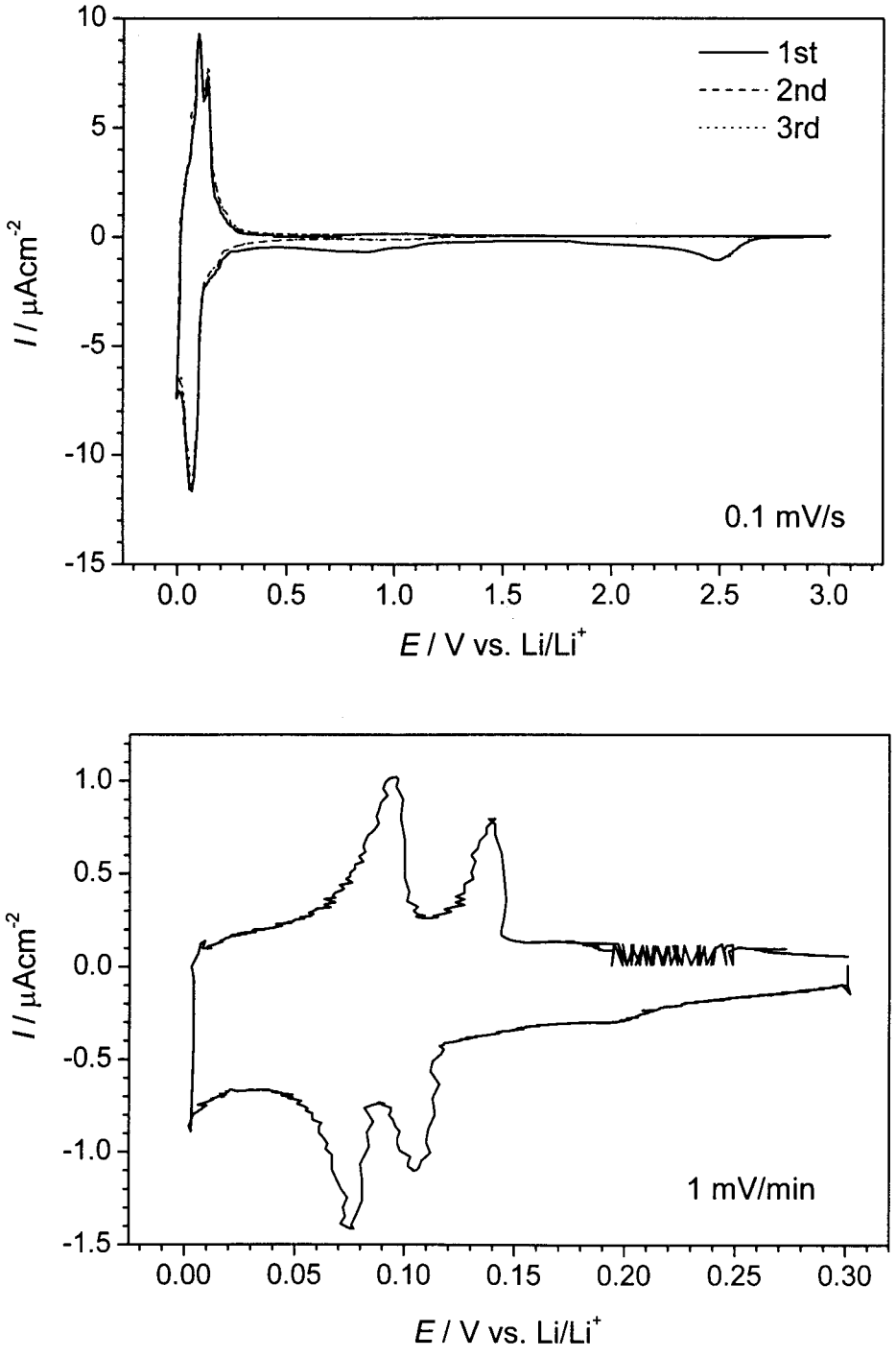

Fig. 4.3. Cyclic voltammograms of carbonaceous thin-film electrode prepared at 10 W in 1 mol dm^{-3} $LiClO_4$/PC. Sweep rate; (top) 0.1 mV/s, and (bottom) 1 mV/min.

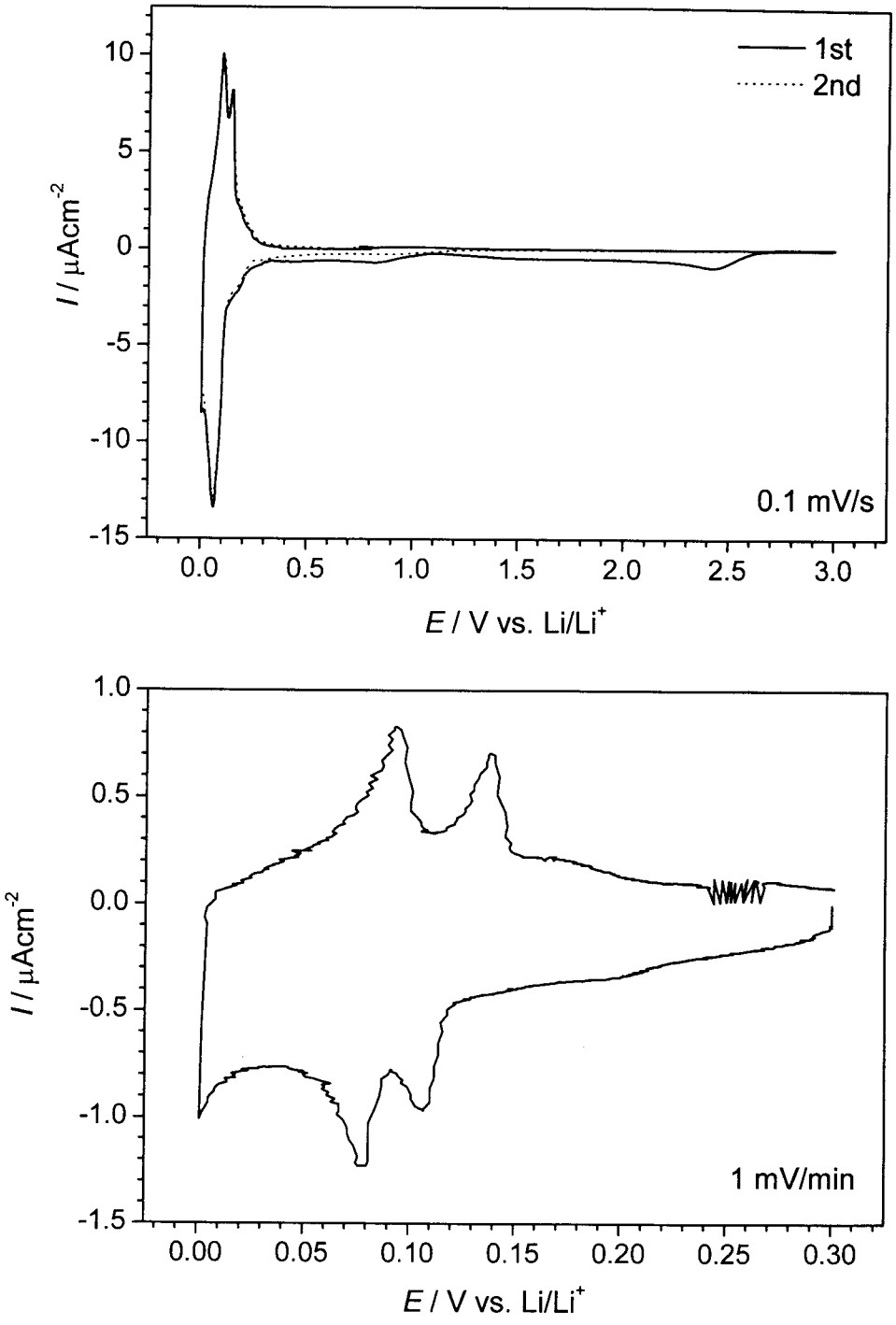

Fig. 4.4. Cyclic voltammograms of carbonaceous thin-film electrode prepared at 10 W in 1 mol dm^{-3} $LiClO_4$/EC+DEC (1:1). Sweep rate; (top) 0.1 mV/s, and (bottom) 1 mV/min.

Therefore, co-intercalation of PC should be suppressed and lithium-ion intercalation occurred. Second cycle of cyclic voltammetry given in Fig. 4.3 revealed that the lithium-ion intercalation occurred from ca. 0.3 V, and that no reduction and oxidation currents were observed above 0.3 V. These results indicate that little capacity is available for the potential above 0.3 V. Lithium-ion insertion into low crystallized carbonaceous materials takes place at around 1.0 V. And hence the thickness of less crystallized part should be very small.

4.4 Conclusion

Highly graphitized carbonaceous thin films have been prepared by plasma CVD, and the thin films were very flat and pin-hole-free. The electrochemical properties of carbonaceous thin-film electrodes were quite different from those of graphite negative electrodes in electrolyte of PC containing 1 mol dm^{-3} $LiClO_4$, which is ascribed to the less crystallized surface of the present thin films.

References

1. Z. Ogumi and M. Inaba, *Bull. Chem. Soc. Jpn.*, **71**, 521 (1998).
2. M. Winter, J. O. Besenhard, M.E. Spahr, and P. Novak, *Adv. Mater.*, **10**, 725 (1998).
3. E. Peled, *J. Electrochem. Soc.*, **126**, 2047 (1979).
4. A. N. Dey and B. P. Sullivan, *J. Electrochem. Soc.*, **117**, 222 (1970).
5. R. Fong, U. von Sacken, and J. R. Dahn, *J. Electrochem. Soc.*, **137**, 2009 (1990).
6. M. Winter, G. H. Wrodnigg, J. O. Besenhard, W. Biberacher, and P. Novak, *J. Electrochem. Soc.*, **147**, 2427 (2000).
7. G. H. Wrodnigg, J. O. Besenhard, and M. Winter, *J. Electrochem. Soc.*, **146**, 470 (1999).
8. G. H. Wrodnigg, T. M. Wrodnigg, J. O. Besenhard, and M. Winter, *Electrochem. Lett.*, **1**, 148 (1999).
9. O. Chusid, Y. Ein-Eli, D. Aurbach, M. Babai, and Y. Carmeli, *J. Power Sources*, **43/44**, 47 (1993).
10. A. Wang, H. Nakamura, K. Komatsu, M. Yoshio, and H. Yoshitake, *J. Power Sources*, **74**, 142 (1998).
11. Z. X. Shu, R. S. McMillan, and J. J. Murray, *J. Electrochem. Soc.*, **140**, L101 (1993).
12. Y. Ein-Eli, S. R. Thomas, and V. R. Koch, *J. Electrochem. Soc.*, **144**, 1159 (1997).

13. I. Kuribayashi, M. Yokoyama, and M. Yamashita, *J. Power Sources*, **54**, 1 (1995).
14. W. Qiu, G. Zhang, S. Lu, and Q. Liu, *Chin. J. Power Sources*, **23**, 7 (1999).
15. M. Yoshio, H. Wang, K. Fukuda, Y. Hara, and Y. Adachi, *J. Electrochem. Soc.*, **147**, 1245 (2000).
16. T. Abe, T. Fukutsuka, M. Inaba, and Z. Ogumi, *Carbon*, **37**, 1165 (1999).
17. T. Fukutsuka, T. Abe, M. Inaba, and Z. Ogumi, *Mol. Cryst. Liq. Cryst.*, **340**, 517 (2000).
18. T. Fukutsuka, T. Abe, M. Inaba, and Z. Ogumi, *J. Electrochem. Soc.*, **148**, A989 (2001).
19. F. Tuinstra and J. L. Koenig, *J. Chem. Phys.*, **53**, 1126 (1970).
20. G. Katagiri, *Tanso*, **175**, 304 (1996).
21. J. R. Dahn, R. Fong, and M. J. Spoon, *Phys. Rev.*, **B42**, 6424 (1990).
22. J. R. Dahn, *Phys. Rev.*, **B44**, 9170 (1991).
23. T. Ohzuku, Y. Iwakoshi, and K. Sawai, *J. Electrochem. Soc.*, **140**, 2490 (1993).
24. M. Inaba, H. Yoshida, Z. Ogumi, T. Abe, Y. Mizutani, and M. Asano, *J. Electrochem. Soc.*, **142**, 20 (1995).
25. K. Tatsumi, N. Iwashita, H. Sakaebe, H. Shioyama, S. Higuchi, A. Mabuchi, and H. Fujimoto, J. Electrochem. Soc., 142, 716 (1995).

Part 2

Surface plasma modification of carbonaceous thin-film electrodes and their electrochemical properties

Chapter 5

Surface modification of carbonaceous thin films by NF_3 plasma and their effects on electrochemical properties

5.1 Introduction

For the recent development of mobile devices, lithium-ion batteries have been extensively studied because of their high performance and potentialities [1]. In regard to the negative electrode, highly crystallized graphite has been used in commercial market because lithium-ion intercalation/de-intercalation proceeds in graphite at the potential as low as redox potential of lithium metal [2]. However, carbonaceous materials have been still extensively investigated as negative electrode materials to improve the performance of lithium-ion batteries [3-10].

At the first charge of lithium-ion batteries, it is well known that reduction of electrolyte on the negative electrode occurs and that passivation film (solid electrolyte interface: SEI) is formed around 1.0 V vs. Li/Li^+ [1, 2]. Although the formation of SEI results in the large part of irreversible capacity, the SEI is essential for suppression of the further decomposition of electrolyte, leading to almost 100 % columbic efficiency.

Various surface modifications on graphite electrodes have been applied for the formation of effective SEI [11-13]. In part 1, the synthesis of sp^2-type carbonaceous thin films by plasma-assisted chemical vapor deposition (plasma CVD) and studied their electrochemical properties as the binder free negative electrodes were reported [14-18]. Homogeneous surface modification of the thin films is quite easy, because of the thin film's flatness and smoothness. Therefore, the effect of surface modification of carbonaceous materials on electrochemical properties can be clearly elucidated.

In this chapter, surface modification of carbonaceous thin films by nitrogen trifluoride (NF_3) plasma and their effects on structures and electrochemical properties of the thin films as negative electrodes for lithium-ion batteries were discussed.

5.2 Experimental

Carbonaceous thin films were deposited on substrates of nickel sheets from acetylene and argon. Substrates were placed on a ground electrode keeping at 873 K. The applied rf power was set to 50 W. The detail procedure was shown in the part 1 [14, 18].

The same apparatus was used for surface plasma modification of the films. NF_3 (Kanto Denka Kogyo Co., Ltd.) was used as fluorine sources and argon was plasma assist gas, and the temperature of films was kept below 373 K. The flow rate of NF_3 was set at 5, 10 and 20 sccm. Applied rf power was chosen to be 50 W, and the treatment time was 5 minutes. The use of NF_3 for surface treatment makes it possible to fluorinate carbonaceous thin films without heating, because NF_3 can release fluorine radicals in plasma, and the polymerization compound is not formed because of the absence of carbon atom in NF_3.

Resultant thin films were characterized by Raman spectroscopy (Jobin-Yvon, T64000) with 514.5 nm line of an argon ion laser. X-ray photoelectron spectroscopy (XPS) was used for surface chemical analysis of the thin films (JEOL, JAMP-7800F). Auger electron spectroscopy (AES) with field emission type electron gun (JEOL, JAMP-7800F) was used for the local elemental analysis of the thin films.

A three-electrode electrochemical cell was employed for electrochemical measurements. Lithium metal was used as counter and reference electrodes. The electrolyte solution was a mixture (1:1 by volume) of ethylene carbonate (EC) and diethyl carbonate (DEC) containing 1 mol dm^{-3} $LiClO_4$ (Tomiyama Pure Chemical Industries, Ltd). The cell was assembled in an argon-filled glove box. Electrochemical properties were studied by cyclic voltammetry (RADIOMETER, VoltaLab 21) with a sweep rate of 1 mV/s in the potential range of 3 to 0 V vs. Li/Li^+.

5.3 Results and discussion

The surface of carbonaceous thin film prepared by plasma CVD was apparently flat and no pin-hole was observed within the SEM image [18]. The Raman spectra of carbonaceous thin films treated by NF_3 plasma are shown in Fig. 5.1. In these Raman spectra, obvious change by plasma treatment was not recognized.

From XPS spectra for pristine thin film, only one peak appeared at 284 eV for C1s spectrum. This peak is assigned to C-C bonding (graphite). No peak was observed for F1s

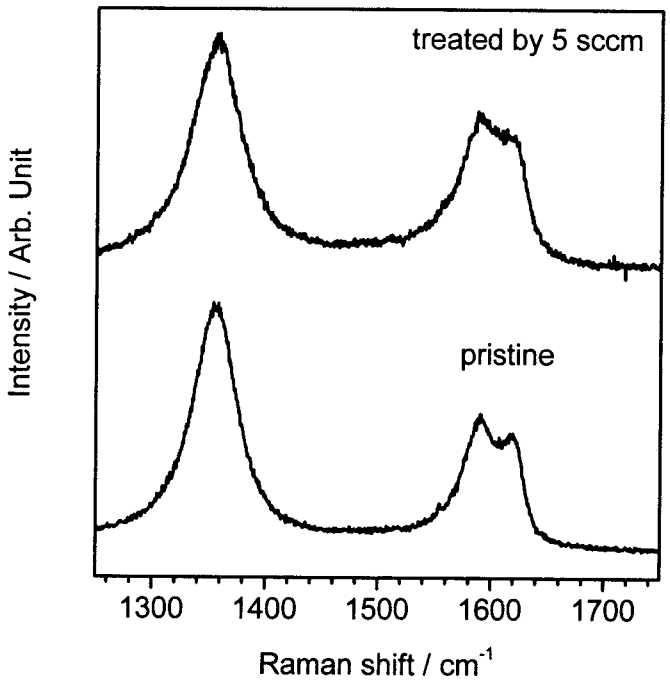

Fig. 5.1. Raman spectra of carbonaceous thin films treated by NF_3 plasma at rf power of 50 W for 5 min. Flow rates of NF_3; 5 sccm.

spectrum. XPS spectra for treated thin films gave two peaks in C1s spectrum at around 284 eV and 288 eV. The former is assigned to C-C bonding and the latter is reported as semi-ionic or semi-covalent C-F bonding observed in stage 1 fluorine-graphite intercalation compounds, C_2F-$C_{2.5}F$ [19]. And for all F1s spectra, only one peak appeared at 687 eV, corresponding to semi-ionically bonded fluorine atoms. From these results, carbonaceous thin films were fluorinated by NF_3 plasma treatment, and fluorine atoms on the carbonaceous thin films are semi-ionically bonded to carbon atoms. AES was used for the evaluation of degree of fluorination by the change of flow rate of NF_3. Table 5.1 shows the atomic ratio of fluorine atom to carbon atom (F/C) of thin films evaluated from the peak intensity of derivative Auger spectra (peak to peak method). The F/C value increased with increase of the flow rate of NF_3. The values of F/C are in the range of 0.495 to 0.545, and therefore the composition of treated films is close to C_2F, the semi-ionic stage 1 fluorine-graphite intercalation compound C_2F [19]. From the above results, it is clear that increment of flow rate of NF_3 lead to the increment of the degree of fluorination.

In Fig. 5.2, cyclic voltammograms (CVs) of the 1st and 2nd cycles for carbonaceous thin-film electrodes are shown. For pristine thin-film electrode (Fig. 5.2(a)), small peak at about 0.8 V and large peak at about 0.6 V appear in the 1st reduction process. These peaks suggest the decomposition of solvent, and the decomposition products act as SEI on the surface of carbonaceous thin-film electrodes [1, 2]. Obvious change was observed for the CVs of plasma treated thin-film electrodes. For the CV of carbonaceous thin-film electrode treated at 5 sccm (Fig. 5.2(b)), the reduction peak about 0.6 V drastically decreased as compared with that for pristine thin-film electrode. The reduction peak became small by increasing the flow rates of NF_3, and the peak at 0.6 V almost disappeared for the film treated by 20 sccm. In addition, the shapes of cyclic voltammograms of the 2nd cycle for surface treated thin-film electrodes are very similar with that of the 2nd cycle for pristine thin-film electrode. Therefore, surface fluorination of carbonaceous thin-film electrodes only affects on the 1st cycle of CV. Open circuit potential (OCP) of treated thin-film electrodes (ca 3.8 V) are much higher than that of pristine thin-film electrode (ca. 3.2 V), which results in the fluorine atoms bonded to the carbonaceous thin film. After the 1st sweep, the OCP becomes almost the same as that of pristine thin-film electrode, which indicates that the fluorine atom on the thin-film electrode is reduced at the 1st sweep.

TABLE 5.1. The F/C values of carbonaceous thin film evaluated from AES spectra

Flow rate of NF_3	Atomic rate (F/C)
5 sccm	0.495
10 sccm	0.535
20 sccm	0.545

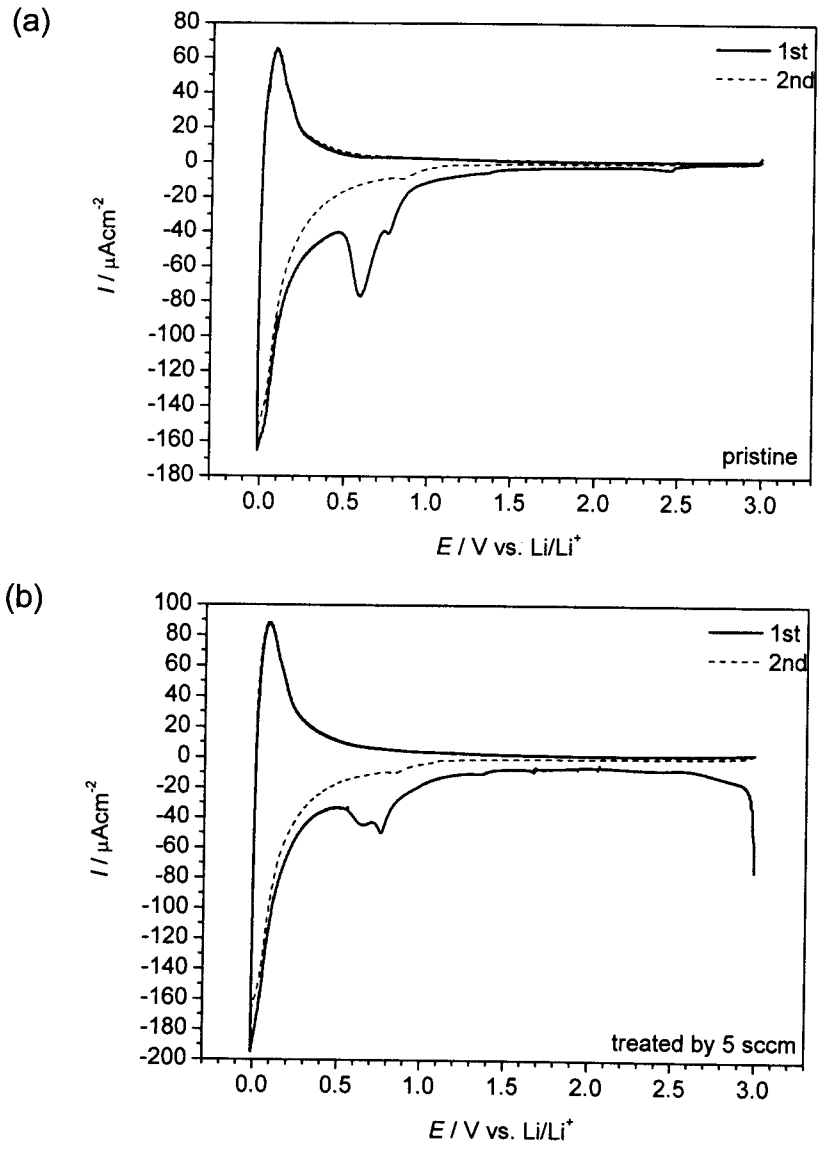

Fig. 5.2. Cyclic voltammograms of carbonaceous thin-film electrodes treated by NF_3 plasma; (a) pristine and (b) treated by 5 sccm.

From the above results, fluorine atoms bonded to the carbonaceous thin film should act as a passivation layer (such as LiF) by the reaction with Li [20], which suppresses the reduction of solvent taking place at 0.6 V. However, the reduction of solvent taking place at 0.8 V was not suppressed by the surface treatment. Hence, reduction of the solvent should be responsible for passivation layer formed at 0.8 V.

5.4 Conclusion

Carbonaceous thin films prepared by plasma CVD were treated by NF_3 plasma to give surface fluorinated thin films. The degree of fluorination evaluated by AES was dependent on the flow rates of NF_3. From cyclic voltammograms, the decomposition of solvent at the 1st reduction process was suppressed by the fluorination. In addition, plasma treatment gave no change to the bulk electrochemical characteristics of carbonaceous thin-film electrodes. It is concluded that surface modification of carbonaceous thin-film electrode by NF_3 plasma affects on the reduction of solvent in the lithium-ion batteries.

References

1. M. Winter, J. O. Besenhard, M. E. Spahr, and P. Novák, *Adv. Mater.*, **10**, 725 (1998).
2. Z. Ogumi and M. Inaba, *Bull. Chem. Soc. Jpn.*, **71**, 521 (1998).
3. J. R. Dahn, T. Zheng, Y. Liu, and J. S. Xue, *Science*, **270**, 590 (1995).
4. N. Imanishi, H. Kashiwagi, T. Ichikawa, Y. Takeda, O. Yamamoto, and M. Inagaki, *J. Electrochem. Soc.*, **140**, 315 (1993).
5. I. Mochida, C.-H. Ku, S.-H. Yoon, and Y. Korai, *J. Power Sources*, **75**, 214 (1998).
6. T. Zheng, J. S. Xue, and J. R. Dahn, *Chem. Mater.*, **8**, 389 (1996).
7. M. Inaba, H. Yoshida, Z. Ogumi, T. Abe, Y. Mizutani, and M. Asano, *J. Electrochem. Soc.*, **142**, 20 (1995).
8. M. Inaba, H. Yoshida, and Z. Ogumi, *J. Electrochem. Soc.*, **143**, 2572 (1996).
9. Y.-S. Han, J.-S. Yu, G.-S. Park, and J.-Y. Lee, *J. Electrochem. Soc.*, **146**, 3999 (1999).
10. M. Inaba, M. Fujikawa, T. Abe and Z. Ogumi, *J. Electrochem. Soc.*, **147**, 4008 (2000).
11. E. Peled, C. Menachem, D. Bar-Tow, and A. Melman, *J. Electrochem. Soc.*, **143**, L4 (1996).
12. T. Nakajima, M. Koh, R. N. Singh, and M. Shimada, *Electrochim. Acta*, **44**, 2879 (1999).

13. M. Yoshio, H. Wang, K. Fukuda, Y. Hara, and Y. Adachi, *J. Electrochem. Soc.*, **147**, 1245 (2000).
14. T. Abe, T. Fukutsuka, M. Inaba, and Z. Ogumi, *Carbon*, **37**, 1165 (1999).
15. T. Fukutsuka, T. Abe, M. Inaba, and Z. Ogumi, *Tanso*, **190**, 252 (1999).
16. T. Fukutsuka, T. Abe, M. Inaba, and Z. Ogumi, *Mol. Cryst. Liq. Cryst.*, **340**, 517 (2000).
17. T. Fukutsuka, T. Abe, M. Inaba, Z. Ogumi, Y. Matsuo, and Y. Sugie, *Carbon Science*, **1**, 129 (2001).
18. T. Fukutsuka, T. Abe, M. Inaba, and Z. Ogumi, *J. Electrochem. Soc.*, **148**, A1260 (2001).
19. Y. Matsuo and T. Nakajima, *Z. Anorg. Allg. Chem.*, **621**, 1943 (1995).
20. T. Nakajima, *J. Fluorine Chem.*, **100**, 57 (1999).

Chapter 6

Surface modification of carbonaceous thin-film electrodes by using oxygen plasma

6.1 Introduction

For the recent development of mobile devices, lithium-ion batteries have been extensively studied because of their high performance and potentialities [1]. Regarding to the negative electrodes, highly crystallized graphite has been used in commercial market because lithium-ion intercalation/de-intercalation proceeds in graphite at potential as low as redox potential of lithium metal [2]. However, carbonaceous materials have been still extensively investigated as negative electrode materials to improve the performance of lithium-ion batteries. In particular, various surface modifications on graphite electrodes have been applied for the improvement of electrode performance, such as fluorination [3], mild oxidation [4], metal thin-film coating [5] and ceramic thin-film coating [6, 7]. These modifications have led to the increasing of reversible capacity [3, 4] and high rate performance [5-7]. Mainly composite electrodes have been used in the above studies, and therefore it is a little bit difficult to focus the effect of surface modification in detail. In chapter 6, it was cleared that the side reaction at the 1st reduction process was suppressed by the surface nitrogen trifluoride (NF_3) plasma treatment of carbonaceous thin-film electrodes [8]. By use of plasma, mild surface modification can be made without changing the bulk electrochemical properties, and in addition, carbonaceous thin-film electrodes enabled us to study the effect of surface modification in detail.

In this chapter, surface O_2 plasma modification of carbonaceous thin-film electrodes and their effects on electrochemical properties of the thin-film electrodes as negative electrodes of lithium-ion batteries were discussed.

6.2 Experimental

Carbonaceous thin films were deposited on substrates of nickel sheets from acetylene

and argon, and thickness of resultant thin films were less than 1.0 μm. Substrates were placed on a ground electrode keeping at 873 K. The applied rf power was set to 50 W. The detail procedure was shown in previous part [9, 10]. The same apparatus was used for surface O_2 plasma modification of the obtained thin-film electrodes. Temperature of thin-film electrodes was kept below 373 K during surface modification. The flow rate of O_2 was set at 0 - 40 sccm. Applied rf power was chosen to be 50 W. Surface modification was conducted for 5 min.

Raman spectroscopy was used to characterize the thin-film electrodes. The measurement was carried out at 298K using a Jobin-Yvon T64000 spectrometer equipped with a multi-channel CCD detector, and the scattered light was collected in a backscattering geometry. The thin-film electrodes were excited with a 514.5 nm line of Ar^+ laser. The power of incident laser light was maintained at 50 mW. X-ray photoelectron spectroscopy (XPS) was used for surface chemical analysis of the thin-film electrodes.

A three-electrode electrochemical cell was employed for electrochemical measurements. Carbonaceous thin-film electrode was used as a working electrode and lithium metal was used as counter and reference electrodes. Electrolyte solutions were mixture (1:1 by volume) of ethylene carbonate (EC) and diethyl carbonate (DEC) containing 1 mol dm^{-3} $LiClO_4$ (Kishida Kagaku), EC containing 1 mol dm^{-3} $LiClO_4$ (Kishida Kagaku), and DEC containing 1 mol dm^{-3} $LiClO_4$ (Kishida Kagaku). Vinylene carbonate (VC; Aldrich) and ethylene sulfite (ES; Aldrich) were used as additives (5 volume %) for EC solution. The cell was assembled in an argon-filled glove box. Electrochemical properties were studied by cyclic voltammetry (RADIOMETER, VoltaLab 21) with a sweep rate of 1 mV/s in the potential range of 3 to 0 V. Unless otherwise stated, potential is referred to against Li/Li^+.

6.3 Results and Discussion

Raman spectra of carbonaceous thin-film electrodes are shown in Figs. 6.1(a) and 1(b). The thin-film electrode was modified by O_2 plasma with a flow rate of 40 sccm. Raman spectrum of surface modified thin-film electrode is almost similar to that of pristine thin-film electrode, indicating that the crystallinity of the surface modified thin-film electrode should not be changed. The same tendency was observed for NF_3 plasma treated thin-film electrode [8]. These results indicated that the thin-film electrodes were not damaged by the present plasma treatment.

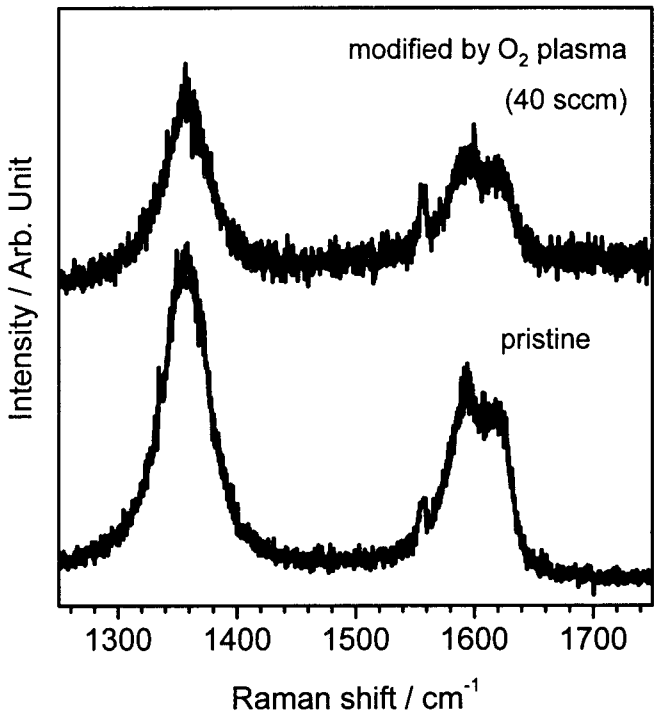

Fig. 6.1. Raman spectra of surface modified carbonaceous thin-film electrodes by O_2 plasma (40 sccm).

From XPS measurements, content of oxygen atom is increased with increasing flow rate of O_2 and the O/C values were calculated as follows; 0.021 (pristine), 0.107 (modified by 5 sccm), 0.111 (modified by 20 sccm), and 0.117 (modified by 40 sccm). Figure 6.2 shows XPS C1s and O1s spectra for surface modified thin-film electrode by O_2 plasma using the flow rate of 40 sccm. As is give in Fig. 6.2, the C1s XPS spectrum gave two peaks at around 284.3 eV and 286.5 eV. The former peak is assigned to C-C bonding of graphitic carbon and the latter one can be identified as C-O bonding. In O1s spectrum, only one peak appeared at 532.6 eV. This peak also represents the existence of O-H, namely C-O-H. From these results, it can be concluded that O_2 plasma modification introduced C-O bonding into the thin film electrodes and the degree of oxidation can be controlled by the flow rates of O_2.

In Fig. 6.3 are shown cyclic voltammograms (CVs) of the 1st cycle for carbonaceous thin-film electrodes modified by O_2 plasma (5 and 40 sccm) in the solution of EC+DEC. For pristine thin-film electrode (solid line), small peak at 0.8 - 0.7 V and large peak at about 0.6 V appeared in the reduction process. These peaks suggest that the decomposition of solvent and formation of SEI on the surface of thin-film electrodes occurred. Obvious change was observed in the CV for surface modified thin-film electrodes as given by dotted and dashed lines (5 and 40 sccm, respectively) in Fig. 6.3; the reduction peak about 0.6 V drastically decreased and almost disappeared (shown by arrows) as compared with pristine thin-film electrode. This result was quite similar to the result of the thin-film electrode modified by NF_3 plasma [8]. And from the 2nd cycle of CVs (not shown here), CVs did not differ for all the thin-film electrodes, indicating bulk electrochemical properties should be remained unchanged. Therefore, surface modification of thin-film electrodes only affected on the 1st cycle of CV. This result is identical with the result of Raman measurement. From the above results, it is conducted that the surface modification of carbonaceous thin-film electrodes by O_2 plasma suppressed the reductive decomposition of solvent taking place at 0.6 V with remaining the bulk electrochemical properties unchanged and these effect is probably due to the C-O bonding from XPS analysis.

Next, CV was measured in electrolyte solutions containing single solvent of EC or DEC to elucidate which solvents (EC or DEC) decompose at 0.6 V. The CV obtained in EC was almost the same with the solid line given in Fig. 6.3. On the other hand, the CV obtained in DEC was quite different from solid line in Fig. 6.3. Two peaks appeared at 0.8 V (small)

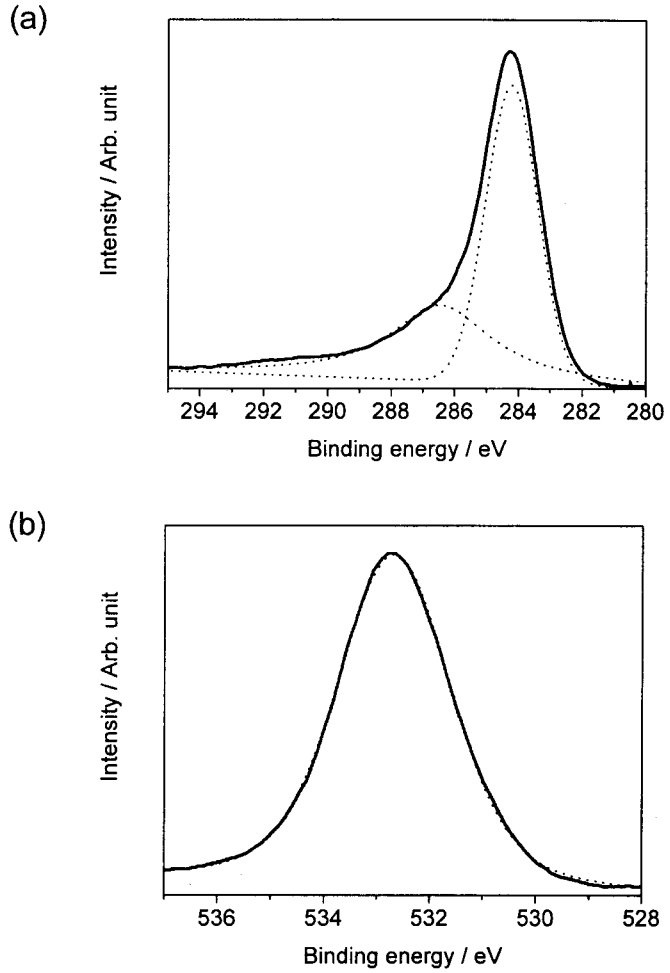

Fig. 6.2. XPS C1s and O1s spectra of surface modified carbonaceous thin-film electrodes by O_2 plasma (40 sccm). (a) C1s spectrum and (b) O1s spectrum.

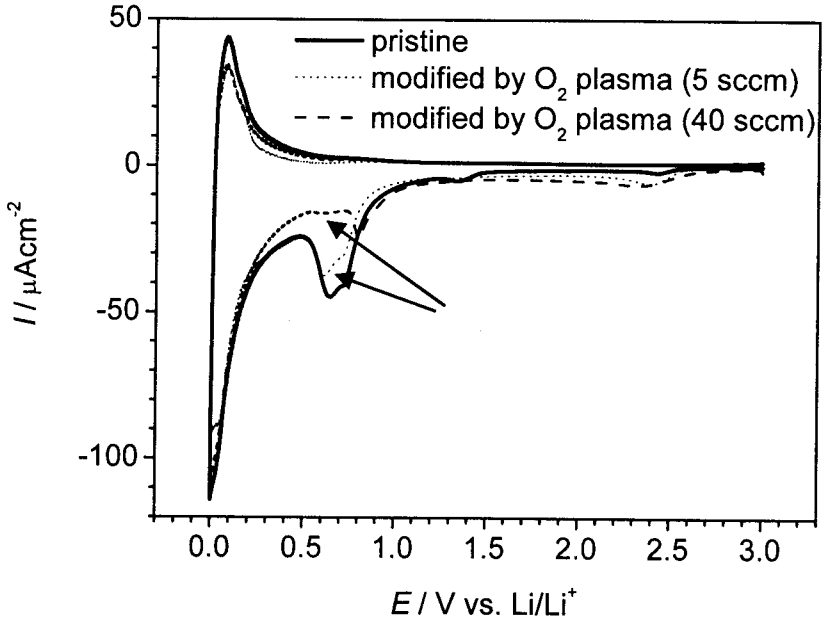

Fig. 6.3. Cyclic voltammograms (1st sweep) of surface modified carbonaceous thin-film electrodes by O_2 plasma (5 and 40 sccm). Solid line represents pristine thin-film electrode and dotted and dashed lines represent surface modified thin-film electrodes (5 and 40 sccm, respectively). Sweep rate is 1 mV/s.

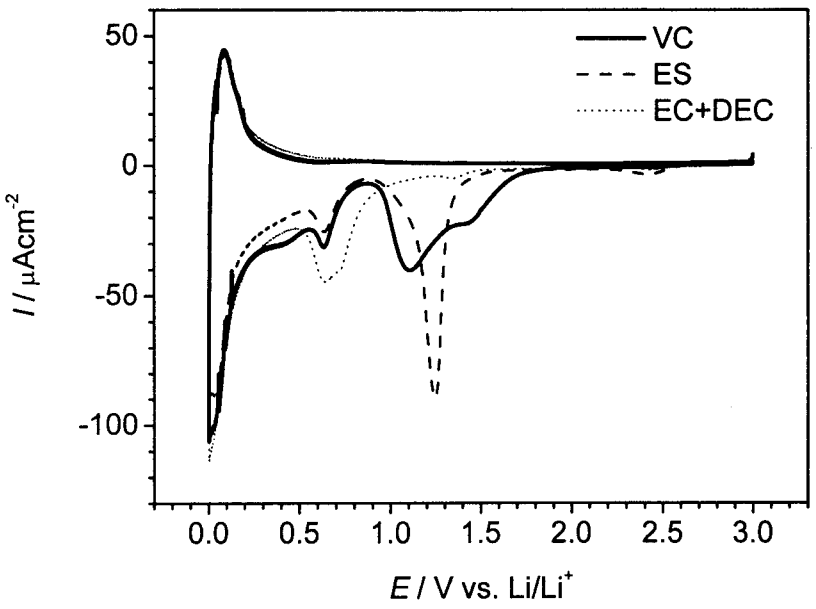

Fig. 6.4. Cyclic voltammograms (1st sweep) of pristine carbonaceous thin-film electrodes in EC solution containing additives. Solid line is obtained in the solution containing VC and dashed line is obtained in the solution containing ES. The dotted line represents the CV in EC solution. Sweep rate is 1 mV/s.

and 0.3 V (large), and lithium-ion insertion into the carbonaceous thin-film electrode in DEC based electrolyte did not occur, which is in good agreement with the literature [11]. Hence, the reduction peak at 0.6 V can be assigned to the decomposition of EC. The remained question is whether the reaction occurred at 0.6 V is related to the SEI formation at the intercalation sites. To characterize this peak, electrolytes of EC solution containing VC or ES were used. Figure 6.4 shows CVs of the pristine thin-film electrodes in EC solution containing VC (solid line) or ES (dashed line) and dotted line represents the CV in EC solution. In Fig. 6.4, VC decomposed around 1.8 - 0.9 V in the reduction process and the large peak observed in EC solution at around 0.6 V was decreased as compared with the dotted line in Fig. 6.4. Similar result was obtained by using ES; as is given in dashed line in Fig. 6.4, ES decomposed at around 1.3 V and the peak at 0.6 V was also decreased. It is well known that VC and ES are decomposed at higher potential than EC and the decomposed products form SEI at intercalation sites [12, 13]. These results indicated that the intercalation sites of carbonaceous thin film electrodes should be covered by SEI at the higher potential via the reductive decomposition of VC and ES. Therefore, VC or ES derived SEI at the intercalation sites suppressed the reductive reaction of EC at about 0.6 V. Hence, the reaction occurred at 0.6 V observed in EC solution in Fig. 6.3 is related to the SEI formation at intercalation sites.

From the above discussion and the result, the following mechanism would be predicted: oxygen atoms on carbonaceous thin-film electrodes gave C-O bonding, and the reaction products formed by the chemical or electrochemical reaction between these bonding and solvent, acted as SEI at the intercalation sites on the thin-film electrodes, leading to the suppression of further reductive reaction at about 0.6 V to form SEI.

6.4 Conclusion

Carbonaceous thin films prepared by plasma CVD were treated by O_2 plasma to conduct surface modification. The XPS measurements revealed that oxygen atoms were introduced into thin-film electrodes and C-O bonding was formed. Cyclic voltammograms showed that the decomposition of EC at the 1st reduction process was suppressed by the plasma modification and that this reduction process suppressed by surface modification is related to the formation of SEI. It is concluded that O_2 plasma modification is available for decrease of the irreversible capacity of carbon negative electrodes in the lithium-ion batteries.

References

1. Z. Ogumi and M. Inaba, *Bull. Chem. Soc. Jpn.*, 71, 521 (1998).
2. M. Winter, J. O. Besenhard, M. E. Spahr, and P. Novák, *Adv. Mater.*, 10, 725 (1998).
3. T. Nakajima, M. Koh, R. N. Singh, and M. Shimada, *Electrochim. Acta*, 44, 2879 (1999).
4. E. Peled, C. Menachem, D. Bar-Tow, and A. Melman, *J. Electrochem. Soc.*, 143, L4 (1996).
5. T. Takamura, *Bull. Chem. Soc. Jpn.*, 75, 21 (2002).
6. S.-S. Kim, Y. Kadoma, H. Ikuta, Y. Uchimoto, and M. Wakihara, *Electrochem. Solid-State Lett.*, 4, A109 (2001).
7. I. R. M. Kottegoda, Y. Kadoma, H. Ikuta, Y. Uchimoto, and M. Wakihara, *Electrochem. Solid-State Lett.*, 5, A275 (2002).
8. T. Fukutsuka, Y. Matsuo, Y. Sugie, T. Abe, M. Inaba, and Z. Ogumi, *Mol. Cryst. Liq. Cryst.*, 388, 117 (2002).
9. T. Abe, T. Fukutsuka, M. Inaba, and Z. Ogumi, *Carbon*, 37, 1165 (1999).
10. T. Fukutsuka, T. Abe, M. Inaba, and Z. Ogumi, *J. Electrochem. Soc.*, 148, A1260 (2001).
11. T. Iijima, K. Suzuki, and Y. Matsuda, *Synth. Metals*, 73, 9 (1995).
12. P. Biensan. J. M. Bodet, F. Perton, M. Broussely, C. Jehoulet, S. Barusseau, S. Herreyre, and B. Simon, Extended Abstracts of The 10th International Meeting on Lithium Batteries, Como, Italy, Abs. No. 286 (2000).
13. G. H. Wrodnigg, J. O. Besenhard, and M. Winter, *J. Electrochem. Soc.*, 146, 470 (1999).

Part 3

Lithium-ion transfer at interface between carbonaceous thin-film electrode and electrolyte

Chapter 7

Lithium-ion transfer at interface between carbonaceous thin-film electrode/electrolyte

7.1 Introduction

Since graphite and non-graphitizable carbonaceous materials have been used as negative electrode materials in lithium-ion batteries, various other kinds of carbonaceous materials have been extensively studied as negative electrodes for further improvement of lithium ion-batteries [1, 2]. Lithium-ion batteries have expanded their application area such as portable electronic devices and their production amount, and recently lithium-ion batteries are expected as an essential power sources for electric vehicles (EVs) and hybrid electric vehicles (HEVs) due to their high performance. The rate performance of lithium-ion batteries should be improved because high power density is required for use in EVs and HEVs.

The rate performance of lithium-ion batteries should be influenced by diffusion coefficients of lithium ion through active materials and by lithium-ion transport in electrolytes. In addition, it is reported that the interfacial lithium-ion transfer between electrode and electrolyte is a slow process [3, 4], and the lithium-ion transfer at the electrode/electrolyte interface should also affect the rate performance of lithium-ion batteries. However, the latter process has been ignored so far because structurally defined electrode/electrolyte interface including real active surface area was not easily attainable, while that is essential for precise studies on interfacial phenomena.

A thin-film electrode is preferable for the fabrication of structurally defined electrode/electrolyte interface. Various methods such as sputtering, pulsed laser deposition, chemical vapor deposition can give a thin film of various materials. Among these methods, Pulsed laser deposition is suitable for the preparation of positive thin-film electrodes [5-8] and plasma-assisted chemical vapor deposition (plasma CVD) is suitable for negative thin-film electrode of carbonaceous materials [9-12]. Electrochemical properties of fabricated thin-film electrodes have been examined and electrochemical properties of the thin-film electrodes are

identical to those of bulk positive and negative active materials. These results give the value of investigating on the interfacial phenomena, namely, ion transfer at interface employing the thin films of positive and negative electrodes.

In this chapter, lithium-ion transfer at the interface between the carbonaceous negative thin film electrode and the electrolyte is described and the high activation barrier at the interface for lithium-ion transfer is discussed.

7.2 Experimental

Carbonaceous thin films were deposited on substrates of nickel sheets from acetylene and argon by plasma CVD as shown in previous chapters. Substrates were placed on a ground electrode whose temperature was kept at 873 K and the applied rf power was set at 10 and 90 W. The resultant thin-film electrode was characterized by X-ray diffraction (XRD) (Rigaku, Rint-2500), Raman spectroscopy (Jobin-Yvon T64000), and transmission electron microscopy (TEM, Hitachi-9000).

Lithium-ion transfer through the interface between the resultant carbonaceous thin-film electrode and the electrolyte (a mixture (1:1 by volume) of ethylene carbonate (EC) and diethyl carbonate (DEC) containing 1 mol dm^{-3} $LiClO_4$) was studied by electrochemical impedance analysis using Sorlatron 1255 in the frequency range of 100 kHz - 10 mHz with a three-electrode cell. Lithium metal was used as counter and reference electrodes. Unless otherwise stated, potential is referred against Li/Li^+. Measurements of AC impedance spectra were carried out from 3 to 0.02 V. The electrode was held at each potential for 1 h to attain the condition of sufficiently low residual current after potential change. Prior to AC impedance measurements, cyclic voltammetry was conducted at a scan rate of 1 mV/s over 3 - 0 V, leading to the formation of passivating film on the carbonaceous thin-film electrodes.

7.3 Results and discussion

Fig. 7.1 shows XRD patterns of the resultant thin films prepared at applied rf powers of 10 and 90 W. As is obvious from Fig. 7.1, broad peaks are observed at around 26° in 2θ. This diffraction angle gives a value of d_{002} of ca. 0.342 nm, and therefore the crystallinity of these carbonaceous thin films is low. No obvious difference in crystallinity was obtained from XRD patterns between two thin carbonaceous thin films prepared at different rf powers.

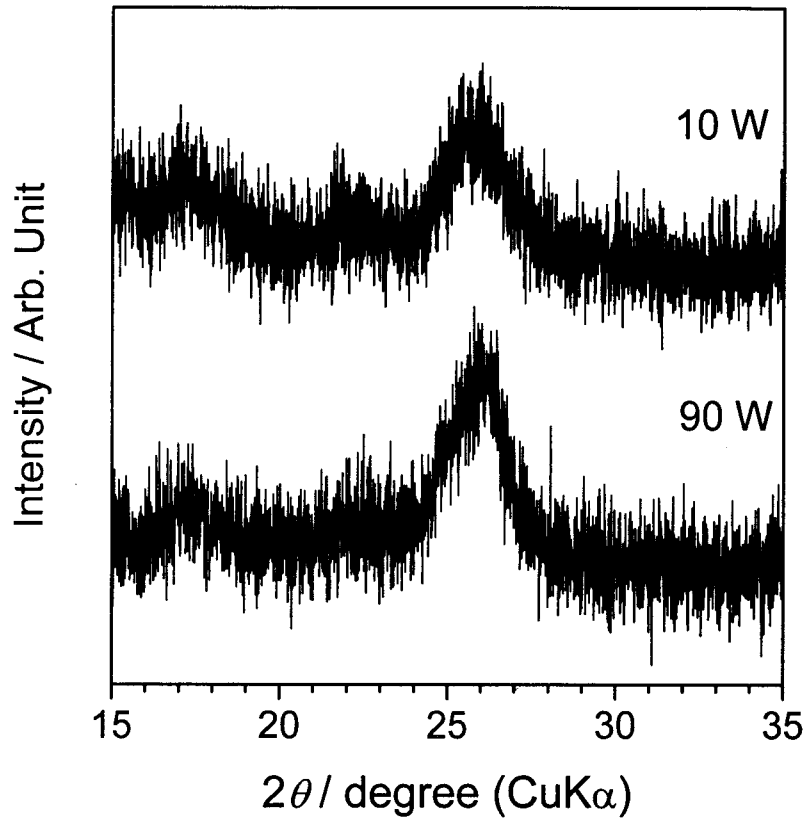

Fig. 7.1. XRD patterns of carbonaceous thin films prepared at applied rf powers of 10 and 90 W. Substrate was Ni sheet kept at 873 K.

In Fig. 7.2 are shown Raman spectra for resultant thin films prepared at different rf powers of 10 and 90 W. The spectra differ from each other in Raman active E_{1g} mode frequencies around 1600 cm^{-1}. For a thin film prepared at 10 W, only one broad peak appeared at 1600 cm^{-1}, while two peaks at 1580 and 1620 cm^{-1} were observed for a thin film prepared at 90 W. Full width at half maximum of peak for the E_{1g} mode is well known to be correlated with the crystallinity of carbonaceous materials [13], and hence the crystallinity of the thin film prepared at 90 W is somewhat higher than that at 10 W. This is supported by the TEM results; many lamellar structures were observed in the TEM image for the thin film prepared at 90 W while only a fewer lamellar structures appeared for the thin film prepared at 10 W.

The above facts given by XRD and TEM indicate that the bulk crystallinity of the carbonaceous thin films is not influenced significantly by the applied rf powers. On the other hand the crystallinity is lower at the surface zone than that at the bulk and the crystallinity at the surface zone is dependent on the applied rf powers.

Cyclic voltammograms for carbonaceous thin-film electrodes showed lithium-ion insertion and extraction mainly take place at potentials below 0.5 V, which agrees with the previous chapter. Figure 7.3 shows Nyquist plots for carbonaceous thin-film electrode prepared at applied rf power of 10 W. At potentials over 0.8 V, no semi-circle appeared and only capacitive behavior was observed. This fact indicates that no lithium-ion insertion into the carbonaceous thin-film electrode should occur at this potential. In contrast, one semi-circle in the higher frequency region was observed at potential below 0.5 V, and the resistances of the semi-circles decreased with decreasing the electrode potential. In chapter 1, the electrical conductivities of the carbonaceous thin films were evaluated to be 1 - 100 S/cm [9]. Since the thickness of the present films is around 0.3 - 0.5 μm, the resistances of the semi-circles should not be ascribed to the electrical resistances. In addition, the semi-circle was dependent on the salt concentration of electrolytes. Hence, the semi-circles should be ascribed to a relaxation process related to the lithium ion. Consequently, the semi-circles given in Fig. 7.3 can be assigned as charge-transfer (lithium-ion transfer) resistances.

In Fig. 7.4 are shown Nyquist plots for the carbonaceous thin-film electrode prepared at applied rf power of 90 W. Similarly to the results in Fig. 7.3, the semi-circles are observed at potential below 0.5 V, and the resistances decrease with decreasing the electrode potentials. In a similar manner, the semi-circles can be assigned again as the charge-transfer resistance.

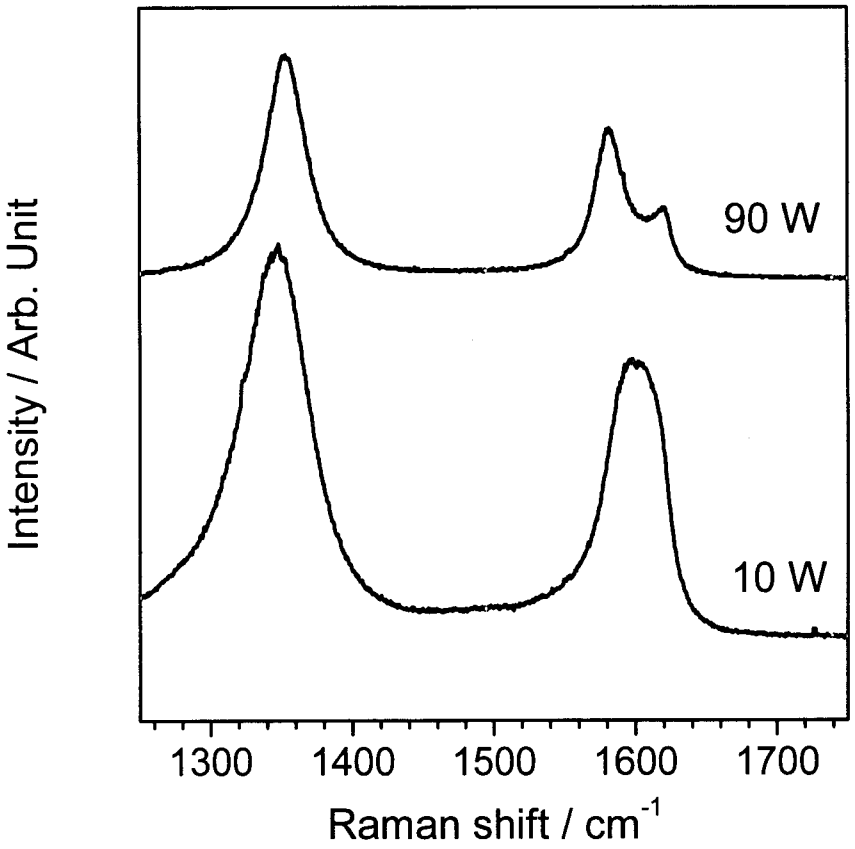

Fig. 7.2. Raman spectra of carbonaceous thin films prepared at applied rf powers of 10 and 90 W.

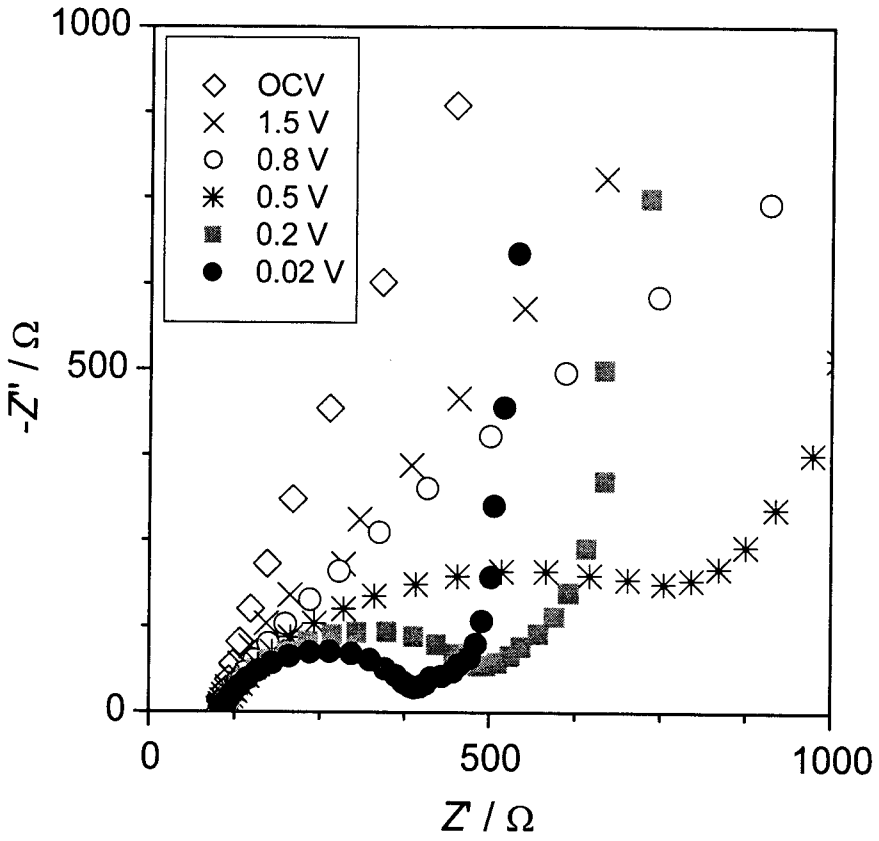

Fig. 7.3. Nyquist plots of carbonaceous thin-film electrode prepared at applied rf power of 10 W for lithium-ion insertion at various electrode potentials at ambient temperature. Super-imposed AC voltage for impedance measurement was set at 5 mV.

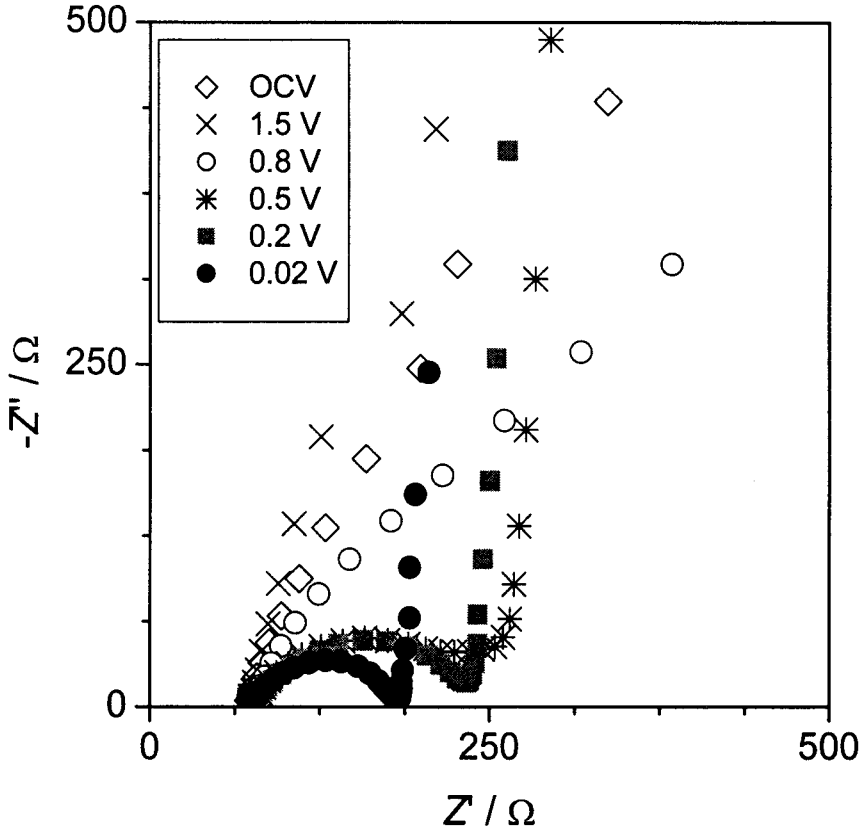

Fig. 7.4. Nyquist plots of carbonaceous thin-film electrode prepared at applied rf power of 90 W for lithium-ion insertion at various electrode potentials at ambient temperature. Super-imposed AC voltage for impedance measurement was set at 5 mV.

Two features should be pointed out for the comparison of the results as given in Figs. 7.3 and 7.4. One is the value of charge-transfer resistances. The carbonaceous thin-film electrode prepared at applied rf power of 90 W showed the charge-transfer resistance of half the value of that at 10 W. The charge-transfer resistances are correlated with reaction areas. Comparing the values of charge-transfer resistance, the reaction sites for lithium-ion insertion and extraction at the carbonaceous thin-film electrode prepared at rf power of 90 W is larger than those of thin-film electrode by rf power of 10 W, which is in good agreement with the TEM observation as mentioned above. The other point is the existence of Warburg impedance. In the intermediate frequency region in Fig. 7.3 at electrode potentials below 0.5 V, the Warburg impedances can be observed in the narrow region, and then capacitive behaviors appeared. On the contrary, no Warburg impedances can be seen in Fig. 7.4. That should be due to the film thickness. It is generally known that the larger rf power decreases the rate of thin-film deposition in plasma CVD such as plasma polymerization because of accelerated ablation [14], and therefore, the carbonaceous thin-film electrode prepared at rf power of 90 W was too thin to give Warburg impedances while the thickness was too low to be precisely estimated by weight increase.

The Nyquist plots in Fig. 7.3 should be interpreted by Voigt-Frumkin and Melik-Gaykazyan impedance as suggested by Levi et al. [15].

As mentioned above, the present thin-film electrode is sufficiently thin that one can obtain apparent lithium-ion diffusion coefficients using the following equation [16]:

$$D(\mathrm{Li}^+) = h^2 / 3R_{\mathrm{LF}}C_{\mathrm{LF}} \qquad \cdots \quad (1)$$

where C_{LF} is the limiting low frequency capacitance, R_{LF} the limiting low frequency resistance, and h denotes the film thickness. Fig. 7.5 shows the "apparent" lithium-ion diffusion coefficients evaluated by the above Eq. (1). The diffusion coefficients gave the maximum value at a potential around 0.3 V for both lithium-ion insertion and extraction. Nishizawa et al. [17] reported the electron and ion-transport properties for a single particle of mesocarbon microbeads heat-treated at 1273 K (MCMB1000). The electrical conductance and diffusion coefficient of lithium-ion for MCMB1000 were dependent on the lithium-ion content, and the dependency changed around 0.6 V, at which potential lithium-ion insertion

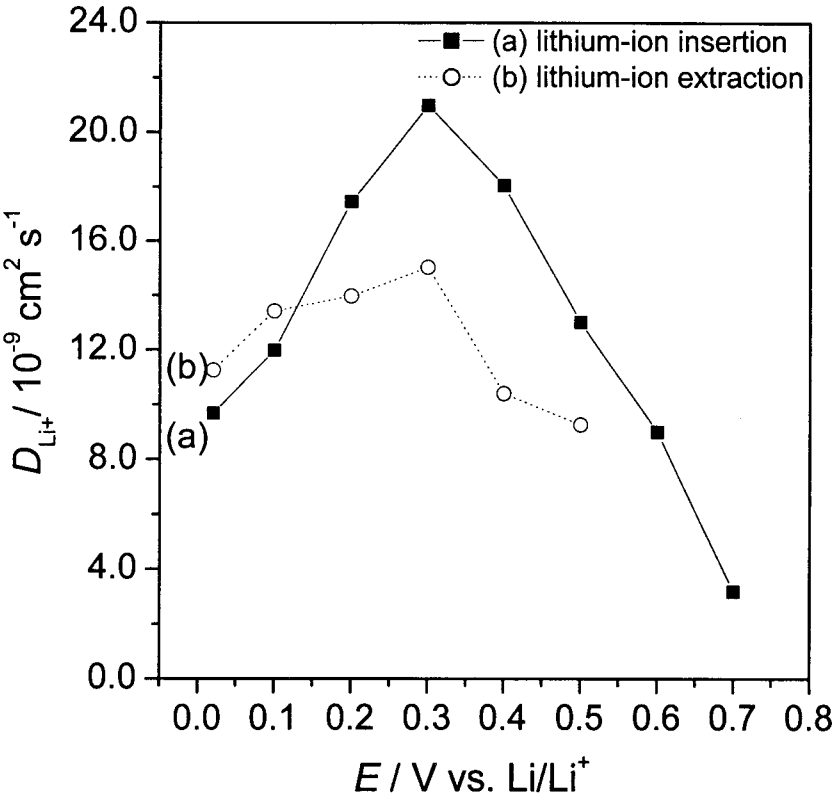

Fig. 7.5. Potential dependence of apparent diffusion coefficient D_{Li+} through carbonaceous thin-film electrode prepared at applied rf power of 10 W.

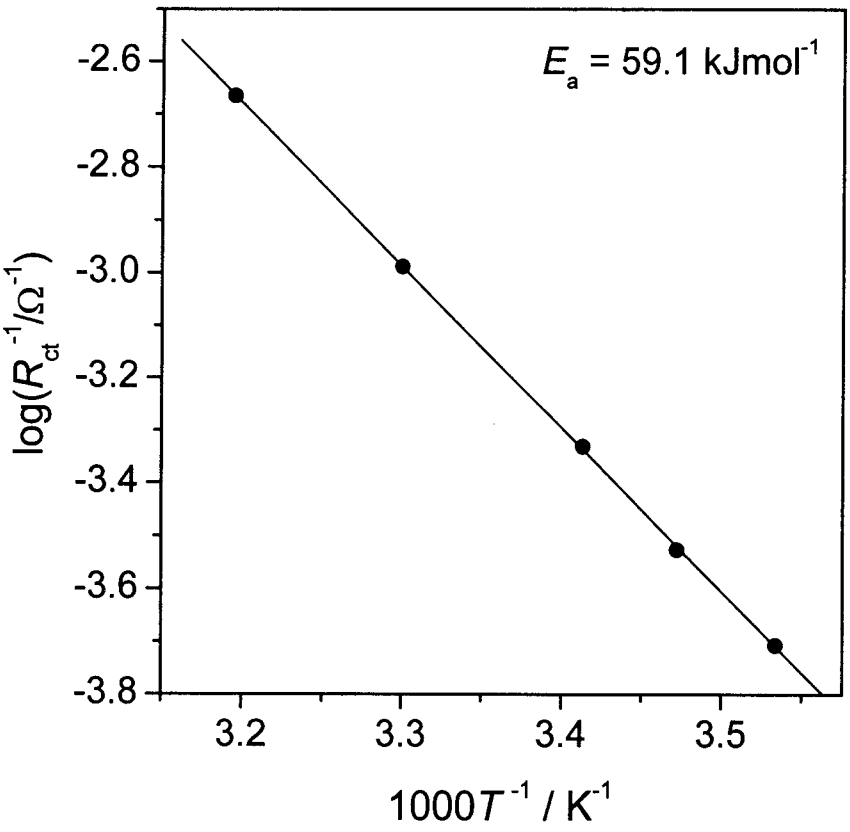

Fig. 7.6. Temperature dependence of charge-transfer resistance at the interface between carbonaceous thin-film electrode (prepared by applied rf power of 10 W) and electrolyte against reciprocal temperatures. The activation energy was evaluated by the least-square fitting.

mechanism should change [17]. These results are in good agreement with those reported by Nishizawa et al., although the potential at which the dependence of diffusion coefficients changes (0.3 V) is different.

It is well known that lithium-ion intercalation of graphite occurs below the potential of around 0.25 V vs. Li/Li^+ [18]. Raman spectroscopy and transmission electron microscopy revealed that the thin-film electrodes in this work possess graphitized and non-graphitized structures. Hence, the variation of diffusion coefficients given in Fig. 7.5 should be related to the change in lithium-ion insertion mechanism; "lithium-ion insertion into graphitized structures" or " lithium-ion insertion into non-graphitized structures".

The activation energy for interfacial lithium-ion transfer at a potential of 0.1 V was evaluated from the temperature dependence of the charge-transfer resistances as is shown in Fig. 7.6. As a result, a value of 59.1 $kJmol^{-1}$ was obtained for the carbonaceous thin-film electrode prepared at applied rf power of 10 W. Almost the same activation energies were obtained for a thin-film electrode prepared at rf power of 90 W. This value of activation energy is very large in comparison with the activation energy for lithium-ion conduction through crystalline solids of fast lithium-ion transfer [19] and through positive active material of $LiCoO_2$ [20]. Therefore, high barriers of activation for lithium-ion transfer exist at the interface between the solid-insertion electrode and electrolyte. Thus the lithium-ion transfer through the interface between electrode and electrolyte gives a significant influence on rate performance of lithium-ion batteries.

7.4 Conclusion

Carbonaceous thin films have been prepared by plasma CVD to obtain structurally defined electrode/electrolyte interface. Lithium-ion transfer at the interface between the thin-film electrode and the electrolyte were investigated by AC impedance spectroscopy. In the Nyquist plots, one semi-circle due to charge-transfer resistances appeared, and the values were dependent on electrode potentials. Lithium-ion diffusion coefficients were also evaluated by using the finite diffusion model. The diffusion coefficient was dependent on the electrode potentials. A high activation barrier was shown for interfacial lithium-ion transfer through the interface between carbonaceous thin-film electrode and electrolyte.

References

1. M. Winter, J. O. Besenhard, M. E. Spahr, and P. Novák, *Adv. Mater.*, **10**, 725 (1998).
2. Z. Ogumi and M. Inaba, *Bull. Chem. Soc. Jpn.*, **71**, 521 (1998).
3. A. Funabiki, M. Inaba, and Z. Ogumi, *J. Power Sources*, **68**, 227 (1997).
4. I. Yamada, T. Abe, Y. Iriyama, M. Inaba, and Z. Ogumi, *Electrochem. Commun.*, **5**, 502 (2003).
5. M. Inaba, Y. Iriyama, Z. Ogumi, Y. Todzuka, A. Tasaka, *J. Raman Spectrosc.*, **28**, 613 (1997).
6. Y. Iriyama, M. Inaba, T. Abe, and Z. Ogumi, *J. Power Sources*, **94**, 175 (2000).
7. Y. Iriyama, M. Inaba, T. Abe, and Z. Ogumi, *Solid State Ionics*, **135**, 95 (2000).
8. M. Inaba, T. Doi, Y. Iriyama, T. Abe, and Z. Ogumi, *J. Power Sources*, **82**, 554 (1999).
9. T. Abe, T. Fukutsuka, M. Inaba, and Z. Ogumi, *Carbon*, **37**, 1165 (1999).
10. T. Fukutsuka, T. Abe, M. Inaba, and Z. Ogumi, *J. Electrochem. Soc.*, **148**, A1260 (2001).
11. T. Fukutsuka, T. Abe, M. Inaba, and Z. Ogumi, *Mol. Cryst. Liq. Cryst.*, **340**, 517 (2000).
12. T. Abe, K. Takeda, T. Fukutsuka, Y. Iriyama, M. Inaba, and Z. Ogumi, *Electrochem. Commun.*, **4**, 310 (2002).
13. G. Katagiri, *Tanso*, **175**, 304 (1996) (*in Japanese*).
14. H. Yasuda and T. Hsu, *Surf. Sci.*, **76**, 232 (1978).
15. M. D. Levi, E. Levi, Y. Gofer, D. Aurbach, E. Vieil, and J. Serose, *J. Phys. Chem.*, **103**, 1499 (1999).
16. C. Ho, I. D. Raistrick, and R. A. Huggins, *J. Electrochem. Soc.*, **127**, 343 (1980).
17. M. Nishizawa, H. Koshika, R. Hashitani, T. Itoh, T. Abe, and I. Uchida, *J. Phys. Chem.*, **103**, 4933 (1999).
18. K. Tatsumi, N. Iwashita, H. Sakaebe, H. Shioyama, S. Higuchi, A. Mabuchi, and H. Fujimoto, *J. Electrochem. Soc.*, **142**, 716 (1995).
19. Y. Inaguma, C. Liquan, M. Itoh, and T. Nakamura, *Solid State Comm.*, **86**, 689 (1993).
20. K. Nakamura, H. Ohno, K. Okamura, Y. Michihiro, I. Nakabayashi, and T. Kanashiro, *Solid State Ionics*, **135**, 143 (2000).

Chapter 8

Influences of ion-solvent interaction on lithium-ion transfer at the interface of carbonaceous thin film-electrode/electrolyte

8.1 Introduction

Lithium-ion batteries have expanded their production area commencing with portable devices, such as handy phones, personal computers, camcorders, etc. [1, 2]. Moreover, lithium-ion batteries have been expected as power sources in electric vehicles and hybrid electric vehicles due to their high energy densities. For these applications, high rate performance of lithium-ion batteries should be improved because high power densities are required for electric vehicles and hybrid electric vehicles.

Lithium-ion transfer at the carbon negative electrode is divided into some processes shown as follows; 1) migration and/or diffusion in the electrolyte, 2) migration and/or diffusion in the passivation film (solid electrolyte interface; SEI), 3) diffusion in the solid phase (carbonaceous material), and 4) lithium-ion transfer at the interface between electrode and electrolyte. Among them, the processes of 1) and 3) have been studied by many researchers. It is very difficult to clarify the second process, since the SEI layer is too thin. The study about the lithium-ion transfer at the electrode/electrolyte interface, the process of 4), has been dismissed so far. In chapter 7, it was clarified that the activation energy of lithium-ion transfer at electrolyte/electrolyte interface is high [3]. In addition, T. Abe et al. reported that the activation energy of solvated lithium-ion transfer was smaller than that of lithium-ion transfer accompanying with de-solvation process [4]. These results indicate that the lithium-ion transfer at the electrode/electrolyte interface should be a slow process in the lithium-ion battery system. And therefore, lithium-ion transfer process will impair the rate performance of lithium-ion batteries. Hence, to clarify the details of lithium-ion transfer at interface accompanying with de-solvation process is very important.

In order to study the interfacial phenomena at the carbonaceous electrode in detail, structurally defined electrode/electrolyte interface is required. To construct well-defined

electrode/electrolyte interface, there are two important points; flat surface electrode, which enables us to evaluate reaction area of electrode and good contact between electrolyte and electrode are essential. The former, thin-film electrodes are ideal for fabrication of structurally defined electrode/electrolyte interface. In our previous studies, it was clear that surface of carbonaceous thin film is very flat and pin-hole-free and the film is suitable for evaluating the electrochemical properties as active materials for negative electrodes [3, 5-11]. In terms of the latter point, the good contact between electrolyte and electrode can be attained by using electrolyte solutions. Based on these considerations, we have constructed electrode/electrolyte interface by using carbonaceous thin-film electrode and electrolyte solution.

In this chapter, the well-defined interfaces between carbonaceous thin-film electrode and various electrolyte solutions are constructed and the influences of ion-solvent interaction on the activation energy of lithium-ion transfer at the interface of carbonaceous thin-film electrode/electrolyte was discussed.

8.2 Experimental

Carbonaceous thin films were deposited on substrates of nickel sheet from acetylene and argon as shown in the previous chapters. Substrates were placed on a ground electrode whose temperature was kept at 873 K and the applied rf power was set at 10 W.

A three-electrode cell was used to perform the electrochemical measurements. Lithium metal was used as counter and reference electrodes, and the electrolyte solutions were 1 mol dm^{-3} $LiClO_4$/ethylene carbonate (EC)+diethyl carbonate (DEC) (1:1 by volume), 1 mol dm^{-3} $LiClO_4$/propylene carbonate (PC), 1 mol dm^{-3} $LiCF_3SO_3$/dimethyl sulfoxide (DMSO), 1 mol dm^{-3} $LiClO_4$/dimethyl carbonate (DMC), and 1 mol dm^{-3} $LiCF_3SO_3$/1,2-dimethoxy ethane (DME). Unless otherwise stated, the potential is referred against Li/Li^+. The cell was assembled in an argon-filled glove box. Cyclic voltammetry (CV) and electrochemical impedance spectroscopy (EIS) are performed as electrochemical measurements. Cyclic voltammograms were obtained from the range of 3 - 0 V with the sweep rate for 1 mV/s (RADIOMETER, VoltaLab 21) and EIS was conducted by using Sorlatron 1260 impedance gain-phase analyzer and Sorlatron 1286 electrochemical interface in the frequency range of 100 kHz - 10 mHz by using ZPlot 2 program. Measurement was carried out with ac amplitude 5 mV. Lithium-ion transfer at the interface between

(a)

Procedure 1 (Proc.1)

Cyclic voltammetry in each objective electrolyte solution
(three cycles)

↓

Holding potential at 0.05 V or 0.1 V for 12 h

↓

Holding potential at 0.1 V until current is under 1 μA

↓

AC impedance measurement at various temperature

(b)

Procedure 2 (Proc.2)

Cyclic voltammetry in 1 mol dm^{-3} $LiClO_4$ / EC+DEC (1:1)
(first sweep)

↓

Holding potential at 0.05 V for 12 h

↓

Washing the electrode by DMC and changing to objective electrolyte solution

↓

Cyclic voltammetry in changed electrolyte solution
(second sweep)

↓

Holding potential at 0.1V for 12 h

↓

AC impedance measurement at various temperature

Fig. 8.1. Flow charts of experimental procedures in this study. (a) Procedure 1 (Proc.1) and (b) Procedure 2 (Proc.2).

carbonaceous thin-film electrodes and electrolytes was studied by the following two methods. The procedures (Proc.1 and Proc.2) of two methods are shown in Fig. 8.1. The difference between Proc.1 and Proc.2 is the formation process of SEI on the carbonaceous thin-film electrodes. For Proc.1, SEI is formed from the decomposition of each solvent, and for Proc.2, SEI is formed in EC+DEC solution in advance. The effect of the different methods mentioned above on lithium-ion transfer at carbonaceous thin-film electrode will be described later.

8.3 Results and Discussion

Structure of carbonaceous thin films is described in the previous chapters. Typical Nyquist plot of carbonaceous thin-film electrode at 0.05 V in EC+DEC solution is shown in Fig. 8.2. At potentials above 1.1 V, no clear semi-circle appeared and only blocking-electrode-type behaviors were observed. This fact indicates that almost no lithium-ion insertion into the carbonaceous thin-film electrode should occur at this potential, which is in good agreement with the previous results [8, 10]. In contrast, one semi-circle in the higher frequency region was observed at potential below 1.0 V, and the resistances of the semi-circles decreased with decreasing the electrode potential. In chapter 1, the electrical conductivities of the carbonaceous thin films were evaluated to be 1 - 100 S/cm [5]. Since the thickness of the present thin films is around 0.6 μm, the resistances of the semi-circles should not be ascribed to the electrical resistances. In addition, the semi-circle was dependent on the salt concentration of electrolytes [3, 10]. Hence, the semi-circles should be ascribed to a relaxation process related with lithium ion. Consequently, the semi-circle given in Fig. 8.2 can be assigned as the lithium-ion transfer resistance at the electrode/electrolyte interface.

Cyclic voltammograms (CVs) for the carbonaceous thin-film electrodes in each electrolyte solution (EC+DEC, PC, DMSO, and DMC solutions) are shown in Fig. 8.3. For the first sweep, large irreversible reduction was observed from the potential around 1.3 to 0.4 V in all electrolyte solutions. However, it almost disappeared after the second sweep. And reduction/oxidation peak for lithium-ion insertion/extraction is clearly observed at around 0.1 V. These results indicate that the decomposition of solvent and formation of SEI on the surface of carbonaceous thin-film electrodes occurred effectively and lithium-ion insertion/extraction can take place at the carbonaceous thin-film electrode in all electrolyte solutions.

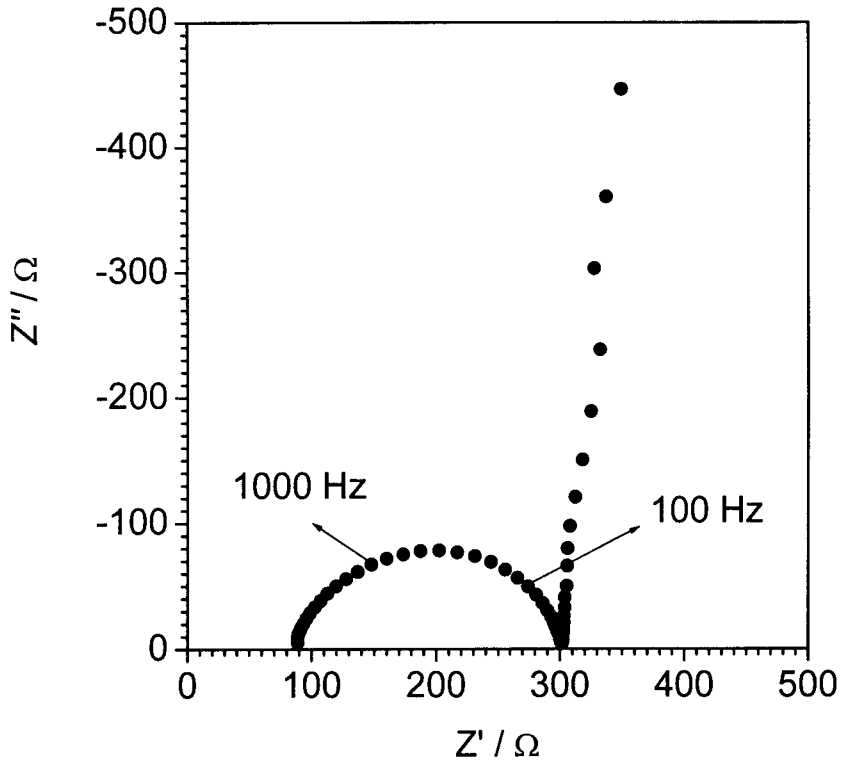

Fig. 8.2. Typical Nyquist plot of carbonaceous thin-film electrode obtained in 1 mol dm^{-3} $LiClO_4$/EC+DEC at 0.05 V.

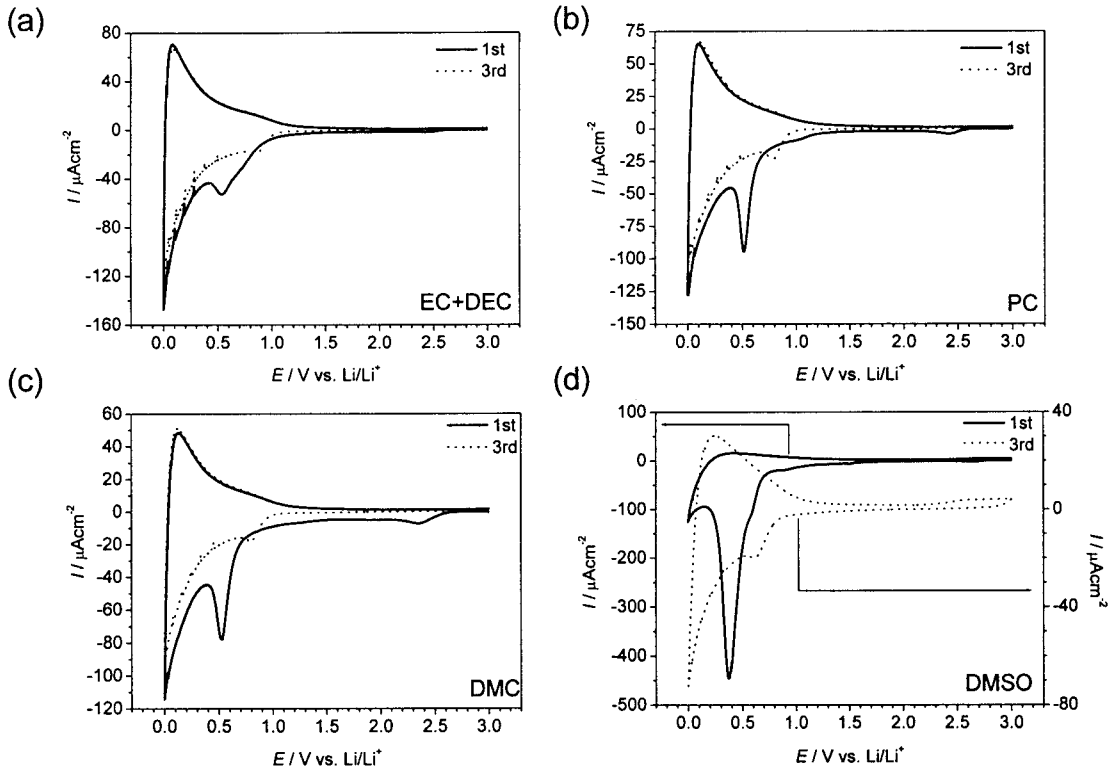

Fig. 8.3. Cyclic voltammograms (1st and 3rd sweep) of carbonaceous thin-film electrodes. Electrolyte solutions are (a) 1 mol dm^{-3} $LiClO_4$/EC+DEC, (b) 1 mol dm^{-3} $LiClO_4$/PC, (c) 1 mol dm^{-3} $LiClO_4$/DMC, and (d) 1 mol dm^{-3} $LiCF_3SO_3$/DMSO. Sweep rate is 1 mV/s.

Nyquist plots for the carbonaceous thin-film electrodes at 0.1 V in each solution are shown in Fig. 8.4. Electrode potential was held at 0.05 V or 0.1 V to attain the steady state. The semi-circles shown in Fig. 8.4 are assigned to the charge-transfer resistance as described above. The value of the charge-transfer resistances were dependent on the solutions used. Since the number of reaction sites for lithium-ion insertion/extraction and the nature of SEI affect the charge-transfer resistances, we cannot simply discuss about the values of charge-transfer resistances. Then, the energy barriers of activation at the interface between an electrode and each electrolyte solution were evaluated by the temperature dependency of the charge-transfer resistances. Figure 8.5 shows Arrhenius plots of the charge-transfer resistances using the Proc.1 described in the experimental section. In this Proc.1, SEI is formed by the reductive decomposition of the electrolyte solutions. The activation energies calculated from the slopes in Fig. 8.5 were in the order of DMSO (84.2 kJ mol^{-1}), PC (61.3 kJ mol^{-1}), EC(+DEC) (59.1 kJ mol^{-1}), and DMC (62.4 kJ mol^{-1}). To some extent, the order of the activation energies corresponds with the Gutmann's donor number [12], which is defined as the negative enthalpy change for the interaction of the electron-donor solvent with $SbCl_5$ in dichloroethane. Donor numbers of DMSO, EC, and PC are reported to be 29.8, 16.4, and 15.1, respectively [12]. Although the donor number of DMC has not been reported, the donor number of DEC, whose structure is similar to that of DMC, is reported to be 15.1 [12]. The donor number of DMC may be similar to that of DEC. It is very clear that the solvents giving high activation energies possess high value of donor numbers. Therefore, it is concluded that ion-solvent interaction in electrolytes gives large influence on the activation barriers at electrode/electrolyte interface.

Based on the above results, activation energies of lithium-ion transfer at electrode/electrolyte interface are ascribed to the energy gap between the energy of activated state and that of solvated lithium ion. From above results, it is found that the energies of solvated lithium ion directly affect the activation energies. However, the influence of the SEI on the energy of activated state was not considered. If SEI affects the energy of activated state, SEI may change the activated states. In the Proc.1, the SEI on the carbonaceous thin-film electrodes was formed by the decomposition of each solution, and therefore, the nature of SEI should be dependent on the solvents used. It is necessary to eliminate the influence of SEI on the energies of activated states for the detail analysis of activation energies for lithium-ion

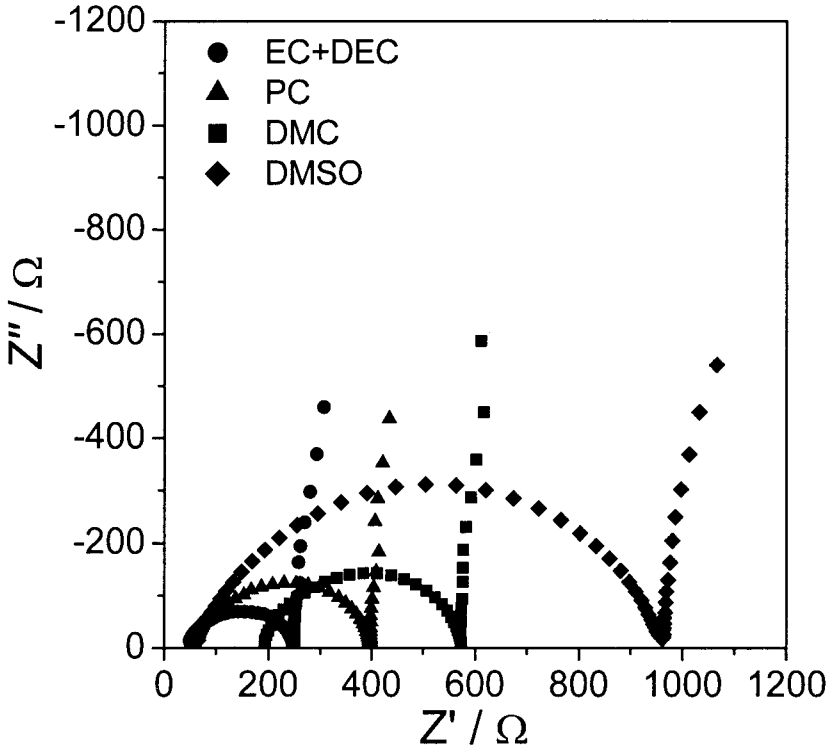

Fig. 8.4. Nyquist plots of carbonaceous thin-film electrodes obtained in various electrolytes at 0.1 V. Electrolyte: 1 mol dm^{-3} $LiClO_4$/EC+DEC, 1 mol dm^{-3} $LiClO_4$/PC, 1 mol dm^{-3} $LiClO_4$/DMC, and 1 mol dm^{-3} $LiCF_3SO_3$/DMSO.

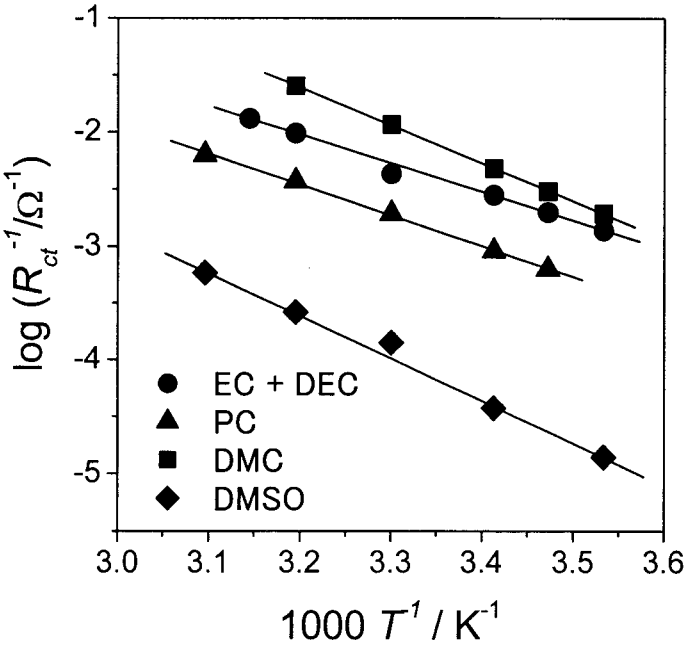

Fig. 8.5. Temperature dependence of charge-transfer resistances at the electrode/electrolyte interface for carbonaceous thin-film electrodes in various electrolytes. Electrolytes are 1 mol dm^{-3} $LiClO_4$/EC+DEC, 1 mol dm^{-3} $LiClO_4$/PC, 1 mol dm^{-3} $LiClO_4$/DMC, and 1 mol dm^{-3} $LiCF_3SO_3$/DMSO. Electrode potential is 0.1 V.

transfer.

Then, the Proc.2 in Fig. 8.1 was selected to eliminate the influence of SEI on the energies of activated states. In the Proc.2, the process to form SEI was carried out by using EC+DEC solution. Previously, it was confirmed that the SEI on carbonaceous thin-film electrodes in EC+DEC solution was formed by the decomposition of EC [11]. It is assumed that the SEI formed on carbonaceous thin-film electrodes in EC+DEC is formed from EC and serves as effective SEI in other solutions. In order to confirm above assumption, CVs were measured by using the solution, in which lithium-ion insertion/extraction dose not easily occur at carbonaceous thin-film electrode. Figure 8.6(a) shows CVs (first and second sweep) of carbonaceous thin-film electrode in 1 mol dm^{-3} $LiCF_3SO_3$/DME solution. In Fig. 8.6(a), clear oxidative peak was not observed at 0.1 V, corresponding to lithium-ion extraction. Therefore, it is not easy for lithium ion to insert/extract into/from the carbonaceous thin-film electrode in DME solution, indicating that the SEI on the electrode should not be available. Figure 8.6(b) shows CV of carbonaceous thin-film electrode in DME solution, after holding the electrode potential at 0.05 V for 12 h in EC+DEC solution to sufficient thick SEI [13] and then replacing the electrolyte. The shape of CV was similar to the shape at second sweep obtained in EC+DEC and lithium-ion insertion/extraction into/from carbonaceous thin-film electrode occurred in DME solution. Therefore it is concluded that SEI formed by the reductive decomposition of EC exist on the carbonaceous thin-film electrode by Proc.2 and that SEI serves effectively. By using carbonaceous thin-film electrode treated by Proc.2, the SEI is the same in all electrode/electrolyte interfaces, so that the influence of SEI can be eliminated, which makes it possible that only the influence of solvent can be discussed.

To clarify the influence of ion-solvent interaction on lithium-ion transfer at electrode/electrolyte interface, CV and EIS measurements were carried out by using Proc.2. The shapes of CV (second sweep) in each solution were almost identical with that in Fig. 8.6(b), indicating that SEI formed in EC+DEC serves effectively in all solutions. Nyquist plots for carbonaceous thin-film electrodes at 0.1 V in each solution (EC+DEC, PC, DMSO, and DMC) are shown in Fig. 8.7. Nyquist plots in Fig. 8.7 show semi-circles in the middle frequency range ascribing to the charge-transfer resistances. Figure 8.8 shows the temperature dependency of the charge-transfer resistances at the carbonaceous thin-film electrode. The activation energies calculated from the slopes were in the order of DMSO (82.3 kJ mol^{-1}) >

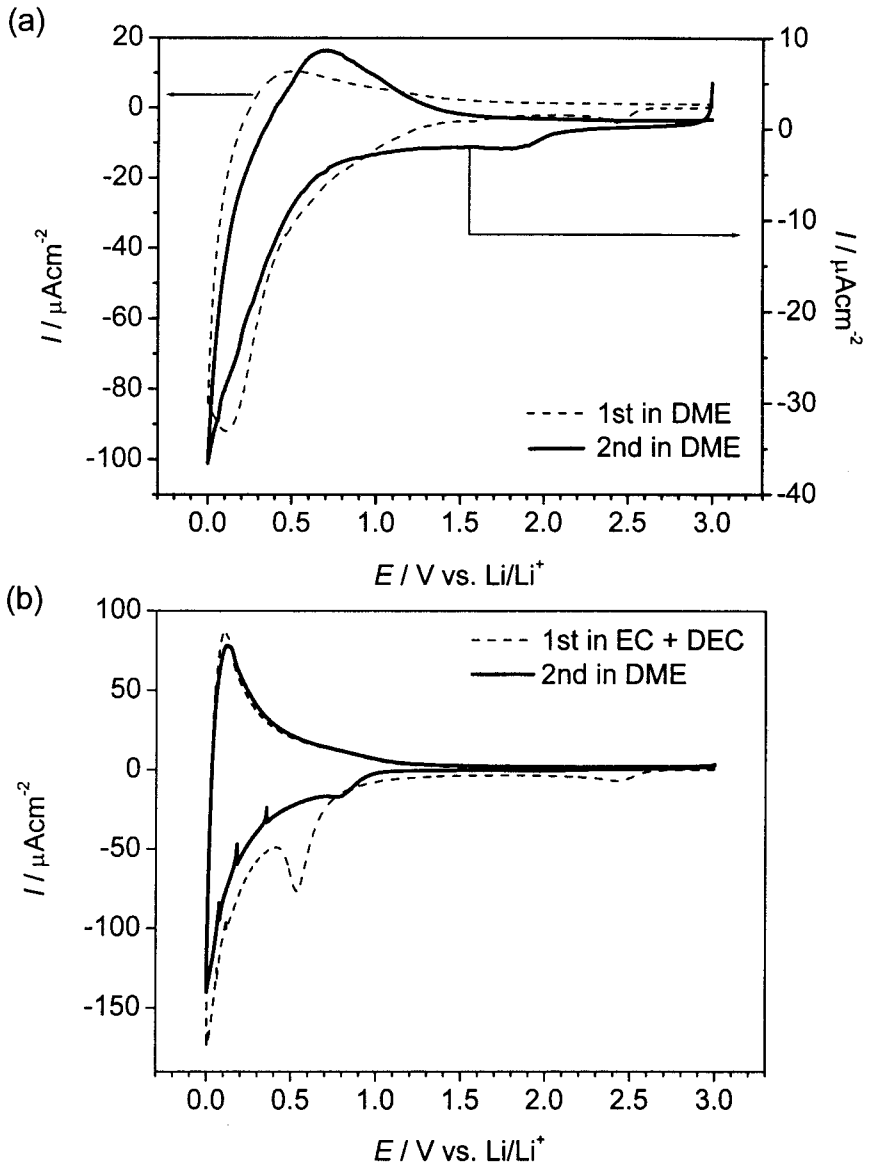

Fig. 8.6. Cyclic voltammograms of carbonaceous thin-film electrodes. (a) Pristine carbonaceous thin-film electrode, and electrolyte solution is 1 mol dm^{-3} $LiCF_3SO_3$/DME. (b) 1st cycle is pristine carbonaceous thin-film electrode in 1 mol dm^{-3} $LiClO_4$/EC+DEC. 2nd cycle is carbonaceous thin-film electrode with SEI formed from EC in 1 mol dm^{-3} $LiCF_3SO_3$/DME. Sweep rate is 1 mV/s.

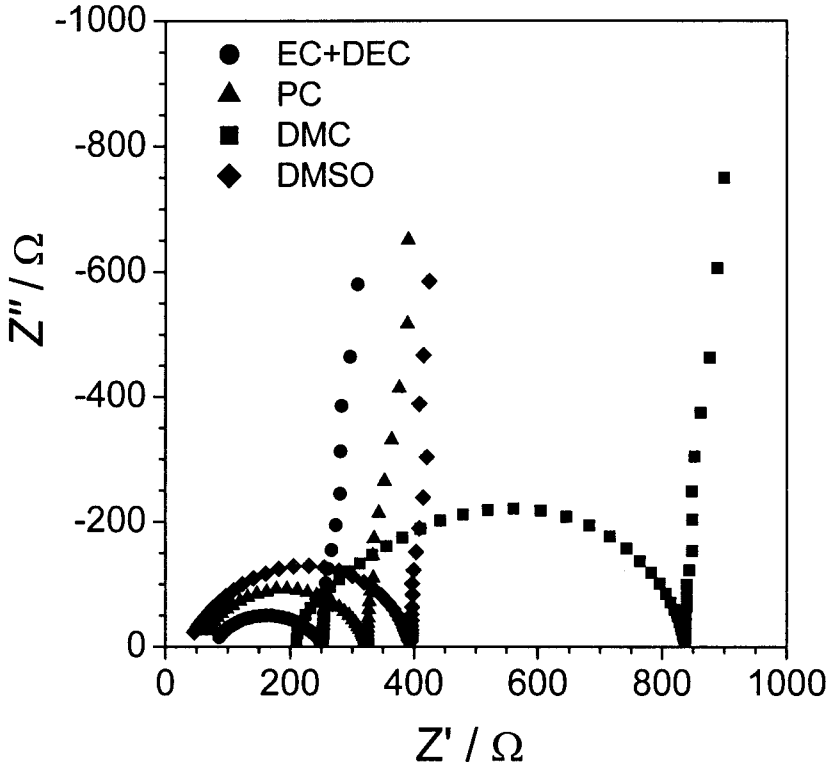

Fig. 8.7. Nyquist plots of carbonaceous thin-film electrodes with SEI formed from EC obtained in various electrolytes at 0.1 V. Electrolytes are 1 mol dm^{-3} $LiClO_4$/EC+DEC, 1 mol dm^{-3} $LiClO_4$/PC, 1 mol dm^{-3} $LiClO_4$/DMC, and 1 mol dm^{-3} $LiCF_3SO_3$/DMSO.

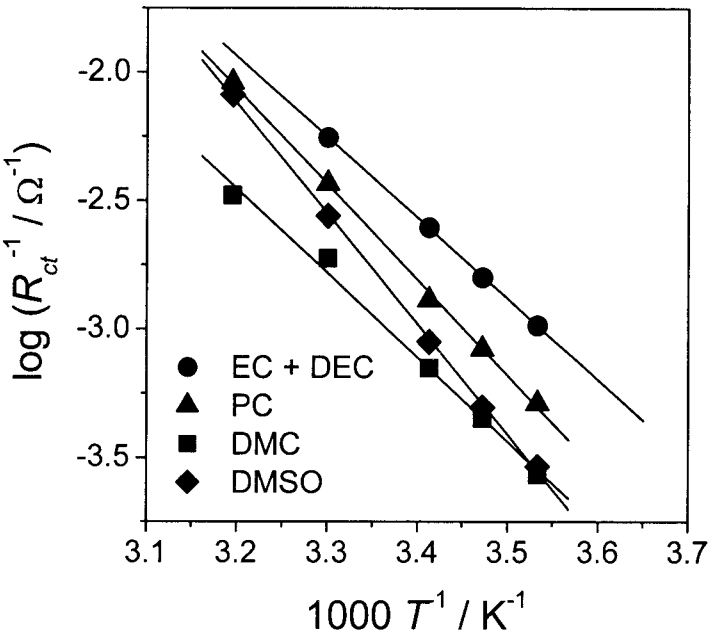

Fig. 8.8. Temperature dependence of charge-transfer resistances at the electrode/electrolyte interface for carbonaceous thin-film electrodes with SEI derived from EC in various electrolytes. Electrolyte: 1 mol dm^{-3} $LiClO_4$/EC+DEC, 1 mol dm^{-3} $LiClO_4$/PC, 1 mol dm^{-3} $LiClO_4$/DMC, and 1 mol dm^{-3} $LiCF_3SO_3$/DMSO. Electrode potential is 0.1 V.

PC (71.2 kJ mol^{-1}) > DMC (62.8 kJ mol^{-1}) ≈ EC (+DEC) (60.2 kJ mol^{-1}). These values are almost identical with those obtained by Proc.1 except for the value in PC solution. This result suggests that activation energy of lithium-ion transfer at the electrode/electrolyte interface should be strongly influenced by ion-solvent interaction as mentioned above, since the energy of activated state is not affected by the difference of SEI using this process of Proc.2. The reason why activation energies using PC solution vary by the method of SEI formation is not cleared. From above results, it is concluded that the activation energies of lithium-ion transfer at electrode/electrolyte interface are determined by the energies of solvated lithium ion, that is, ion-solvent interaction of lithium-ion batteries. These results suggest that improvement of rate performance requires the decrease of interaction between lithium ion and solvent.

8.4 Conclusion

Interfacial lithium-ion transfer was examined by using carbonaceous thin-film electrodes and various solutions. The activation energies of lithium-ion transfer at the interface of carbonaceous thin-film electrode/electrolyte were influenced by the electron donicities of the solvents used. Further, it made clear that SEI does not affect the activation energies. Therefore, the lithium-ion transfer at the carbonaceous electrode is concluded to be influenced by the degree of interaction between lithium ion and solvents.

References

1. M. Winter, J. O. Besenhard, M. E. Spahr, and P. Novák, *Adv. Mater.*, **10**, 725 (1998).
2. Z. Ogumi and M. Inaba, *Bull. Chem. Soc. Jpn.*, **71**, 521 (1998).
3. Z. Ogumi, T. Abe, T. Fukutsuka, S. Yamate, and Y. Iriyama, *J. Power Sources*, **127**, 72-75 (2004).
4. T. Abe, H. Fukuda, Y. Iriyama, and Z. Ogumi, *J. Electrochem. Soc.*, **151**, A1120 (2004).
5. T. Abe, T. Fukutsuka, M. Inaba, and Z. Ogumi, *Carbon*, **37**, 1165 (1999).
6. T. Fukutsuka, T. Abe, M. Inaba, and Z. Ogumi, *Mol. Cryst. Liq. Cryst.*, **340**, 517 (2000).
7. T. Fukutsuka, T. Abe, M. Inaba, Z. Ogumi, Y. Matsuo and Y. Sugie, *Carbon Science*, **1**, 129 (2001)
8. T. Fukutsuka, T. Abe, M. Inaba, and Z. Ogumi, *J. Electrochem. Soc.*, **148**, A1260 (2001).
9. T. Abe, K. Takeda, T. Fukutsuka, Y. Iriyama, M. Inaba, and Z. Ogumi, *Electrochem.*

Commun., **4**, 310 (2002).

10. T. Abe, T. Fukutsuka, S. Yamate, Y. Iriyama, M. Inaba, and Z. Ogumi, *Mol. Cryst. Liq. Cryst.*, **388**, 141 (2002).
11. T. Fukutsuka, Y. Matsuo, Y. Sugie, T. Abe, M. Inaba, and Z. Ogumi, *Mol. Cryst. Liq. Cryst.*, **388**, 117 (2002).
12. V. Gutmann, *Electrochim. Acta*, **26**, 661 (1976).
13. M. Umeda, K. Dokko, Y. Fujita, M. Mohamedi, I. Uchida, and J. R. Selman, *Electrochim. Acta*, **47**, 885 (2001).

Chapter 9

Electrochemical properties of graphitized carbonaceous thin films prepared by plasma-assisted chemical vapor deposition

9.1 Introduction

Natural graphite and highly graphitized artificial graphite have been used as negative electrodes in lithium-ion batteries [1, 2]. Lithium-ion batteries are used worldwide in the portable electronic devices such as cellular phones, notebook computers, PDAs, etc. Lithium-ion batteries have also attracted attention because of their potential use in hybrid electric vehicles (HEVs). The high power performance of lithium-ion batteries is required for use in HEVs, and therefore fast charge and discharge reactions, i.e., the rapid transport of lithium-ion from the positive to negative electrodes via electrolyte is essential. One of the practical approaches to achieving rapid ion-diffusion is to decrease the diffusion path in the battery active materials. In this sense, the fabrication of thin-film electrodes is a very ideal approach. Much work has been conducted on the preparation of positive thin-film electrodes by using sputtering [3-5], pulsed laser deposition [6-9], sol-gel method [10, 11], etc. In contrast, little attention has been paid to the preparation of graphitized thin-film electrodes [12, 13].

In the chapter 4, it was reported the preparation of graphitized thin films by using plasma-assisted chemical vapor deposition (plasma CVD). The obtained thin film showed a highly graphitized structure with a less-crystallized surface, i.e., core-shell-type thin films were synthesized [12]. Since the surface shows low crystallization, the electrochemical properties of the electrode in propylene carbonate (PC)-based electrolyte were almost the same as those in ethylene carbonate (EC)-based electrolytes. The use of PC-based electrolytes should be beneficial for the lower-temperature use of lithium-ion batteries. The thickness of the resultant thin-film electrode is less than 1.0 μm. Therefore, lithium-ion should diffuse very rapidly in this electrode. Another problem using thin-film electrodes is charge-transfer resistance. The surface area of a thin-film electrode is restricted compared to a composite

electrode. Therefore, interfacial reactions between thin-film electrodes and the electrolyte should be studied.

In this chapter, graphitized carbonaceous thin-film electrodes with different bulk crystallinities were synthesized by plasma CVD, and their electrochemical properties together with interfacial reactions were studied by cyclic voltammetry and AC impedance spectroscopy. Lithium-ion transfer at the interface between the electrode and electrolyte will be discussed.

9.2 Experimental

The apparatus used for plasma CVD has been described in detail in previous chapters. The starting materials of acetylene and argon gases were used as a carbon source and plasma assist gas, respectively. Carbonaceous thin films were deposited on substrates of nickel sheets kept at a temperature of 1023 K [13]. The deposition time was 3 h. Glow discharge plasma was generated between rf and ground electrodes by an rf power supply of 13.56 MHz, and the applied rf power was set at 10, 50 and 90 W. The flow rates of argon and acetylene were set at 25 and 10 sccm, respectively. The total pressure of the reaction chamber was kept at 133 Pa.

The resultant thin films were characterized by scanning electron microscopy (SEM), X-ray diffraction (XRD; Rint-2200), and Raman spectroscopy (Jobin-Yvon, T64000).

Electrochemical properties were studied by cyclic voltammetry using a three-electrode cell. Carbonaceous thin-film electrode was used as a working electrode. Lithium metal was used for both counter and reference electrodes. The scanning range was 0 - 3 V vs. Li/Li^+ with a sweep rate of 0.1 mV/s. Electrolytes consisting of PC and a mixture of EC and diethyl carbonate (DEC) (1:1 by volume) containing 1 mol dm^{-3} $LiClO_4$ were used. Interfacial reactions between the electrode and electrolyte were studied by AC impedance spectroscopy using VoltaLab40 (Radiometer) over the frequency region from 100 kHz to 10 mHz using the same three-electrode cell. All experiments were conducted under an Ar atmosphere.

9.3 Results and discussion

Figures 9.1(a), 9.1(b), and 9.1(c) show XRD patterns of the carbonaceous thin films prepared by applied rf powers of 10, 50, and 90 W, respectively. As shown in Fig. 9.1(a), a very sharp peak appeared at 26.6° in 2θ. The peak position for the thin film prepared at 50 W

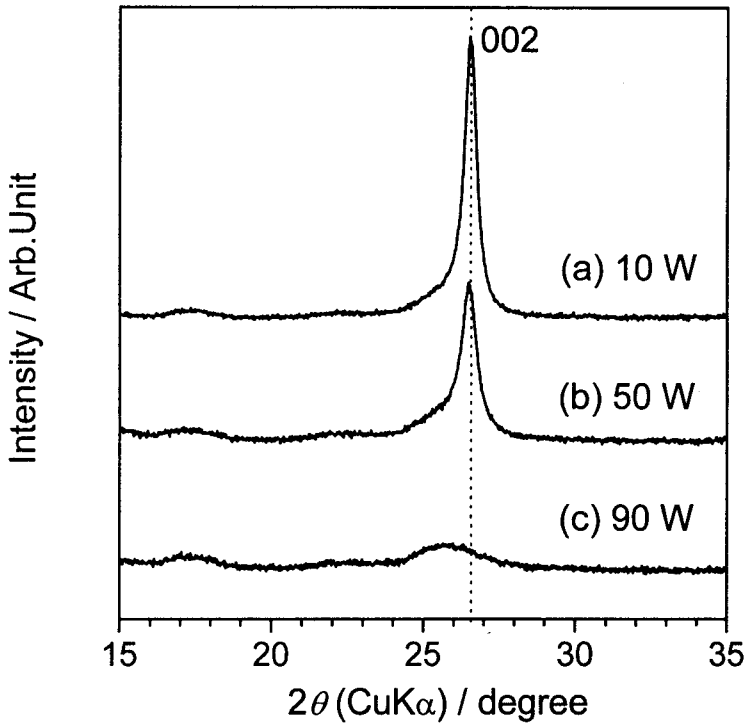

Fig. 9.1. XRD patterns of carbonaceous thin films prepared at applied rf powers of (a) 10 W, (b) 50 W, and (c) 90 W.

is also observed at 26.6°, however, the full width at half maximum of the peak in Fig. 9.1(b) is slightly wider than that in Fig. 9.1(a), indicating that the thin film prepared at 10 W is more crystallized than that at 50 W. In Fig. 9.1(c), a very broad peak was observed at around 26°. Therefore, the crystallinity of the thin film prepared at 90 W should be very low. A substrate of nickel sheet should act as a catalyst, leading to the graphitization of carbonaceous thin films. At 90 W, the rate of etching for carbon is much faster than at 10 and 50 W. Therefore, bulk graphitization did not occur.

Figure 9.2 shows Raman spectra for thin films prepared at rf powers of 10, 50, and 90 W. Three peaks appeared at around 1350, 1580, and 1620 cm^{-1}. The peaks at 1350 and 1620 cm^{-1} are ascribed to the crystal imperfection of graphite [17], and the peak at 1580 cm^{-1} corresponds to G band, which is related to the graphitic structure [17]. The G band is clearly seen for the film prepared at 90 W, indicating that the thin film surface has higher crystallinity than those in thin films prepared at 10 and 50 W. After deconvolution, the intensity ratio of the peaks at 1350 and 1580 cm^{-1}, I_{1350}/I_{1580}, was evaluated. The ratio of I_{1350}/I_{1580} is correlated with the crystallinity of carbonaceous materials [18]. In contrast to the XRD results, crystallinity increased with increasing rf power, which is in good agreement with the chapter 2 [16]. Since Raman spectroscopy gives information near the surface, the carbonaceous thin films in the present work likely possess high crystallinity inside the bulk with a less-crystallized surface, and the difference in crystallinity between inside the bulk and the surface increases with a decrease in the applied rf power.

SEM observation revealed that the obtained thin films were less than 1.0 μm thick. The thin films were so thin that the ratios of highly crystallized to less-crystallized carbons could not be evaluated.

Cyclic voltammograms for carbonaceous thin-film electrodes prepared at an rf power of 10 W have been reported [13]. Figure 9.3 shows the cyclic voltammograms of graphitized carbonaceous thin-film prepared at 50 W in an electrolyte of EC+DEC containing 1 mol dm^{-3} $LiClO_4$. For the first sweep, an irreversible reduction current was observed at around 0.8 V vs. Li/Li^+, but it almost disappeared after the second sweep, indicating that SEI was formed on the carbonaceous thin-film electrode at the first sweep. Even for the second sweep, redox peaks are observed at around 0.9 V. Based on the findings by XRD and Raman spectroscopy given in Figs. 9.1 and 9.2, carbonaceous thin film prepared at 50 W contains a less

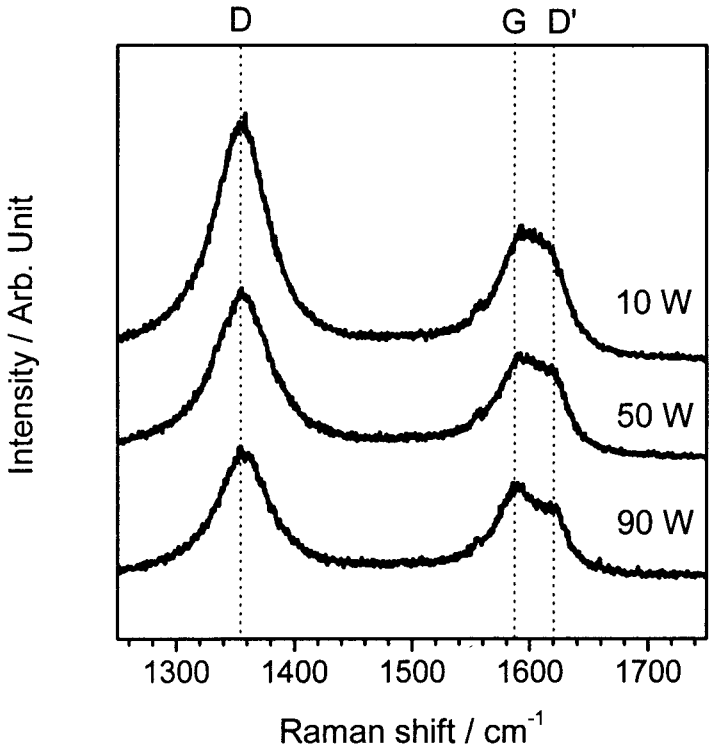

Fig. 9.2. Raman spectra of carbonaceous thin films prepared at applied rf powers of 10, 50, and 90 W.

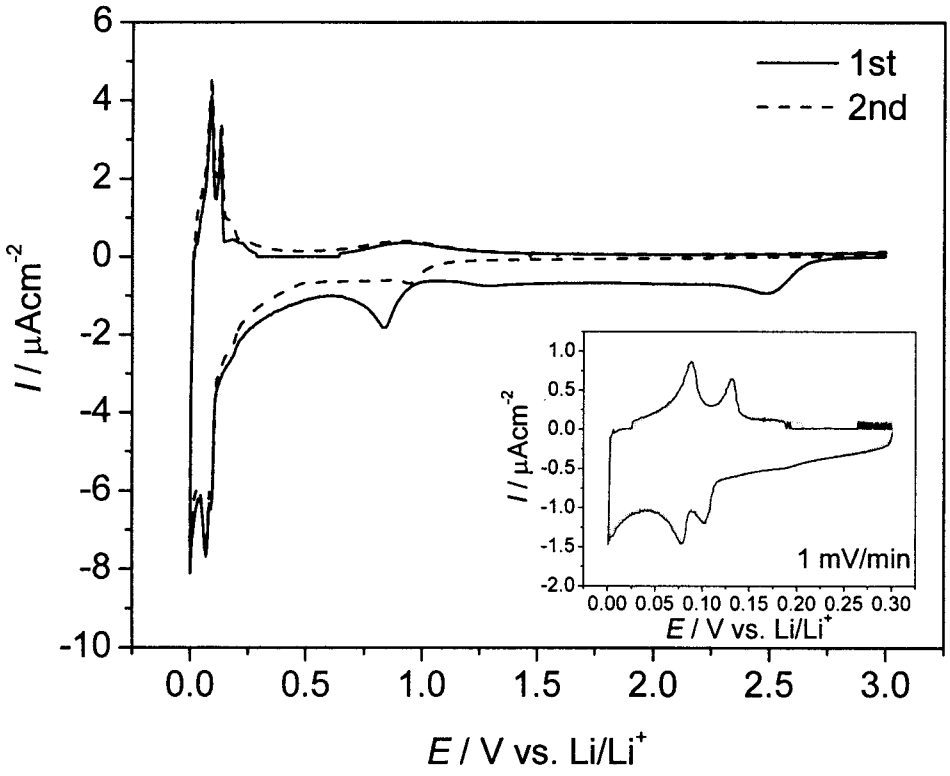

Fig. 9.3. Cyclic voltammograms of carbonaceous thin-film electrode prepared at applied rf power of 50 W in 1 mol dm^{-3} $LiClO_4$/EC+DEC (1:1). Sweep rate; 0.1 mV/s. Inset is referred to cyclic voltammogram of the same electrode in the potential range of 0 - 0.3 V at a sweep rate of 1 mV/min.

crystallized part. Therefore, insertion of lithium-ion into the less-crystallized part occurred at higher potentials. The capacities at higher potentials were also confirmed by charge and discharge measurements. As is readily apparent from the inset in Fig. 9.3, oxidation and reduction peaks at around 0.1 V were split. Splitting of the peak at around 0.1 V is observed for a graphite negative electrode due to stage transformation [19-22]. Hence, the electrochemical properties of the present thin-film electrodes are very similar to those of graphite negative electrodes [23], which is in good agreement with structural considerations. The cyclic voltammogram for a carbonaceous thin-film electrode prepared at 90 W is almost the same as that reported for the less-crystallized carbonaceous thin-film electrodes [16].

Figure 9.4(a) shows Nyquist plots for a carbonaceous thin-film electrode prepared at an rf power of 10 W in an electrolyte of EC+DEC (1:1 by volume) containing 1 mol dm^{-3} $LiClO_4$. Electrode potentials were 0.8 - 1.2 V. Cyclic voltammetry was conducted for two cycles in the range of 3 - 0 V in advance to form SEI on the electrode. At a potential of 1.2 V, only one semi-circle appeared in the higher frequency region followed by capacitive behavior. Based on the results of the cyclic voltammogram, no lithium-ion insertion or extraction occurs at this potential, and therefore the thin-film electrode should act as a blocking electrode. The semi-circle in the higher frequency region is derived from SEI on the electrode. When the potential decreased to 1.0 V, a large semi-circle with a characteristic frequency of 2.5 Hz appeared. The resultant carbonaceous thin-film electrode shows an electric conductivity of greater than 100 S/cm [14], and hence this semi-circle is not due to electrical resistance of the electrode. In addition, this semi-circle was dependent on the salt concentration of the electrolyte, indicating that the semi-circle in the lower frequency region is associated with the relaxation process related to lithium ion. Based on these considerations, this semi-circle can be identified as charge-transfer (lithium-ion transfer) resistance. Unless otherwise stated, charge-transfer resistance was clarified by chaining the salt concentration of electrolyte and electrode potential dependency. The charge-transfer resistance drastically decreased with a decrease in the electrode potentials. Figure 9.4(b) shows the Nyquist plots for carbonaceous thin film electrodes at potentials of 0.02 - 0.5 V. As is clear from this figure, semi-circles due to SEI and charge-transfer resistance completely overlap and apparently only one semi-circle is observed. By deconvolution of the Nyquist plot at a potential of 0.9 V, the semi-circle at a higher frequency region gives a resistance of ca. 250 Ω. By considering the resistance of SEI,

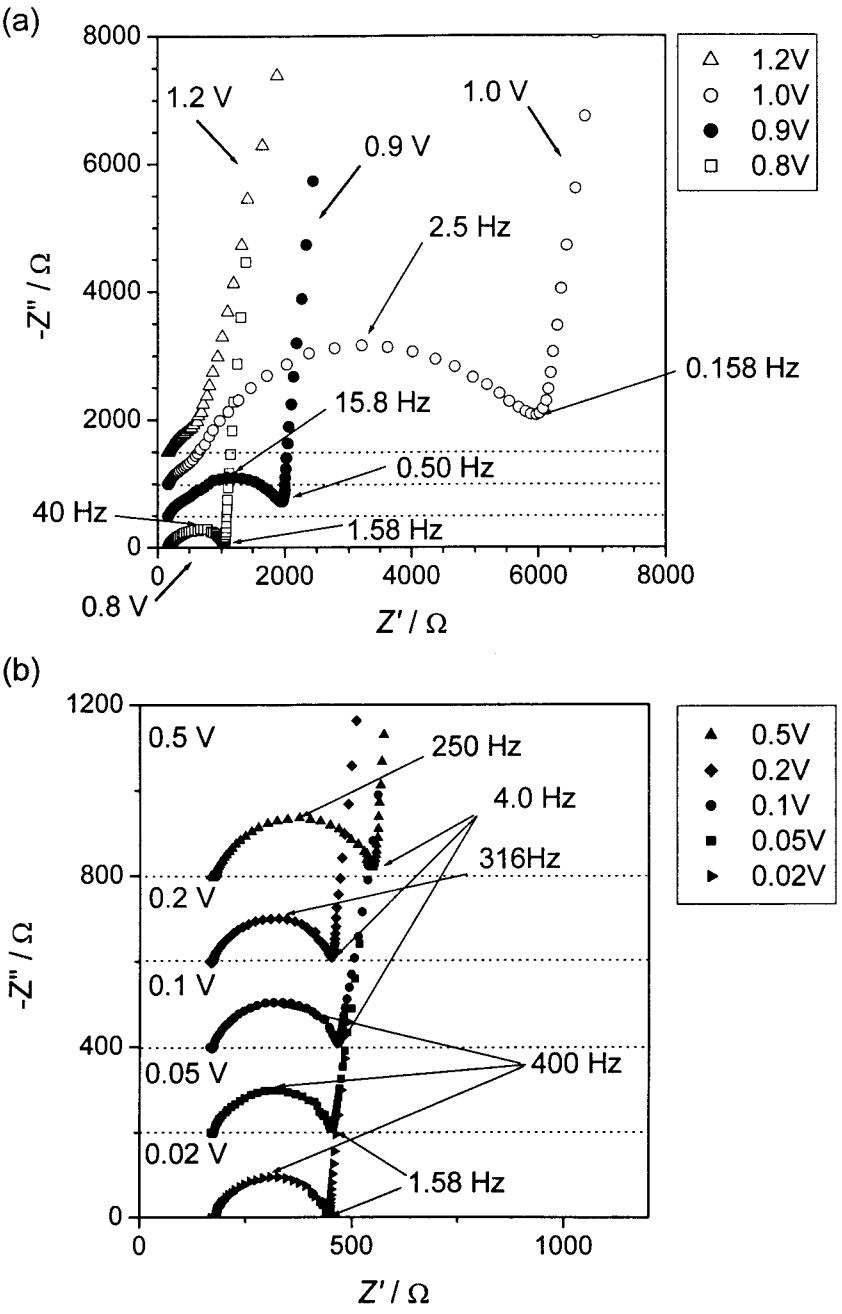

Fig. 9.4. Nyquist plots of carbonaceous thin-film electrode prepared at applied rf power of 10 W in 1 mol dm^{-3} $LiClO_4$/EC+DEC (1:1). (a) Electrode potential is kept at 0.8, 0.9, 1.0, and 1.2 V vs. Li/Li^+. (b) Electrode potential is kept at 0.02, 0.05, 0.1, 0.2 and 0.5 V vs. Li/Li^+.

the charge-transfer resistance becomes very low at lower potentials. The apparent surface area for the thin-film electrodes in this work was kept constant at 0.58 cm^2. Even for such small areas, charge-transfer resistance is very small. This is due to the less-crystallized surface. If the present thin-film electrode shows *c*-axis orientation, the effective sites for lithium-ion insertion and extraction would become small, leading to high charge-transfer resistance. In this sense, the present core-shell-type carbonaceous thin-film electrodes are very suitable for the fabrication of thin-film batteries.

Figure 9.5(a) shows Nyquist plots for a carbonaceous thin-film electrode prepared at an rf power of 50 W in an electrolyte of EC+DEC containing 1 mol dm^{-3} $LiClO_4$. Electrode potentials were 0.6 - 0.9 V. Similar to the result given in Fig. 9.4(a), only one semi-circle due to SEI was observed at a higher frequency region followed by capacitive behavior at a potential of 0.9 V. At a lower potential of 0.8 V, charge-transfer resistance was observed in the mid to low frequency regions. Again, similar to the carbonaceous thin-film electrode prepared at 10 W, the charge-transfer resistance decreased with a decrease in the electrode potentials, as shown in Figs. 9.5(a) and 9.5(b).

Figures 9.6(a) and 9.6(b) show the Nyquist plots for a carbonaceous thin-film electrode prepared at an rf power of 90 W. Similar to the thin-film electrodes prepared at 10 and 50 W, the charge-transfer resistance showed an identical dependence on the electrode potential. The charge-transfer resistance was the greatest for a carbonaceous thin-film electrode prepared at 90 W as is readily seen in Figs. 9.4(b), 9.5(b), and 9.6(b). Charge-transfer resistance is principally due to the effective reaction sites of the electrode. By Raman spectroscopy, the highest crystallinity of the carbonaceous thin-film electrode surface was seen for 90 W thin film, which was associated with fewest reaction sites for lithium-ion insertion and extraction. Therefore, it is quite reasonable that the largest charge-transfer resistance is seen for 90 W thin film.

For the fabrication of a thin-film battery using a carbonaceous thin-film electrode, the bulk electrochemical properties of graphite should be the best due to its flat potential as low as lithium metal, reversibility, etc. On the other hand, the surface of the thin film should be less crystallized because a PC-based electrolyte can be used, thus enabling lithium-ion batteries to be used at a lower temperature. Based on these requirements, carbonaceous thin-film electrodes prepared at an rf power of 10 W should be ideal for the fabrication of thin

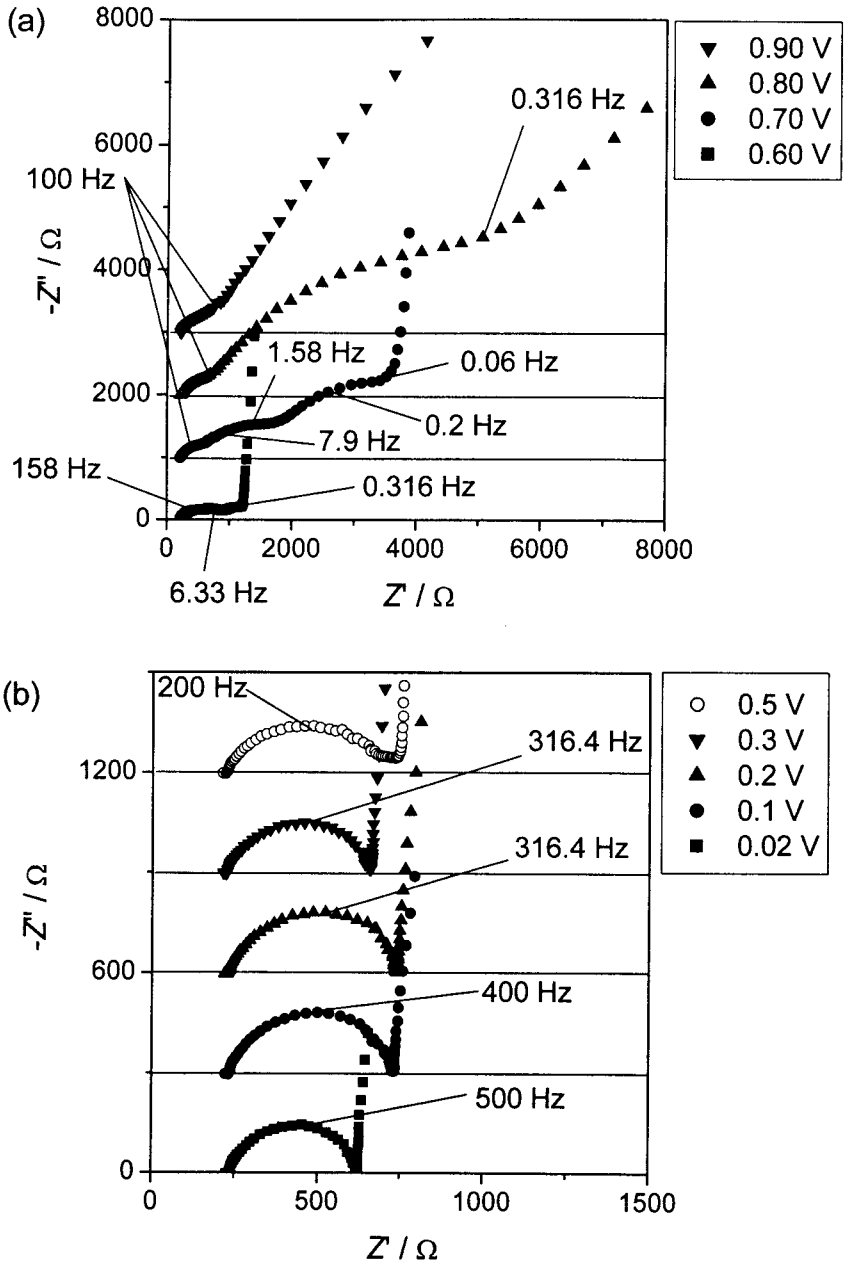

Fig. 9.5. Nyquist plots of carbonaceous thin-film electrode prepared at applied rf power of 50 W in 1 mol dm^{-3} $LiClO_4$/EC+DEC (1:1). (a) Electrode potential is kept at 0.6, 0.7, 0.8, and 0.9 V vs. Li/Li^+. (b) Electrode potential is kept at 0.02, 0.1, 0.2, 0.3 and 0.5 V vs. Li/Li^+.

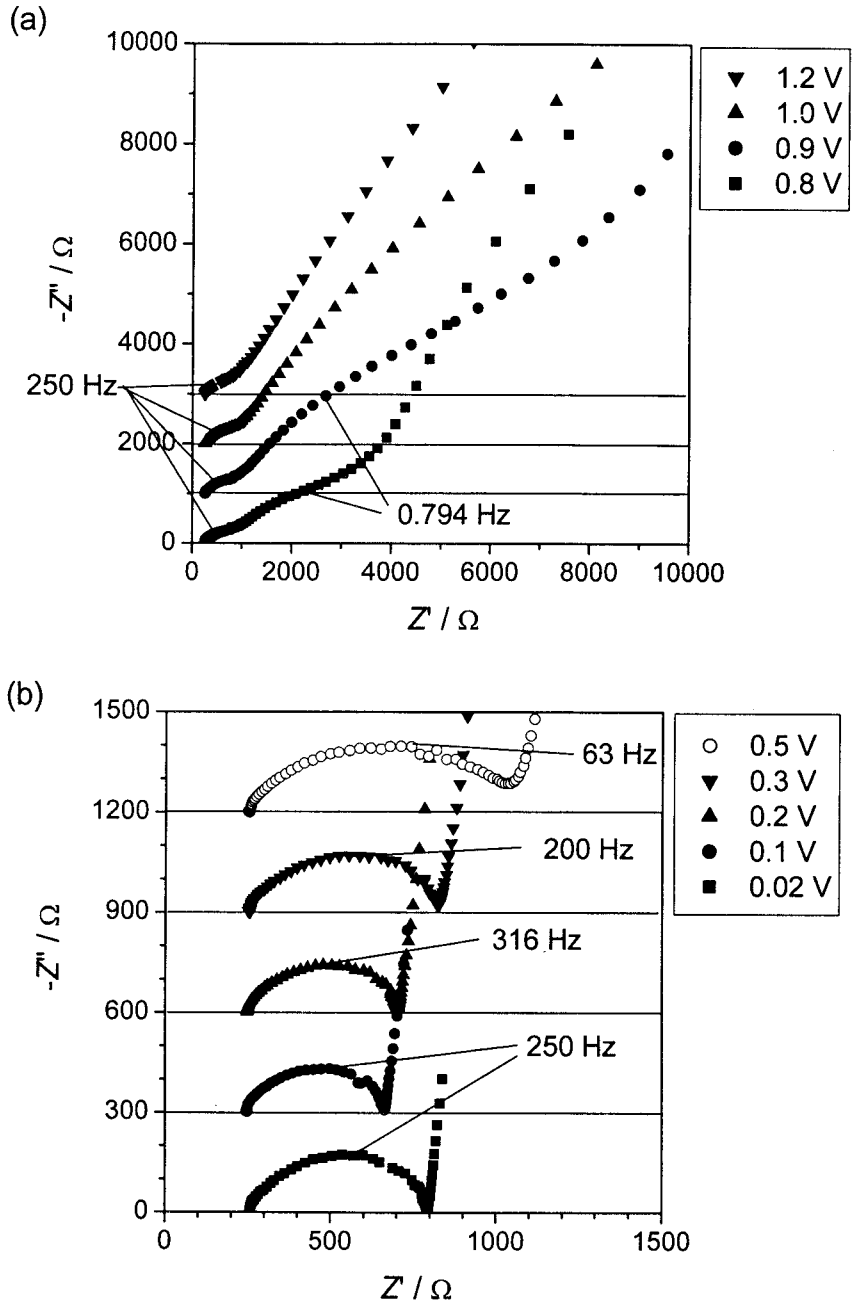

Fig. 9.6. Nyquist plots of carbonaceous thin-film electrode prepared at applied rf power of 90 W in 1 mol dm^{-3} $LiClO_4$/EC+DEC (1:1). (a) Electrode potential is kept at 0.8, 0.9, 1.0, and 1.2 V vs. Li/Li^+. (b) Electrode potential is kept at 0.02, 0.1, 0.2, 0.3 and 0.5 V vs. Li/Li^+.

film batteries, as also supported by the least total resistance in the Nyquist plots.

9.4 Conclusion

Core-shell-type carbonaceous thin film electrodes were prepared by plasma-assisted chemical vapor deposition (plasma CVD). This CVD process gave a highly graphitized carbonaceous thin-film electrode with a less-crystallized surface. By changing the applied rf power, the difference in crystallinity between the interior bulk and surface could be controlled. Since the surface of the thin films was less crystallized, propylene carbonate-based electrolyte can be used for graphitized carbonaceous thin-film electrodes.

AC impedance spectroscopy revealed the charge-transfer resistances of the resultant thin-film electrodes, and a carbonaceous thin-film electrode prepared at an rf power of 10 W showed the minimum value of charge-transfer resistance.

These results suggest that highly graphitized carbonaceous thin films with a much less-crystallized surface should be ideal electrodes for the fabrication of thin film batteries.

References

1. Z. Ogumi and M. Inaba, *Bull. Chem. Soc. Jpn.*, **71**, 521 (1998).
2. M. Winter, J. O. Besenhard, M. E. Spahr, and P. Novak, *Adv. Mater.*, **10**, 725 (1998).
3. B. Wang, J. B. Bates, F. X. Hart, B. C. Sales, R. A. Zuhr, and J. D. Robertson, *J. Electrochem. Soc.*, **143**, 3203 (1996).
4. S. Yamamura, H. Koshika, M. Nishizawa, T. Matsue, and I. Uchida, *J. Solid State Electrochem.*, **2**, 211 (1998).
5. B. J. Neudecker, R. A. Zuhr, J. D. Robertson, and J. B. Bates, *J. Electrochem. Soc.*, **145**, 4160 (1998)
6. Y. Iriyama, M. Inaba, T. Abe, and Z. Ogumi, *J. Power Sources*, **94**, 175 (2001).
7. Y. Iriyama, T. Abe, M. Inaba, and Z. Ogumi, *Solid State Ionics*, **135**, 95 (2000).
8. M. Inaba, T. Doi, Y. Iriyama, T. Abe, and Z. Ogumi, *J. Power Sources*, **82**, 554 (1999).
9. P. J. Bouwman, B. A. Boukamp, H. J. M. Bouwmeester, and P. H. L. Notten, *J. Electrochem. Soc.*, **149**, A699 (2002).
10. M. K. Kim, H. T. Chung, Y. J. Park, J. G. Kim, J. T. Son, K. S. Park, and H. G. Kim, *J. Power Sources*, **99**, 34 (2001).

11. S. I. Pyun, S. W. Kim, and J. M. Ko, *J. New Mater. Electrochem. Systems*, **5**, 135 (2002).
12. M. Mohri, N. Yanagisawa, Y. Tajima, T. Tanaka, T. Mitate, S. Nakajima, M. Yoshida, M. Yoshimoto, T. Suzuki, and H. Wada, *J. Power Sources*, **26**, 545 (1989).
13. T. Abe, K, Takeda, T. Fukutsuka, Y. Iriyama, M. Inaba, and Z. Ogumi, *Electrochem. Commun.*, **4**, 310 (2002).
14. T. Abe, T. Fukutsuka, M. Inaba, and Z. Ogumi, *Carbon*, **37**, 1165 (1999).
15. T. Fukutsuka, T. Abe, M. Inaba, and Z. Ogumi, *Mol. Cryst. Liq. Cryst.*, **340**, 517 (2000).
16. T. Fukutsuka, T. Abe, M. Inaba, and Z. Ogumi, *J. Electrochem. Soc.*, **148**, A989 (2001).
17. F. Tuinstra and J. L. Koenig, *J. Chem. Phys.*, **53**, 1126 (1970).
18. G. Katagiri, *Tanso*, **175**, 304 (1996) (in Japanese).
19. J. R. Dahn, R. Fong, M. J. Spoon, *Phys. Rev. B*, **42**, 6424 (1990).
20. J. R. Dahn, *Phys. Rev. B*, **44**, 9170 (1991).
21. T. Ohzuku, Y. Iwakoshi, and K. Sawai, *J. Electrochem. Soc.*, **140**, 2490 (1993).
22. M. Inaba, H. Yoshida, Z. Ogumi, T. Abe, Y. Mizutani, M. Asano, *J. Electrochem. Soc.*, **142**, 20 (1995).
23. K. Tatsumi, N. Iwashita, H. Sakaebe, H. Shioyama, S. Higuchi, A. Mabuchi, and H. Fujimoto, *J. Electrochem. Soc.*, **142**, 716 (1995).

General Conclusion

Carbonaceous thin films were prepared by plasma-assisted chemical vapor deposition (plasma CVD) and their structure and electrochemical lithium-ion insertion/extraction were studied for the development of LIBs. In particular, surface modification and interfacial lithium-ion transfer for the resultant carbonaceous thin-film electrodes were focused. The summary of the present work is given as follows:

In chapter 1, carbonaceous thin films were prepared by plasma CVD from acetylene/argon plasma at 873 K. The resultant thin films were sp^2-type carbonaceous thin films and relatively high crystallinity. The physical properties of these carbonaceous thin films are strongly dependent on the applied rf power.

In chapter 2, electrochemical lithium-ion insertion/extraction was examined by using carbonaceous thin-film electrodes prepared in chapter 1. The electrochemical properties were dependent on their crystallinity. The lithium-ion insertion/extraction mechanism into the carbonaceous thin-film electrodes was clarified by using cyclic voltammetry, charge-discharge measurements, and linear sweep voltammetry.

In chapter 3, carbonaceous thin films were prepared by C_2H_4 / NF_3 glow discharge plasma. Addition of NF_3 into plasma was found to affect the growth rates and crystallinity of carbonaceous thin films. Electrochemical properties of the resultant carbonaceous thin-film electrodes were also influenced by the flow rates of NF_3.

In chapter 4, highly graphitized carbonaceous thin films have been prepared by plasma CVD at lower temperature of 1073 K. The electrochemical properties of the highly graphitized carbonaceous thin-film electrodes were different from those of graphite negative electrodes in electrolyte of PC containing 1 mol dm^{-3} $LiClO_4$, which is ascribed to the less crystallized surface of the present thin films.

In chapter 5, carbonaceous thin-film electrodes prepared by plasma CVD were

treated by NF_3 plasma to give surface fluorinated thin films. The degree of fluorination was dependent on the flow rates of NF_3. From cyclic voltammograms, the decomposition of solvent at the 1st reduction process was suppressed by the fluorination. In addition, plasma treatment gave no change to the bulk electrochemical characteristics of carbonaceous thin-film electrodes. The results indicated that surface modification of carbonaceous thin-film electrode by NF_3 plasma affects the mechanism for the reductive decomposition of solvent during the first charge in the LIBs.

In chapter 6, carbonaceous thin-film electrodes prepared by plasma CVD were treated by O_2 plasma to conduct surface modification. The XPS measurements revealed that oxygen atoms were introduced into the carbonaceous thin-film electrodes and C-O bonding was formed. Cyclic voltammograms showed that the decomposition of EC at the 1st reduction process was suppressed by the plasma modification and that this reduction process suppressed by surface modification is related to the formation of SEI. It is indicated that O_2 plasma modification is available for decrease of the irreversible capacity of carbon negative electrodes in the LIBs as well as surface fluorination.

In chapter 7, structurally defined electrode/electrolyte interface was prepared from the carbonaceous thin-film electrode described in the previous chapters. Lithium-ion transfer at the interface between the carbonaceous thin-film electrode and the electrolyte was investigated by AC impedance spectroscopy. In the Nyquist plots, one semi-circle due to charge-transfer resistances appeared, and the values of charge-transfer resistance were dependent on electrode potentials. Lithium-ion diffusion coefficients were also evaluated by adopting the finite diffusion model. The diffusion coefficient was dependent on the electrode potentials. A high activation barrier was shown for interfacial lithium-ion transfer through the interface between a carbonaceous thin-film electrode and an electrolyte.

In chapter 8, interfacial lithium-ion transfer was examined by using carbonaceous thin-film electrodes and various solutions. A relationship was derived for the activation energy of interfacial lithium-ion transfer and ion-solvent interaction. The solvents that strongly interact with lithium ion, such as DMSO, gave high activation energies. These results indicate that activation energy is dependent on the ion-solvent interaction. Hence, reduction of ion-solvent interaction is essential to decrease the activation energy at the interfacial lithium-ion transfer to improve the rate performance of LIBs.

In chapter 9, core-shell-type carbonaceous thin films were prepared by plasma CVD. This CVD process gave a highly graphitized carbonaceous thin-film electrode with a less-crystallized surface. By changing the applied rf power, the difference in crystallinity between the interior bulk and surface could be controlled. Since the surface of the thin films was less crystallized, PC-based electrolyte can be used for graphitized carbonaceous-thin film electrodes as mentioned in chapter 4. AC impedance spectroscopy revealed that the charge-transfer resistances of the carbonaceous thin-film electrode prepared at an rf power of 10 W showed the minimum value of charge-transfer resistance.

Carbonaceous thin-film electrodes prepared in this study are used as a model electrode of carbonaceous negative electrodes for LIBs, and based on the above results, detail lithium-ion insertion/extraction mechanism into lower crystallized carbonaceous materials, effect of surface modification of carbonaceous materials on electrochemical properties, and interfacial lithium-ion transfer at carbonaceous electrodes were clarified.

Publication List

Part 1

Chapter 1

1) Synthesis of sp^2-type carbonaceous thin films by glow discharge plasma.
Takeshi Abe, Tomokazu Fukutsuka, Minoru Inaba, and Zempachi Ogumi
Carbon, **37**, 1165-1168 (1999).

Chapter 2

2) Electrochemical properties of carbonaceous thin films prepared by plasma chemical vapor deposition.
Tomokazu Fukutsuka, Takeshi Abe, Minoru Inaba, and Zempachi Ogumi
Journal of the Electrochemical Society, **148**, A1260 -A1265 (2001).

3) Electrochemical intercalation of Li into carbon thin films prepared by plasma CVD.
Tomokazu Fukutsuka, Takeshi Abe, Minoru Inaba, and Zempachi Ogumi
Molecular Crystals and Liquid Crystals, **340**, 517-522 (2000).

4) Electrochemical lithium insertion / extraction for carbonaceous thin film electrodes in propylene carbonate solution.
Tomokazu Fukutsuka, Takeshi Abe, Minoru Inaba, Zempachi Ogumi, Yoshiaki Matsuo, and Yosohiro Sugie
Carbon Science, **1**, 129-132 (2001).

Chapter 3

5) Preparation and electrochemical properties of carbonaceous thin films prepared by C_2H_4/NF_3 glow discharge plasma.

Tomokazu Fukutsuka, Takeshi Abe, Minoru Inaba, Zempachi Ogumi, Naoko Tsuji and Akimasa Tasaka

Tanso, **190**, 252-256 (1999).

Chapter 4

6) Synthesis of highly graphitized carbonaceous thin films by plasma assisted chemical vapor deposition and their electrochemical properties in propylene carbonate solution.

Takeshi Abe, Kazuhisa Takeda, Tomokazu Fukutsuka, Yasutoshi Iriyama, Minoru Inaba, and Zempachi Ogumi

Electrochemistry Communications, **4**, 310-313 (2002).

Part 2

Chapter 5

7) Surface modification of carbonaceous thin films by NF_3 plasma and their effects on electrochemical properties

Tomokazu Fukutsuka, Yoshiaki Matsuo, Yosohiro Sugie, Takeshi Abe, Minoru Inaba, and Zempachi Ogumi

Molecular Crystals and Liquid Crystals, **388**, 117-122 (2002).

Chapter 6

8) Surface plasma modification of carbonaceous thin film electrodes

Tomokazu Fukutsuka, Satoshi Hasegawa, Tatsuya Katayama, Yoshiaki Matsuo, Yosohiro Sugie, Takeshi Abe and Zempachi Ogumi

Electrochemistry, **71**, 1111-1113 (2003).

Part 3

Chapter 7

9) Lithium ion transfer at interface between carbonaceous thin film electrode / electrolyte
Zempachi Ogumi, Takeshi Abe, Tomokazu Fukutsuka, Shigeki Yamate, and Yasutoshi Iriyama
Journal of Power Sources, **127(1-2)**, 72-75 (2004).

10) Lithium ion transfer at carbon thin film electrode / electrolyte interface
Takeshi Abe, Tomokazu Fukutsuka, Shigeki Yamate, Yasutoshi Iriyama, Minoru Inaba, and Zempachi Ogumi
Molecular Crystals and Liquid Crystals, **388**, 141-146 (2002).

Chapter 8

11) Influences of ion-solvent interaction on lithium-ion transfer at the interface of carbonaceous thin film electrode/electrolyte
Tomokazu Fukutsuka, Yoshiaki Matsuo, Yosohiro Sugie, Takeshi Abe, and Zempachi Ogumi
Journal of the Electrochemical Society, to be submitted.

Chapter 9

12) Electrochemical properties of graphitized carbonaceous thin films prepared by plasma assisted chemical vapor deposition
Takeshi Abe, Kazuhisa Takeda, Tomokazu Fukutsuka, Yasutoshi Iriyama, and Zempachi Ogumi
Journal of the Electrochemical Society, **151**, C694–C697 (2004).

Paper not included in the thesis is listed below.

Surface modification of carbonaceous thin films by electropolymerization of pyrrole and their effects on electrochemical properties (1)
Takayuki Doi, Kazuhisa Takeda, Tomokazu Fukutsuka, Yasutoshi Iriyama, Takeshi Abe, Zempachi Ogumi
Tanso, **210**, 217-220 (2003).